CELL-SPECIFIC AND PHOSPHORYLATION-DEPENDENT ACTIONS OF NEUROSTEROIDS AT EXTRASYNAPTIC GABA-A RECEPTORS IN THE BRAIN

A Dissertation

by

SHU-HUI CHUANG

Submitted to the Office of Graduate and Professional Studies of
Texas A&M University
in partial fulfillment of the requirements for the degree of

DOCTOR OF PHILOSOPHY

Chair of Committee,	D. Samba Reddy
Committee Members,	Jun Wang
	Peng Li
	Ursula H. Winzer-Serhan
Head of Program,	Warren E. Zimmer

May 2019

Major Subject: Medical Sciences

ABSTRACT

Epilepsy is a chronic neurological disorder characterized by unpredicted recurrent seizures. Dysfunction of GABA-A receptors (GABA-ARs) in the brain plays a key role in the pathophysiology of epilepsy. Neurosteroids are powerful allosteric agonists of GABA-ARs and are more efficacious on extrasynaptic δ subunit-containing GABA-ARs that mediate tonic inhibition. Endogenous neurosteroids such as allopregnanolone (AP) have broad-spectrum anticonvulsant activity and possess therapeutic potential for epilepsy. There are many synthetic neurosteroids in trials. Ganaxolone (GX) is the 3β-methylated synthetic analog of AP. Although GX was previously tested in recombinant GABA-ARs, its precise mechanisms of action on native neurons in the brain, including its ability to modulate extrasynaptic δGABA-ARs, and its interactions with other molecules, remain unknown.

The main objective of this dissertation is to investigate the molecular, cell-specific, and phosphorylation-dependent mechanisms of action of synthetic neurosteroid GX and related neurosteroid agents at extrasynaptic δGABA-ARs using pharmacological, electrophysiological, and behavioral approaches. In addition, structure-activity relationships of analogs are tested in native neurons. Several GABA-AR subunits contain phosphorylation sites regulated by protein kinases. Therefore, this study examines the influences of protein kinase activity on neurosteroid actions in native neurons. In addition, we explore the physiological interactions between neurosteroids and zinc and the potential combination strategy of neurosteroids with other clinical GABAergic agents.

We established concentration-response profiles of GX in two cell types: (i) δ-abundant dentate gyrus granule cells (DGGCs) and (ii) γ-rich CA1 pyramidal cells (CA1PCs). Our results show that GX and analogs are preferential allosteric modulators and direct activators of extrasynaptic δGABA-ARs regulating network inhibition and seizures in the dentate gyrus. The potentiation of tonic inhibition by GX is δ subunit-dependent and

protein kinase C activity-mediated. Zinc concentration-dependently blocks GX-potentiated GABA-gated currents in DGGCs and CA1PCs. Zinc reduces antiseizure activity of GX by the selective blockade of extrasynaptic δGABA-AR-mediated tonic inhibition in the hippocampus. Combination therapies of neurosteroids with clinically used antiepileptic drugs tiagabine and midazolam exhibit strong synergistic effects on antiseizure activity and hippocampal tonic inhibition. Overall, these findings signify a unique role for extrasynaptic δGABA-ARs as key modulators of excitability in the brain and provide valuable mechanistic rationales for the clinical synergistic potential of neurosteroids in epilepsy and seizure disorders.

DEDICATION

This dissertation is dedicated to my family.

ACKNOWLEDGEMENTS

I would like to thank my committee chair and mentor Dr. Samba Reddy for his continual support and guidance of my graduate life and career. Dr. Reddy is an intelligent person with enthusiasm in science. He not only ignites my passion in epilepsy research but fosters an environment with extensive support and resources that allow me to conduct all the experiments without any hesitation. His encouragement and the training and challenge I have been through during my graduate life have led me to mature into an independent scientist. I would also like to thank my committee members, Drs. Ursula Winzer-Serhan, Jun Wang, and Peng Li, for their guidance and feedback throughout the course of this research.

Thanks also go to my friends and colleagues and the department faculty and staff for making my time at Texas A&M University Health Science Center a great experience. I would like to thank Drs. Xin Wu and Chase Carver for the training and help with electrophysiology, Dr. Bryan Clossen for his assistance in animal seizure studies, and Victoria Golub for her assistance and help in the lab. I would also like to thank Dr. Je-Chin Han and Mrs. Han for their encouragement for being participate in public affairs and to thank my friends Kenneth, Mei, Jay, Yi-Tang, Franke, Jeng-Yih, Yu-Syuan, and Szu-Ting for all the fun time we have been spent together.

Finally, thanks to my mother, father, brother and two sisters for their encouragement and support and to my husband Chia-Hung for his endless patience and love. Thanks also go to my adorable son Max for making me a strong mom.

CONTRIBUTORS AND FUNDING SOURCES

Contributors

This work was supervised by a dissertation committee consisting of Professor D. Samba Reddy [advisor] and Professors Ursula H. Winzer-Serhan and Jun Wang of the Department of Neuroscience and Experimental Therapeutics and Professor Peng Li of the Department of Electrical & Computer Engineering.

All the work conducted for the dissertation was completed by the student independently.

Funding Sources

This work was made possible in part by NIH under Grant Number [U01 NS083460] to D. Samba Reddy.

NOMENCLATURE

δKO	GABA-A receptor δ subunit knockout
AED	Antiepileptic drug
AMPA	α-amino-3-hydroxy-5-methyl-4-isoxazolepropionic acid
AP	Allopregnanolone (3α-hydroxy-5α-pregnan-20-one)
AP2	Adaptor protein 2
APV	D,L-2-amino-5-phosphonovaleric acid
BIC	Bicuculline
BLA	Basolateral amygdala
BZ	Benzodiazepine
CaMKII	Ca2+/Calmodulin-dependent protein kinase II
CA1	Cornu Ammonis area 1
CA1PC	Cornu Ammonis area 1 pyramidal cell
CA3	Cornu Ammonis area 3
CAE	Childhood absence epilepsy
CI	Combination index
CL	Confidence limit
CNS	Central nervous system
DGGC	Dentate gyrus granule cell
DHEAS	Dehydroepiandrosterone sulfate
DNQX	6,7-dinitroquinoxaline-2,3-dione
DS	Dravet syndrome
EC_{10}	Effective concentration that produces 10% of the maximal currents
EC_{50}	Median effective concentration
ED_{50}	Median effective dose
$EF_{2\text{-fold endogenous}}$	The effective functional concentration of drug required to double the endogenous tonic response
ER	Endoplasmic reticulum

FDA	Food and Drug Administration
FS	Febrile seizures
GABA	γ-aminobutyric acid
GABA-AR	γ-aminobutyric acid type A receptor
GABA-B	γ-aminobutyric acid type B
GABA-C	γ-aminobutyric acid type C
GABA-T	GABA transaminase
GABRA	The gene encoding the GABA-A receptor α subunit
GABRB	The gene encoding the GABA-A receptor β subunit
GABRD	The gene encoding the GABA-A receptor δ subunit
GABRG	The gene encoding the GABA-A receptor γ subunit
GBZ	Gabazine, SR-95531 (4-[6-imino-3-(4-methoxyphenyl) pyridazin-1-yl] butanoic acid hydrobromide)
GEFS+	Generalized Epilepsy with Febrile Seizures Plus
GX	Ganaxolone
HEK	Human embryonic kidney cell
IPSC	Inhibitory postsynaptic current
JME	Juvenile myoclonic epilepsy
MDZ	Midazolam
mIPSC	Miniature inhibitory postsynaptic current
MT	Metallothionein
NMDA	*N*-Methyl-D-aspartate
NS	Neurosteroid
OP	Organophosphate
PKA	Protein kinase A
PKC	Protein kinase C
PTZ	Pentylenetetrazol
QX-314	*N*-(2,6-Dimethylphenylcarbamoylmethyl)triethylammonium bromide

SE	Status epilepticus
THDOC	Allotetrahydrodeoxycorticosterone (3α,21-dihydroxy-5α-pregnan-20-one)
THIP	Gaboxadol (4,5,6,7-tetrahydroisoxazolo-[5,4-c]pyridin-3-ol
TG	Tiagabine
TM	Transmembrane domain
TSPO	Translocator protein 18kDa
TTX	Tetrodotoxin
VGCC	Voltage-gated calcium channel
WT	Wildtype
Zn^{2+}	Zinc
ZnT	Zn^{2+} transporter

TABLE OF CONTENTS

Page

LIST OF FIGURES

Page

LIST OF TABLES

Page

CHAPTER I

INTRODUCTION AND LITERATURE REVIEW[*]

I. Introduction

Alterations in the structure and function of neurotransmitter receptors play critical roles in the pathophysiology of many brain diseases. Epilepsy is one of the most widespread and debilitating neurological disorders that affects approximately 3.4 million people in the USA and 65 million people worldwide. This disorder is a chronic condition characterized by two or more unpredicted and unprovoked seizures occurring due to excessive or hypersynchronous electrical discharge of neurons in the brain (Hauser 1994; Thurman et al., 2011; Hesdorffer et al., 2013). Many subregions and a wide variety of neurotransmitters are involved in the pathology of epileptic seizures. The GABA-A receptor (GABA-AR), a subtype of receptor activated by the inhibitory neurotransmitter GABA, is a prime target for many seizure medications. While antiepileptic drugs (AEDs) allow for symptomatic control of seizures, epilepsy remains incurable, partially due to our poor understanding of the molecular and electrophysiological basis of epilepsy development. Advances in our understanding of the pathology of epilepsy are crucial for discovering effective treatments for epilepsy and related brain disorders.

Current knowledge indicates that approximately 60% of epilepsy is idiopathic, and 40% stems from developmental or acquired conditions such as a stroke, traumatic brain injury, infections, tumor, drug withdrawal, neurotoxicity, or prolonged seizures and genetic defects (Eslami et al., 2015; Pitkanen et al., 2015; Vezzani et al., 2016). The underlying mechanisms that render a normal brain to progressively develop into a brain with recurring seizures are still elusive. Along with age- and gender-related factors, other physiological abnormalities in neurotransmitter release, functions of ion channels,

---

[*]Reprinted (adapted) with permission from "Genetic and molecular regulation of extrasynaptic GABA-A receptors in the brain: therapeutic insights for epilepsy" by S-H Chuang and DS Reddy, 2018. T*he journal of pharmacology and experimental therapeutics*, 364(2): 180–197, Figures 1 – 6, Table 1 – 4, Copyright © 2018 by The American Society for Pharmacology and Experimental Therapeutics. All rights reserved.

synaptic connectivity, neural circuitries, or the interaction of these factors facilitate seizure development. The term “epileptogenesis” is used to describe the complicated process of the development of acquired epilepsy. Epileptogenesis denotes a plastic progression in which the balance of neuronal excitation/inhibition, neuronal interconnections, and neuronal circuits undergo gradual changes during or after a series of insults, and consequently, transform a normal brain into one that is hyperexcitable, suffers neuronal loss and damage, and, as a result, has recurrent spontaneous seizures.

In this review, we describe briefly the emerging concepts on GABA genetics in epilepsy, with a special emphasis on the functional role of extrasynaptic GABA-ARs in the regulation of network excitability and susceptibility to brain disorders. We also highlight the potential therapeutic implications of modulating extrasynaptic GABA-AR-mediated tonic inhibition in pharmacotherapy of epilepsy, status epilepticus (SE), and other brain disorders.

I.1 GABA-AR Structure and Subtypes

Gamma-aminobutyric acid (GABA) is the most abundant inhibitory neurotransmitter in the brain. It is a highly hydrophilic molecule and hence cannot cross the blood-brain barrier. GABA is synthesized in neurons and stored in synaptic vesicles. Upon neuronal activation, GABA is released from the vesicles into the synapse, where it can act on postsynaptic receptors, or diffuse into the extracellular space. GABA binds with three receptors: GABA-A receptor (GABA-AR), GABA-B, and GABA-C. GABA-AR plays a pivotal role in regulating neuronal excitability and in the pathology of epilepsy (Baulac et al., 2001). GABA exerts fast inhibitory actions by activating postsynaptic GABA-ARs in the brain, causing the influx of negatively charged chloride ions and hyperpolarization of neurons that serves to reduce neuronal excitability and firing. GABA-ARs are pentamers consisting of five subunits. Each subunit has one long extracellular N-terminus that interacts with a variety of drugs including benzodiazepines (BZs), barbiturates, and neurosteroids; four transmembrane domains (TM1-TM4); and one short intracellular loop

that links TM1 and TM2, one short extracellular loop that links TM2 and TM3, one long intracellular loop that links TM3 and TM4 and can be modulated by phosphorylation, and one small extracellular C-terminus. TM2 transmembrane domain of each subunits form a selective channel pore that is permeable for chloride ion passage (Figure 1). GABA-AR isoform distribution plays key roles in regulation of sedation, hypnosis, anxiolysis, anesthesia, and seizure protection (Table 1).

GABA-ARs are made from a repertoire of 19 known subunits: α1-6, β1-3, γ1-3, δ, ε, θ, π, ρ1-3. The most general stoichiometry of GABA-ARs contains 2 αs, 2 βs and 1 γ or 1 δ subunit. GABA-AR subunits have discrete distributions among different brain regions. Approximately 90% of GABA-ARs are γ-containing, but the δ subunit can substitute for γ. The δ subunit has more confined expression in parts of the brain such as the hippocampus, cerebellum, and thalamus. GABA binding sites are located at the junction between subunits α and β, and BZs bind at the interface between subunits α and γ. The genomic location of 19 GABA-AR subunits has been identified (Russek, 1999). The genes encoding subunit α2, α4, β1, and γ1 cluster on chromosome 4p12; subunit α1, α6, β2, γ2, and π genes are mapped on chromosome 5q; subunit α5, β3, and γ3 genes cluster on chromosome 15q12; subunit α3, θ, and ε are located on chromosome Xq28; ρ1 and ρ2 cluster on chromosome 6q15; and the ρ3 and δ subunits are found on chromosome 3q11.2 and chromosome 1p36.3, respectively (Figure 2).

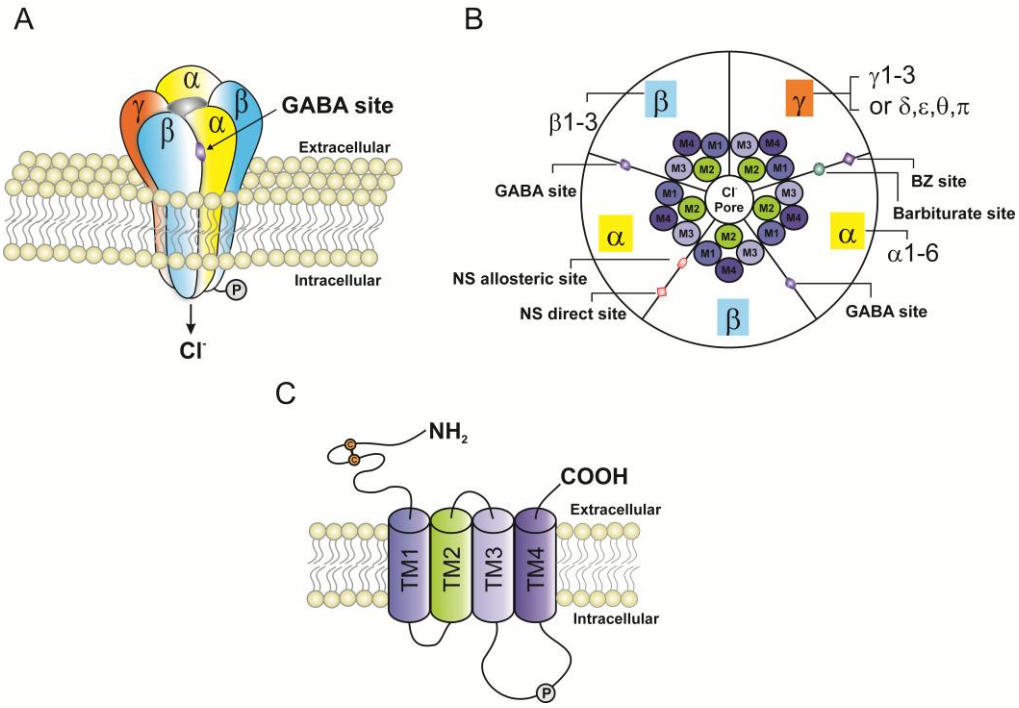

Figure 1 Schematic representation of typical GABA-AR structure and subunit composition.

(A) GABA-A receptors (GABA-ARs) are heteropentamers forming a channel that is permeable to chloride ion passage. (B) A top view of the pentamer. GABA-ARs are made from a repertoire of 19 known subunits: α1-6, β1-3, γ1-3, δ, ε, θ, π, ρ1-3. The most general stoichiometry of GABA-ARs contains 2 αs, 2 βs and 1 γ; the γ subunit can be substituted by δ, ε, θ, or π. Each subunit has four transmembrane domains (TM1-4). TM2 transmembrane domains form a selective channel pore. GABA exerts fast inhibitory actions by activating postsynaptic GABA-ARs in the brain, causing the influx of negatively charged chloride ions and hyperpolarization of neurons which serves to reduce neuronal excitability and firing. The GABA binding sites are located at the junction between subunit α and β, whereas benzodiazepines (BZs) bind at the interface between subunit α and γ. Barbiturates binding sites are distinct from the BZ binding site. The neurosteroids (NSs) have two putative binding sites including allosteric and direct binding sites. The allosteric binding site is located at the α subunit transmembrane domains, whereas the direct binding site is within the transmembrane domains of the α and β subunits. (C) GABA-ARs belong to Cys-loop family of ligand-gated ion channels that also contains nicotinic acetylcholine, glycine, and serotonin 5-HT3 receptors. Each subunit has one long extracellular N-terminus that interacts with a variety of drugs including BZs, barbiturates, and NSs; four transmembrane domains (TM1-TM4); and one short intracellular loop that links TM1 and TM2, one short extracellular loop that links TM2 and TM3, one long intracellular loop that links TM3 and TM4 and can be modulated by phosphorylation, and one small extracellular C-terminus.

A

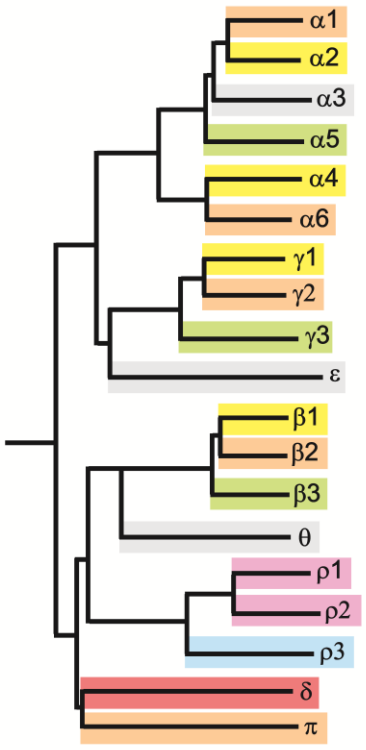

B

Chromosome	Location	Subunit	Gene Name	Gene ID
1	1p36.3	δ	GRBRD	2563
3	3q11.2	ρ3	GRBRR3	200959
4	4p12	α2	GRBRA2	2555
		α4	GRBRA4	2557
		β1	GRBRB1	2560
		γ1	GRBRG1	2565
5	5q34	α1	GRBRA1	2554
	5q34	α6	GRBRA6	2559
	5q34	β2	GRBRB2	2561
	5q34	γ2	GRBRG2	2566
	5q35.1	π	GRBRP	2568
6	6q15	ρ1	GRBRR1	2569
		ρ2	GRBRR2	2570
15	15q12	α5	GRBRA5	2558
		β3	GRBRB3	2562
		γ3	GRBRG3	2567
X	Xq28	α3	GRBRA3	2556
		θ	GRBRQ	55879
		ε	GRBRE	2564

Figure 2 GABA-AR subunit family.

(A) A dendrogram illustrating the 19 known genes encoding for the mammalian GABA-AR subunits and the sequence homologies. (B) Chromosomal clusters of GABA-AR subunit genes.

Table 1 The pharmacological roles of select GABA-AR subunits.

	α1	α2	α3	α4	α5	β2	β3	γ2	δ
ANXIETY								+	-
LEARNING MEMORY					+				-/+
SEIZURE/EPILEPSY	+	-	-		-		+		
EFFECTS OF BENZODIAZEPINES									
MOTOR IMPAIRMENT	-	-	-		-				
SEDATION	+	-	-		-	+			
ANXIOLYSIS	-	+	+		-				
MYORELAXATION	-		+						
ANTICONVULSANT	+	-	-		-				
EFFECTS OF NEUROSTEROIDS									
MOTOR IMPAIRMENT	-								
HYPNOSIS	-								+
ANXIOLYSIS									+
ANTICONVULSANT									+
EFFECTS OF OTHER DRUGS									
SEDATION				+					
ANESTHESIA				+			+		-

(Homanics et al., 1997; Mihalek et al., 1999; Rudolph et al., 1999; Low et al., 2000; McKernan et al., 2000; Collinson et al., 2002; Crestani et al., 2002; Blednov et al., 2003; Jurd et al., 2003; Kralic et al., 2003; Chandra et al., 2005; Wiltgen et al., 2005; Nutt 2006; Jia et al., 2007; Carver et al., 2014)

I.2 Synaptic vs. Extrasynaptic GABA-ARs

GABA-ARs are divided into two categories according to their localization: synaptic and extrasynaptic receptors. Each type of receptor possesses distinct characteristics in its affinity and efficacy to GABA, desensitization rate, and response to BZs and neurosteroids (Bianchi and Macdonald, 2002; Brown et al., 2002; Wohlfarth et al., 2002; Bianchi and Macdonald, 2003; Mortensen et al., 2011). Extrasynaptic GABA-ARs are composed of mainly δ-containing receptors, which have high GABA affinity but low efficacy, low desensitization rate, low sensitivity to BZs, and are highly potentiated by neurosteroids compared to synaptic GABA-ARs (Table 2). Activation of synaptic γ-containing GABA-ARs and extrasynaptic δ-containing GABA-ARs produce phasic and tonic current inhibition, respectively. Rapid and transient phasic current inhibition is generated by presynaptic GABA release and the binding of synaptic γ-containing GABA-ARs, whereas, tonic current inhibition is produced by persistent activation of perisynaptic or extrasynaptic δ-containing GABA-ARs by ambient GABA. Extrasynaptic receptors are only found in specific brain areas such as the hippocampus, amygdala, neocortex, thalamus, hypothalamus, and cerebellum (Stell et al., 2003; Jia et al., 2005; Drasbek and Jensen, 2006; Olmos-Serrano et al., 2010; Mortensen et al., 2011; Carver et al., 2014). Extrasynaptic δ-containing GABA-ARs are tailored to regulate neuronal excitability by controlling the basal tone through shunting and tonic inhibition in neurons (Coulter and Carlson, 2007; Carver and Reddy 2013). They are mostly insensitive to allosteric modulation by BZs such as midazolam (MDZ) (Reddy et al., 2015; Carver and Reddy, 2016).

Table 2 Characterization of synaptic (αβγ2-containing) and extrasynaptic (αβδ-containing) GABA-ARs in the brain.

	SYNAPTIC GABA-ARS	EXTRASYNAPTIC GABA-ARS
SUBUNITS	Pentamer (γ2-containing)	Pentamer (δ-containing)
INHIBITION	Phasic	Tonic
GABA AFFINITY	Low	High
GABA EFFICACY	High	Low
DESENSITIZATION	Pronounced	Moderate/Low
BENZODIAZEPINES	sensitive	insensitive
NEUROSTEROIDS	Potentiated	Highly potentiated
LOW $[Zn^{2+}]$ BLOCKADE	No	Yes
DISTRIBUTION	Highly prevalent	Highly specific regional (e.g. hippocampus, neocortex, thalamus, hypothalamus, cerebellum)

I.3 Distribution of GABA-AR Subtypes

Different subtype combinations respond differently to receptor modulators and contribute distinct functions in each brain area. GABA-ARs have a high molecular heterogeneity because of the abundance of available subunits and the ways in which those subunits can be assembled to form the heteropentameric receptors. The composition and distribution of the GABA-AR isoforms are listed in Table 3. Receptors located in the synaptic sites are primarily made of α, β, and γ2 subunits. α1-, α2-, α3-, and α5-containing receptors are generally sensitive to BZs. γ subunit containing receptors constitute the majority of GABA-ARs. Immunohistochemistry and *in situ* hybridization data showed that α1β2γ2 is the most abundant and widespread subtype accounting for ~43-60% of all GABA-ARs in the adult brain (McKernan and Whiting, 1996; Loup et al., 2000; Mohler et al., 2002). It majorly appears in the synaptic sites. α2β3γ2 and α3β3γ2 receptors, located mostly in the synaptic sites, are also highly prevalent. They represent ~15-20% and ~10-15% of all GABA-ARs, respectively. α4βγ and α4βδ, located in the synaptic and extrasynaptic locations respectively, represent approximately 5%, while synaptic α5β1/3γ2 and α6β2/3γ2 account for less than 5% (McKernan and Whiting, 1996; Pirker et al., 2000; Mohler et al., 2002). Other subtypes have more specific and confined distribution patterns (Figure 3).

Receptors located in the extrasynaptic locations usually contain the δ subunit rather than γ in association with β2 or β3 and a certain isoform of α subunit. The δ subunit with its highly specific regional and subcellular distribution is tailored to generate tonic inhibition. It is abundant in cerebellar and dentate gyrus granule cells (DGGCs), some cortical neurons, and thalamic relay cells (Wisden et al., 1992; Fritschy and Mohler, 1995; Sperk et al., 1997; Pirker et al., 2000; Peng et al., 2002).

In the hippocampus, several isoforms are expressed in distinct regions and cell types. CA1 pyramidal neurons mainly contain α5β3γ2S receptors, which are located at both synaptic and extrasynaptic sites. However, DGGCs, which have the second highest

density of δ subunits, express α3β3γ2S and α4β2/3δ receptors in the synaptic and extrasynaptic site, respectively (Sperk et al., 1997; Peng et al., 2002). The δ subunit is thought to be predominately co-localized and assembled with α4 and/or α6 subunit. α4β2/3δ or α6β2/3δ combinations exhibit the highest GABA affinity with a GABA EC_{50} (concentration required to achieve half-maximal activation) in the nanomolar range. α1β2δ receptors are primarily present in hippocampal interneurons and show lower GABA potency compared to the α4β2/3δ combination. Overall, α1, α4, γ2 and δ subunit are found to be expressed in the extrasynaptic sites of hippocampus (Sun et al., 2004; Glykys and Mody, 2007; Mortensen et al., 2011).

In the cerebellum, cerebellar granule cells, which contain the highest density of δ subunit in the central nervous system (CNS), express α6β2/3δ predominantly at extrasynaptic sites. α6β3 and α6β3γ2S combinations are also found in cerebellar granule cells (Nusser et al., 1998; Farrant and Nusser, 2005; Zheleznova et al., 2009). Notably, α6-containing receptors are almost exclusively expressed in the cerebellar granule cells and, in combination with the δ subunit, exhibit the highest GABA potency. In the thalamus, α4β3γ2S receptors are expressed at synaptic sites in the thalamic relay cells, whereas, α4β3 and α4β3δ receptors are expressed at extrasynaptic sites. In addition, α3β3 receptors are also found in the thalamus.

In the amygdala, the α2 subunit, primarily found in principal neurons, is responsible for the allosteric action of the BZs (Marowsky et al., 2004). The principal neurons in the basolateral amygdala (BLA) also contain γ2 subunits which contribute to the fast synaptic inhibition (Esmaeili et al., 2009). The BZ-sensitive α2βγ2 subtypes are thought to be assembled in the principal neurons of the BLA in the synaptic site and generate phasic inhibition. Extrasynaptic GABA-ARs in the BLA are made up mainly of the α3, α5, and the δ subunits, which contribute to non-desensitizing tonic current inhibition. In particular, the α3 subunit is strongly expressed throughout the BLA nucleus and is responsible for the majority of tonic inhibition since significant reduction of tonic

currents was observed in the BLA neurons from α3 subunit knockout mice (Farrant and Nusser, 2005; Marowsky et al., 2012).

In general, receptors containing a γ2 subunit in combination with α1, α2 or α3 subunits (α1β2/3γ2, α2β2/3γ2 and α3β2/3γ2) are the predominant synaptic receptor subtypes that produce phasic inhibition, whereas receptors containing α4, α5, α6 or δ subunits (α4βδ, α6βδ, and α5βγ2) are the primary extrasynaptic receptor subtypes that generate tonic inhibition.

Table 3 Distribution of GABA-AR subunits in different brain regions and cell types.

Subunit isoforms	Cellular distribution	Main brain locations/cell types	GABA Potency (EC50) (μM)	Pharmacological characterization	References
Synaptic (S)					
α1β2γ2S	S	Ubiquitously express throughout the brain. Most abundant. Constitute ~43-60% of all GABA-ARs	6.6	BZs, zolpidem, and flumazenil sensitive	(Sieghart 1995; McKernan and Whiting 1996; Pirker et al., 2000; Mohler et al., 2002)
α1β3γ2S	S	Widespread	2.1	BZs and zolpidem sensitive	(Sieghart 1995; Mortensen et al., 2011)
α2β3γ2S	S	Widespread. Account for 15-20% of all GABA-ARs. Hippocampal pyramidal neurons, cerebral cortex, amygdala, caudate putamen	13.4	BZs, zolpidem, and flumazenil sensitive	(Sieghart 1995; McKernan and Whiting 1996; Pirker et al., 2000; Mohler et al., 2002; Mortensen et al., 2011)
α3β3γ2S	S	Account for 10-15% of all GABA-ARs. Hippocampal dentate gyrus granule cells, hypothalamic nuclei, thalamic reticular nucleus, cerebral cortex	12.5	BZs, zolpidem, and flumazenil sensitive	(Sieghart 1995; Mohler et al., 2002; Mortensen et al., 2011)
α4β3γ2S	S	Hippocampus, thalamic relay cells	2.1	Furosemide and Ro15-4513 sensitive	(Brown et al., 2002; Mohler et al., 2002; Mortensen et al., 2011)
α6β3γ2S	S	Account for ~2% of all GABA-ARs. Cerebellum granule cells	0.17	Furosemide and Ro15-4513 sensitive	(McKernan and Whiting 1996; Brown et al., 2002; Mohler et al., 2002; Mortensen et al., 2011)
Extrasynaptic (E)					
α1β2δ	E	Hippocampal interneurons	3.7		(Sun et al; 2004; Glykys et al., 2007)
α3/5βδ	E	BLA principle neurons			(Marowsky et al., 2004; Marowsky et al., 2012)
α3β3	E	Thalamus, hypothalamus, locus coeruleus	4.5		(Mortensen et al., 2011)
α4β3	E	Thalamic relay cells	0.97		(Brickley et al., 1999; Mortensen et al., 2011)
α4β2/3δ	E	Hippocampal dentate gyrus granule cells, thalamic relay cells, neostriatum	0.97-1.7	BZs insensitive; Furosemide and THIP sensitive	(Sperk et al., 1997; McKernan and Whiting 1996; Brown et al., 2002; Peng et al., 2002; Farrant and Nusser 2005; Boehm et al., 2006; Mortensen et al., 2011;)
α6β3	E	Cerebellum granule cells	0.076		(Mortensen et al., 2011)

Table 3 Continued

Subunit isoforms	Cellular distribution	Main brain locations/cell types	GABA Potency (EC50) (μM)	Pharmacological characterization	References
α6β2/3δ	E	Account for ~2% of all GABA-ARs. Cerebellum granule cells	0.17	Lacks BZ binding site; Furosemide and THIP sensitive	(Brown et al., 2002; Mohler et al., 2002; Boehm et al., 2006)
Synaptic (S)/ Extrasynaptic (E)					
α5β3γ2S	S/E	Account for ~4% of all GABA-ARs. Hippocampal pyramidal neurons, cerebral cortex, olfactory bulb	1.4	BZs and flumazenil sensitive	(McKernan and Whiting 1996; Mohler et al., 2002; Farrant and Nusser 2005; Mortensen et al., 2011)

The GABA potency (EC_{50}) data is obtained from recombinant HEK293 cells (Mortensen et al., 2011). BZs: GABA-AR allosteric agonists; Zolpidem: a full agonist at α1-containing GABA-ARs, ~10-fold lower affinity at α2- and α3-containing GABA-ARs; Flumazenil: a GABA-AR antagonist; Furosemide: a GABA-AR antagonist; THIP: 4,5,6,7-tetrahydroisothiazolo-[5,4-c]pyridin-3-ol, a GABA-AR agonist.

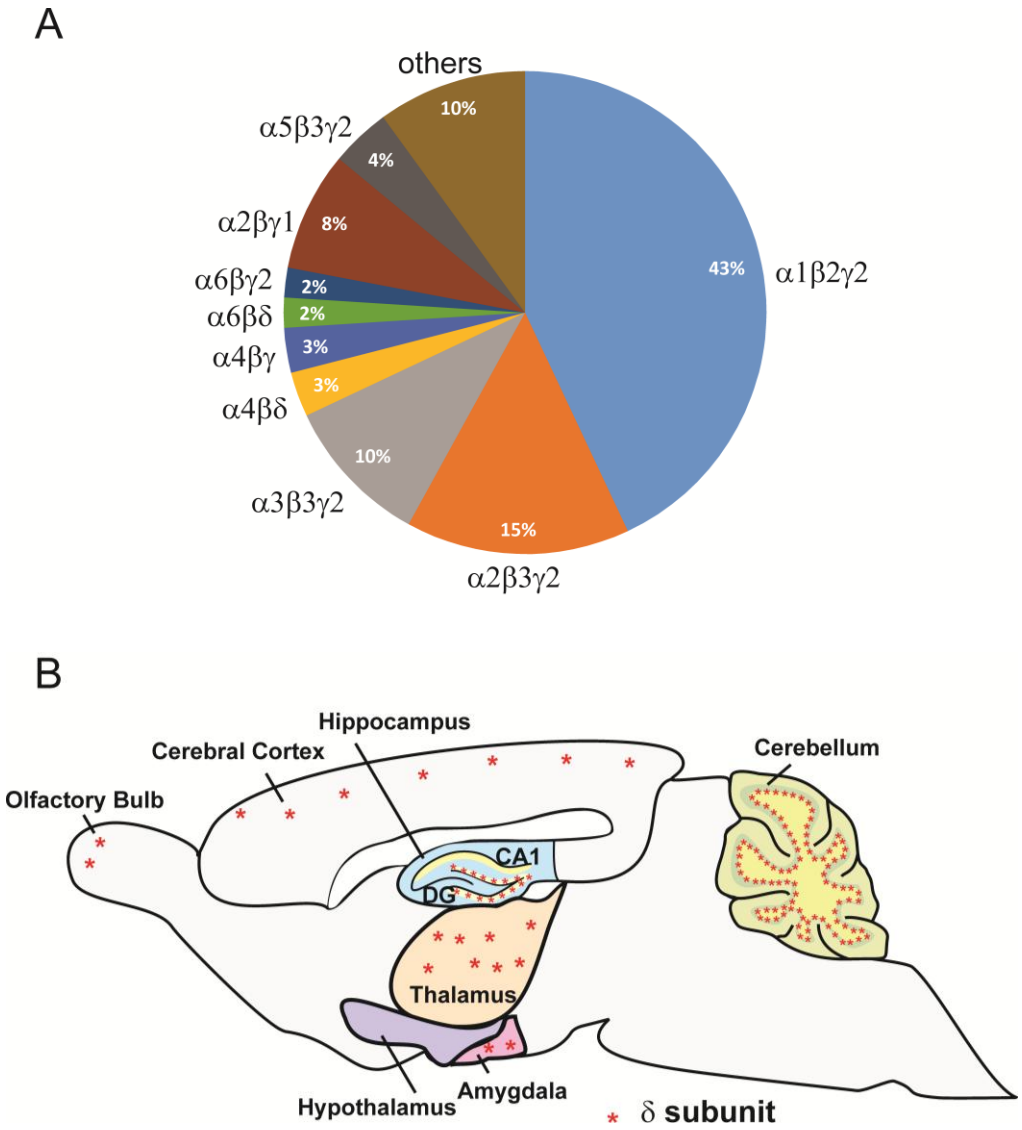

Figure 3 Extrasynaptic GABA-AR δ subunit distribution.

(A) The estimated abundance of GABA-AR subtypes in the rodent brain. (B) GABA-AR δ subunit distribution. *denotes δ subunit.

I.4 Neurosteroid Modulation of GABA-ARs and Tonic Inhibition

Neurosteroids, also referred as neuroactive steroids, are steroids with rapid actions on neuronal excitability through modulation of membrane receptors in the CNS (Kulkarni and Reddy, 1995; Mellon and Griffin, 2002). The terminology on "neurosteroid" and "neuroactive steroid" has been described extensively in the literature (Reddy and Rogawski, 2012). Generally, the terms neurosteroids and neuroactive steroids are used interchangeably to refer to endogenous steroids with rapid membrane actions that were either made de novo in the brain or from peripheral sources of parent steroids that were metabolized in the brain (Baulieu, 1981; Paul and Purdy, 1992; Reddy, 2003ab; 2009a; 2011; 2013b). Parent steroids or neurosteroid precursors (not the steroid metabolites) bind to classic steroid receptors. A brief outline of neurosteroid synthesis is described below. Cholesterol is first translocated across the mitochondrial membrane by the translocator protein 18kDa (TSPO, a key protein that controls the biosynthesis of neurosteroids) and converted into steroid precursor pregnenolone by the P450 side-chain cleavage enzyme in the inner membrane of mitochondria. Pregnenolone is subsequently converted into neurosteroid precursors progesterone, deoxycorticosterone, and testosterone, which go through two sequential A-ring reduction steps and are converted into three prototype endogenous neurosteroids – allopregnanolone (AP, 3α-hydroxy-5α-pregnan-20-one), allotetrahydrodeoxycorticosterone (THDOC), and androstanediol – by the catalysis of two key enzymes called 5α-reductase and 3α-hydroxysteroid oxidoreductase in the brain. These three prototype neurosteroids, AP, THDOC, and androstanediol, are well-studied (Rupprecht, 2003; Belelli and Lambert, 2005; Reddy, 2003ab; 2009a; 2011; Carver and Reddy, 2013; Brown et al., 2015; Porcu et al., 2016).

THDOC potentiates both tonic current conductance and the weighted decay time of spontaneous inhibitory postsynaptic currents (IPSCs) directly in DGGCs and cerebellar granule cells (Vicini et al., 2002; Wohlfarth et al., 2002; Stell et al., 2003). AP at low concentrations (30 and 100 nM) potentiates the decay time of miniature IPSCs (mIPSCs) in CA1 pyramidal cells (Belelli and Herd, 2003). AP also enhances GABA currents in

dissociated neurons and tonic currents in hippocampal slice allosterically and directly (Carver et al., 2014; Carver and Reddy, 2016).

Neurosteroids are powerful modulators of GABA-ARs and can rapidly alter neuronal excitability (Reddy and Estes, 2016). Neurosteroids act at both synaptic and extrasynaptic GABA-ARs but they are more efficacious on extrasynaptic δGABA-ARs that mediate tonic inhibition. At low concentrations (sub-micromolar level), neurosteroids allosterically potentiate GABA-AR currents, whereas at high concentrations (micromolar level), neurosteroids can directly activate GABA-ARs by binding directly at the orthosteric site (Reddy and Rogawski, 2002; Hosie et al., 2007; Reddy and Jian, 2010; Carver and Reddy, 2016). One recent study demonstrated a downregulation of the δ-containing GABA-ARs prior to onset of epilepsy, and a reduction in neurosteroid-induced modulation of tonic inhibition in the SE model of epilepsy, highlighting the role of δGABA-ARs in this disease (Joshi et al., 2017).

Ganaxolone (GX, 3α-hydroxy-3β-methyl- 5α-pregnan-20-one), the 3β-methylated analog of AP, is now being assessed in advanced clinical trials for epilepsy (Pieribone et al., 2007; Porcu et al., 2016). Like AP, GX has been shown to modulate GABA-ARs in *X. Laevis* oocytes expressing human recombinant α1β1γ2L receptors (Carter et al., 1997). Natural neurosteroids have low bioavailability since they can be back-converted to active 3-ketone-containing progesterone metabolites (Rupprecht et al., 1993). The synthetic 3β-substituted GX provides a more promising pharmacokinetic profile as an AED, overcoming the limitations of lower bioavailability by preventing the oxidation of the 3α-hydroxyl group (Carter et al., 1997). GX possesses broad-spectrum anticonvulsant activity in animal seizure models (Reddy and Rogawski, 2000ab; 2010). GX is currently being evaluated in clinical trials for the treatment of epilepsy and related conditions (Nohria and Giller, 2007; Reddy and Rogawski, 2010; 2012; Bialer et al., 2015; Braat et al., 2015; Ligsay et al., 2017).

Progesterone, GX, and AP have been evaluated in clinical trials for seizure conditions (Reddy and Estes, 2016; Younus and Reddy, 2017). GX has been evaluated in more than 1300 subjects in various clinical studies in adults and children with epilepsy (Laxer et al., 2000; Kerrigan et al., 2000; Reddy and Woodward, 2004; Nohria and Giller, 2007; Pieribone et al., 2007; Sperling et al., 2017). Progesterone was evaluated as an adjunct therapy in women with epilepsy (Herzog et al., 2012). The neurosteroid AP has been suggested as an intravenous therapy for refractory SE (Rosenthal et al., 2017) and post-partum depression (Kanes et al., 2017). Overall, synthetic neurosteroid analogs, which activate both synaptic and extrasynaptic GABA-AR-mediated tonic inhibition in the brain, may be promising compounds for clinical development for specific seizure conditions, such as status epileptic and catamenial epilepsy.

I.5 Protein Kinase Modulation of Neurosteroid-Sensitive GABA-ARs

Protein kinases are enzymes that can regulate the function of other proteins by phosphorylating hydroxyl groups on the proteins by which they act. Protein kinase activity influences GABA-AR surface expression, trafficking, chloride conductance, and sensitivity to neurosteroids. Several GABA-AR subunits contain residues that can be phosphorylated by protein kinases including α4, β, and γ2 subunits (Moss and Smart, 1996; Brandon et al., 2000). The serine residue (Ser-443) within the intracellular domain of the α4 subunit is phosphorylated by protein kinase C (PKC) (Abramian et al., 2010). A conserved serine residue (Ser-409 or Ser-410) of the β subunit is phosphorylated by PKC, protein kinase A (PKA), Ca2+/Calmodulin-dependent protein kinase II (CaMKII), and cGMP-dependent protein kinase. Two additional serine residues of the β subunit (Ser-408 and Ser-383) are also phosphorylated by PKA and CaMKII, respectively (McDonald et al., 1998; Saliba et al., 2012). Additionally, the tyrosine residues (Tyr-365 and Tyr-367) and serine residue (Ser-343) of the γ2 subunit are also substrates of tyrosine kinase and PKC, respectively (Krishek et al., 1994; Moss et al., 1995). Phosphorylation of residues within the intracellular loops of the β3 and γ2 subunits maintains the surface expression

of GABA-ARs, whereas, dephosphorylation of these subunits triggers receptor internalization (Kittler et al., 2005; Kittler et al., 2008; Figure 4).

Previous studies have shown PKC activity regulates receptor function, ion conductance and response to receptor modulators. 10-min bath application of PKC activator phorbol 12-myristate 13-acetate increases THDOC-potentiated, GABA-gated chloride currents (Leidenheimer and Chapell, 1997). Treatment with the specific PKC antagonist bisindolylmaleimide 15-min before and during neurosteroid administration diminishes the decay of IPSCs by neurosteroids (Fancsik et al., 2000). Inhibition of either PKA or PKC by intracellular dialysis significantly reduces neurosteroid 5β-pregnan-3α-ol-20-one-mediated prolonged decay of mIPSCs in CA1 pyramidal neurons, whereas activation of PKC has no effect on neurosteroid sensitivity (Harney et al., 2003). Phosphorylation of the serine residue of the β subunits (Ser-383) by L-type voltage-gated Ca^{2+} channel-activated CaMKII leads to rapid surface expression of GABA-ARs and enhanced tonic currents in hippocampal neurons (Saliba et al., 2012). 10-min co-treatment with PKC inhibitor prevents THDOC-upregulated phosphorylation of the α4 subunits and surface expression of α4-containing GABA-ARs (Abramian et al., 2014). Recent study demonstrated that continuous application of AP, but not GX, upregulates the phosphorylation and surface expression of the β3-containing GABA-ARs and tonic current potentiation, effects prevented by the application of PKC inhibitor 15-min before and during neurosteroid application (Modgil et al., 2017).

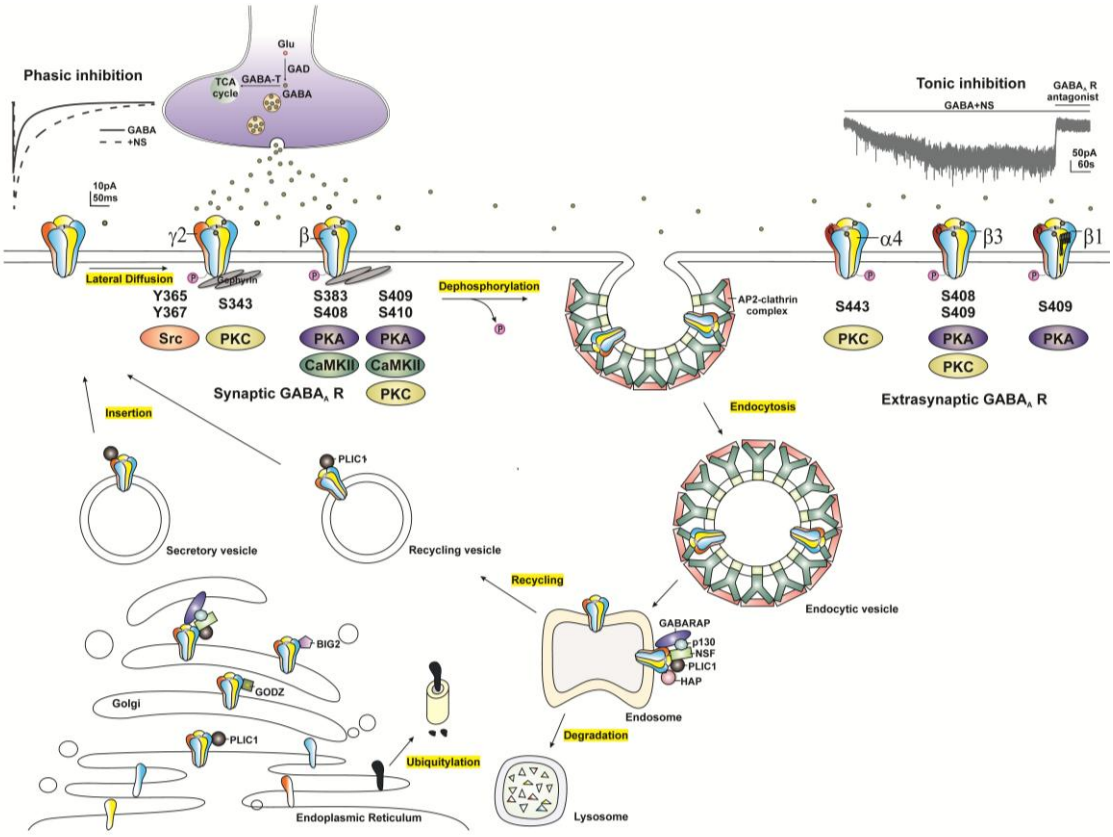

Figure 4 Modulation of extrasynaptic GABA-AR trafficking by phosphorylation.

GABA-ARs subunits including α4, β, and γ2 subunit contain residues that can be phosphorylated by various protein kinases. Phosphorylation of residues within GABA-ARs not only regulates receptor function but maintains their surface expression. Dephosphorylation of these subunits triggers receptor internalization through adaptor protein 2 (AP2)-clathrin complex-dependent endocytosis. Internalized receptors are subsequently transported to the endosomal system, where they can be either recycled to the surface or degraded in the lysosomes. GABA-AR trafficking is facilitated by a variety of protein-protein interactions. GABARAP, a GABA-AR-associated protein, interacts with the γ2 subunit of GABA-ARs and might facilitate receptor insertion into the cell membrane; p130, a phospholipase, shares the same bind site on the γ2 subunit with the GABARAP; NSF, a N-ethylmaleimide sensitive factor, interacts with GABARAP and p130 and plays a crucial role in intracellular transport; PLIC-1, an ubiquitin-like protein, increases receptor stability and enhances membrane insertion of receptors; HAP, a Huntingtin-associated protein, interacts with the β subunit of GABA-ARs and facilitates receptor recycling to the cell membrane; GODZ, a Golgi-specific DHHC zinc finger domain protein, mediates posttranslational palmitoylation; BIG2, a brefeldin A-inhibited GDP/GTP exchange factor, binds to the intracellular loop of β subunits and is involved in the trafficking of receptors. GAD, glutamate decarboxylase; GABA-T, GABA transaminase.

I.6 Zinc Antagonism of Neurosteroid-Sensitive GABA-ARs

Zinc (Zn^{2+}) is an essential cofactor in many cells including neurons. Zn^{2+} is the most abundant transition metal in the vesicles of hippocampal mossy fibers that project from the DG to the CA3 (Frederickson, 1989). During neuronal activity, vesicular Zn^{2+} is released synaptically from certain nerve terminals in the hippocampus (Tian et al., 2010). Excessive release of Zn^{2+} has been shown in epilepsy, and it can decrease the threshold of excitability and seizures (Takeda et al., 1999; Coulter, 2000; Foresti et al., 2008). Zn^{2+} regulation of postsynaptic targets and synaptic plasticity is shown in Figure 5. Zn^{2+} modulates several ligand- and voltage-gated ion channels (Harrison and Gibbons 1994). In particular, Zn^{2+} attenuates GABAergic inhibition at mossy fiber synaptic varicosities that release GABA (Xie and Smart, 1991; Ruiz et al., 2004; Bitanihirwe and Cunningham, 2009). In addition, Zn^{2+} has been shown to negatively modulate synaptic GABA-ARs and modify the excitability of the hippocampal network (Barberis et al., 2000). Three distinct Zn^{2+} binding sites mediate its inhibition of GABA-ARs: one site at the internal surface of the channel pore and two at the external amino-terminus of the α-β interfaces. The incorporation of the γ subunit after GABA-AR co-assembly disrupts two of the Zn^{2+} binding sites, which leads to a reduced sensitivity to Zn^{2+} inhibition (Hosie et al., 2003). Thus, the sensitivity to Zn^{2+} inhibition is different between the two different GABA-AR subtypes (δ-containing and γ-containing) (Smart et al., 1991; Storustovu and Ebert, 2006).

Our recent study demonstrated the δ-containing receptors to be more sensitive to Zn^{2+} inhibition than γ-containing receptors, and Zn^{2+} selectively blocked neurosteroid-sensitive extrasynaptic δGABA-AR-mediated tonic currents in the mouse hippocampus dentate gyrus (Carver et al., 2016). Zn^{2+} blocked AP potentiation of tonic currents in a concentration-dependent manner, while synaptic currents were unaffected. Application of Zn^{2+} chelator prevented the positive shift of tonic currents by Zn^{2+}, confirming the Zn^{2+} blockade of AP-sensitive tonic currents. In the mouse kindling model of epilepsy, intrahippocampal infusion of Zn^{2+} resulted in rapid epileptiform activity and prevention of the antiseizure activity of AP. Therefore, Zn^{2+} inhibition of neurosteroid-potentiated,

extrasynaptic GABA-ARs in the hippocampus has direct involvement in a variety of brain conditions, such as seizures, epileptogenesis, epilepsy, and conditions with compromised balance of excitation/inhibition. Both Zn^{2+} and neurosteroids show high-affinity for extrasynaptic δ-containing GABA-ARs, but their actions are distinctly opposite through the binding of different allosteric sites. Overall, Zn^{2+} hinders neurosteroid activation of extrasynaptic δGABA-AR-mediated tonic inhibition and their ability to promote neuroprotection and inhibit seizure activity in the brain.

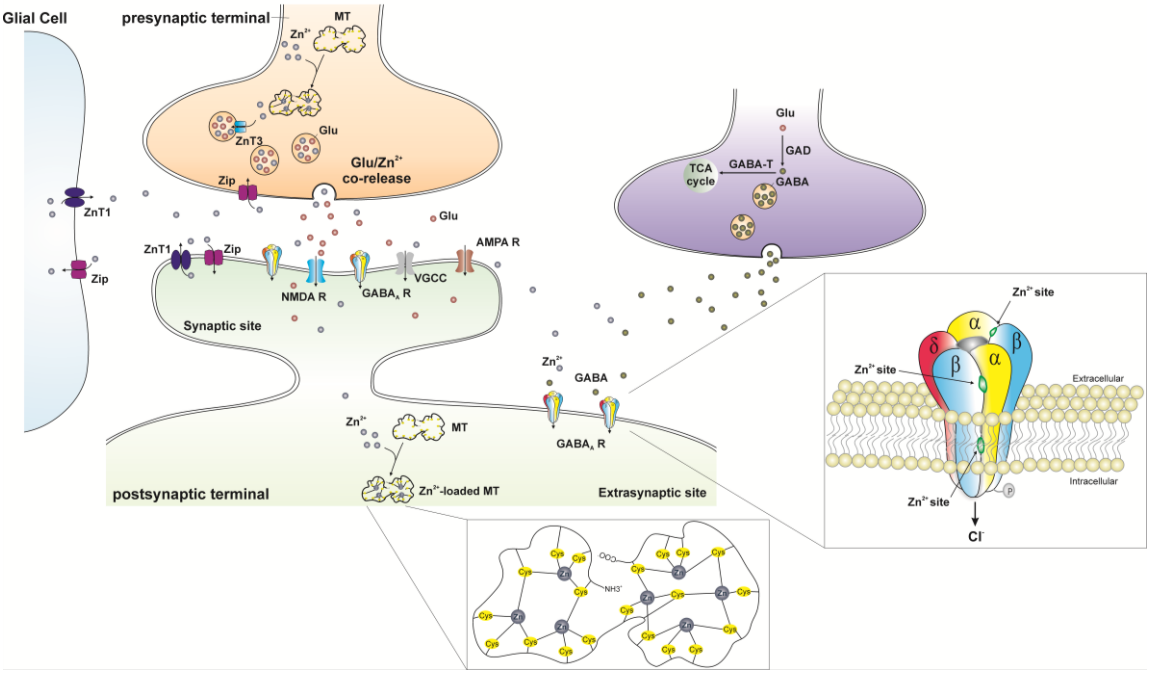

Figure 5 Trafficking of Zn^{2+} at the gluzinergic synapse.

In the gluzinergic terminal, the availability of free Zn^{2+} is regulated by metallothioneins (MTs), the primary intracellular Zn^{2+}-buffering proteins. The MT is a dumbbell-shape, cysteines (Cys)-rich protein comprised of two domains in which seven zinc atoms are tetrahedrally bound to twenty cysteines (*inset, middle*). The Zn^{2+} transporter (ZnT) and Zip proteins are also involved in the regulation of Zn^{2+} in the cytoplasm. ZnT proteins promote Zn^{2+} efflux and vesicular uptake to decrease the amount of intracellular Zn^{2+} while Zip proteins facilitate the influx of extracellular Zn^{2+} into neurons and glial cells to increase the concentration of intracellular Zn^{2+}. Free Zn^{2+} is transferred into synaptic vesicles through the ZnT3 proteins and stored with glutamate. During normal neurotransmission, Zn^{2+}- and glutamate-containing vesicles fuse with cell membrane and co-release Zn^{2+} and glutamate into the synaptic cleft. There are a variety of postsynaptic targets that Zn^{2+} can act at including NMDA receptors (NMDA Rs), AMPA receptors (AMPA Rs), voltage-gated calcium channels (VGCCs), GABA-ARs and a number of other channels, transporters and receptors. Three distinct Zn^{2+} binding sites mediate its inhibition of extrasynaptic δ-containing GABA-ARs (*inset, right*): one site at the internal surface of the channel pore and two at the external amino-terminus of the α-β interfaces.

I.7 Genetic Regulation of GABA-ARs

I.7.1 GABA Epilepsy Genetics

GABA-ARs play a pivotal role in regulating neuronal inhibition in the CNS. Dysregulation of neuronal activity and changes in the composition and function of GABA-ARs contribute to the development of epilepsy. Genetic epilepsies are genetically driven recurrent seizures caused by mutations in genes governing excitation and inhibition. Mutations in GABA-AR subunit genes have been involved in the pathophysiology of several idiopathic generalized epilepsies. Specifically, mutations in the gene encoding the α1 subunit (GABRA1) and the β3 subunit (GABRB3) are mainly associated with Childhood Absence Epilepsy (CAE) and Juvenile Myoclonic Epilepsy (JME), while mutations in the gene encoding the γ2 subunit (GABRG2) and the δ subunit (GABRD) are associated with Febrile Seizures (FS), Generalized Epilepsy with Febrile Seizures Plus (GEFS+) and Dravet Syndrome (DS) (Table 4, Figure 6).

Table 4 Summary of GABA-AR genetic epilepsies.

	Genetic location	Mutation	Sample size	Receptor dysfunction	Phenotype OMIM#
Child Absence Epilepsy (CAE)					
α1 (GABRA1)	5q34	(**975delC, S326fs328X**) A single base pair deletion and premature stop codon in TM3	Sporadic 1 of 98 German IGE patients	Reduced GABA current and surface expression (Maljevic et al., 2006)	611136
α6 (GABRA6)	5q34	(**R46W**) A missense mutation in N terminus, causing the changes of arginine to tryptophan at position 46	1 of 72 IGE, 65 GEFS+, 66 FS patients	Impaired receptor assembly/trafficking; reduced surface expression of δ subunit (Dibbens et al., 2009; Hernandez et al., 2011)	-
β3 (GABRB3)	15q12	**Haplotype 2** promoter in exon 1a	45 CAE patients	Lower transcription activity (Feucht et al., 1999; Urak et al., 2006)	612269
		(**P11S**) A heterozygous missense mutation in exon 1a in signal peptide, causing the changes of proline to serine at position 11	4 of 48 Remitting CAE patients in a Mexican family	Reduced GABA current and increased glycosylation (Tanaka et al., 2008)	
		(**S15F**) A missense mutation in signal peptide, causing the changes of serine to phenylalanine at position 15	1 of 48 Remitting CAE patients from Honduras	Reduced GABA current and increased glycosylation (Tanaka et al., 2008)	
		(**G32R** A missense mutation in exon 2 in N terminus, causing the changes of glycine to arginine at position 32)	2 of 48 Remitting CAE patients in a Honduran family	Reduced GABA current and increased glycosylation (Tanaka et al., 2008)	
γ2 (GABRG2)	5q34	(**R82Q**) A missense mutation in N terminus, causing the changes of arginine to glutamine at position 82	Autosomal dominant form in a large Australian family	Impaired receptor trafficking and reduced surface expression (Wallace et al., 2001)	607681
Juvenile Myoclonic Epilepsy (JME)					
α1 (GABRA1)	5q34	(**A332D**) A heterozygous missense mutation in TM3, causing the changes of alanine to aspartate at position 322	14 members of a French Canadian family	Reduced GABA current and surface expression (Cossette et al., 2002)	611136
δ (GABRD)	1p36.3	(**R220H**) A missense mutation in exon 6 in N terminus, causing the changes of arginine to histidine at position 220	A small GEFS+ family	Reduced surface expression and receptor mean open duration (Dibbens et al., 2004)	613060
Febrile Seizures (FS)					
γ2 (GABRG2)	5q34	(**R82Q**) A missense mutation in N terminus, causing the changes of arginine to glutamine at position 82	Autosomal dominant form in a large Australian family	Impaired receptor trafficking and reduced surface expression (Wallace et al., 2001)	611277
		(**R177G**) A missense mutation in N terminus, causing the changes of arginine to glycine at position 177	1 of 47 unrelated patients	Altered GABA current and kinetics and impaired subunit folding and/or oligomerization (Audenaert et al., 2006)	
		(**K328M**) A missense mutation in extracellular loop between the TM2 and TM3, causing the changes of lysine to methionine at position 328	A large French family	Altered GABA current and kinetics (Baulac et al., 2001)	

Table 4 Continued

	Genetic location	Mutation	Sample size	Receptor dysfunction	Phenotype OMIM#
Generalized Epilepsy with Febrile Seizures Plus (GEFS+)					
γ2 (GABRG2)	5q34	(**K328M**) A missense mutation in extracellular loop between the TM2 and TM3, causing the changes of lysine to methionine at position 328	A large French family with GEFS+	Altered GABA current and kinetics (Baulac et al., 2001)	611277
		(**Q390X**) A nonsense mutation in intracellular loop between the TM3 and TM4, causing a premature stop codon at position 390	A GEFS+ family	ER retention and abolished GABA sensitivity (Harkin et al., 2002; Kang et al., 2010)	
		(**R136X**) A nonsense mutation in N terminus, causing a premature stop codon at position 136	A two-generation family with GEFS+	Reduced receptor current amplitudes and surface expression, ER retention (Sun et al., 2008; Johnston et al., 2014)	
		(**W429X**) A nonsense mutation in intracellular loop between the TM3 and TM4, causing a premature stop codon at position 429	1 of 23 Chinese families with GEFS+	Undetermined, is predicted to translate a truncated protein (Sun et al., 2008; Johnston et al., 2014)	
δ (GABRD)	1p36.3	(**R220C**) A missense mutation in exon 6 in N terminus, causing the changes of arginine to cysteine at position 220	A small GEFS+ family	Reduced GABA current and single channel open duration (Dibbens et al., 2004)	613060
		(**E177A**) A missense mutation in N terminus, causing the changes of glutamate to alanine at position 177	A small GEFS+ family	Reduced GABA current and receptor expression and altered channel gating frequency (Dibbens et al., 2004)	
Dravet Syndrome (DS)					
γ2 (GABRG2)	5q34	(**Q40X**) A nonsense mutation in N terminus, causing a premature stop codon at position 40	Dizygotic twin girls with DS and their apparently healthy father in a Japanese family	Haploinsufficiency and abnormal intracellular trafficking (Hirose 2006; Ishii et al., 2014)	-

The positions of mutations are designated in the immature peptide including the 39 amino acid signal peptide. OMIM: Online Mendelian Inheritance in Man, a daily-updated catalog of human genes and genetic disorders.

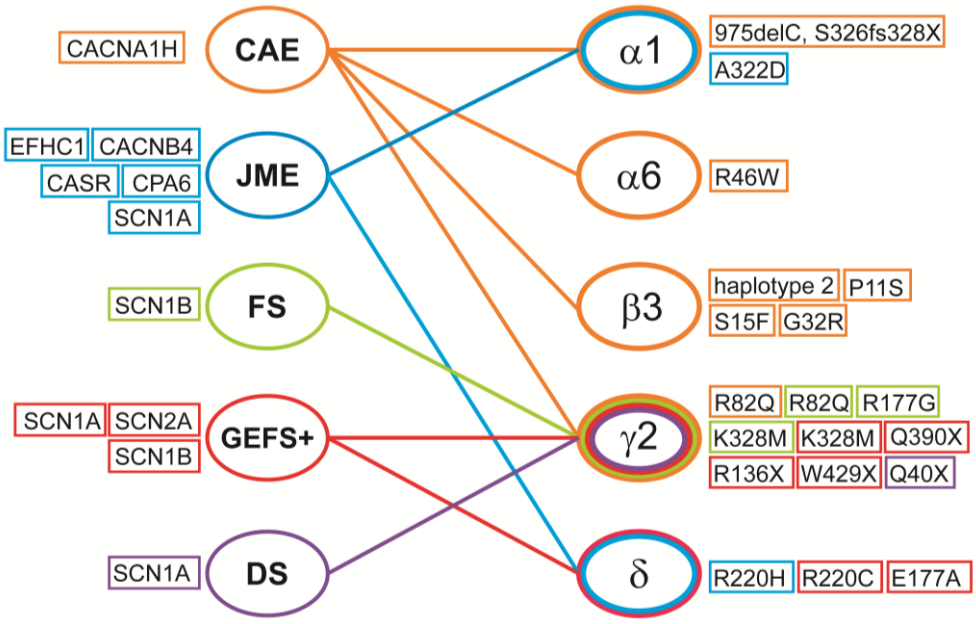

Figure 6 Summary outline of the association of genetic epilepsies with GABA-AR subunits and other genetic factors.

Right: GABA-AR subunits that are involved in genetic epilepsies. Mutations in each subunit are listed. Left: other genetic factors that are associated with genetic epilepsies. CACNA1H (Cav3.2): a voltage-dependent T-type calcium channel alpha1H subunit gene; CACNB4: a voltage-dependent L-type calcium channel beta4 subunit gene; EFHC1: a gene that encodes a protein with an EF-hand domains; CPA6: a gene that encodes carboxypeptidase A6; CASR: a gene that encodes calcium sensor receptor; SCN1A: a sodium voltage-gated channel alpha1A subunit gene; SCN1B: a sodium voltage-gated channel alpha1B subunit gene; SCN2A: a sodium voltage-gated channel alpha2A subunit gene; SCN2B: a sodium voltage-gated channel alpha2B subunit gene. CAE, Childhood Absence Epilepsy; JME, Juvenile Myoclonic Epilepsy; FS, Febrile Seizures; GEFS+, Generalized Epilepsy with Febrile Seizures Plus; DS, Dravet Syndrome.

I.7.2 Mutations of α1 Subunit

A heterozygous missense mutation (A322D) in the TM3 of GABRA1 was identified in an autosomal dominant form of JME in a French Canadian family. This mutation arises by the replacement of the alanine amino acid residue by a larger negatively charged aspartate in the helix of TM3 of the α1 subunit. In *in vitro* studies, HEK 293 cells expressing this mutant GABA-AR ($\alpha1_{A322D}\beta2\gamma2$) exhibited reduced GABA-evoked currents, GABA sensitivity, and α1 subunit protein expression, along with altered current kinetics and accelerated receptor endocytosis and endoplasmic reticulum (ER)-associated degradation via the ubiquitin–proteasome system (Cossette et al., 2002; Gallagher et al., 2004; Krampfl et al., 2005; Gallagher et al., 2007; Bradley et al., 2008; Ding et al., 2010). One study indicated that this mutant GABA-AR ($\alpha1_{A322D}\beta2\gamma2$) causes a dominant negative effect on the composition and surface expression of wildtype (WT) GABA-ARs (Ding et al., 2010). Therefore, the A322D mutation in human GABRA1 results in a loss-of-function of the receptor via several mechanisms including the alteration of receptor functions, a reduction in receptor surface expression, and decreased receptor lifetime on the cell membrane.

A single base pair deletion (975delC) in GABRA1 was found in a patient with sporadic CAE among 98 unrelated idiopathic generalized epilepsy patients. This de novo mutation causes a frameshift and a premature stop codon (S326fs328X), leading to a truncation in the TM3 and ER-associated degradation. In addition, GABA-evoked currents were not detected in the HEK293 cells with mutant α1-containing GABA-ARs. These mutant receptors were not able to be incorporated into the membrane surface, highlighting the involvement of the α1 subunit in inserting the receptors into the cell membrane and overall functional integrity of GABA-AR (Maljevic et al., 2006). However, no dominant negative effects on the WT receptors were observed in these mutant receptors. These findings reveal that a single base pair deletion in GABRA1 causes a loss-of-function and haploinsufficiency of the GABA-ARs.

Two other mutations in GABRA1 associated with impaired membrane delivery of the mature GABA-AR were also identified in a cohort of French Canadian families with idiopathic generalized epilepsy. A 25-bp insertion associated with intron results in the deletion of the TM4 and a premature stop codon (K353delins18X), and a missense mutation that replaces the aspartate 219 residue with an asparagine (D219N). The family with K353delins18X mutation displays afebrile, generalized tonic–clonic seizures, while the family with the D219N mutation in GABRA1 shows mainly febrile seizures and absence seizures (Lachance-Touchette et al., 2011). In addition, 4 novel de novo mutations in GABRA1 were also found in *SCN1A*-negative patients with DS, providing insight into more genetic causes for this syndrome (Carvill et al., 2014). Recently, several novel mutations in the extracellular N-terminus of TM1 or TM2 of GABRA1 have been implicated in several epileptic diseases including infantile epilepsy, West syndrome, Ohtahara syndrome, and early onset epileptic encephalopathy (Johannesen et al., 2016; Kodera et al., 2016). Mutations in GABRA1 of GABA-ARs contribute to the genetic etiology of both mild generalized epilepsies and severe epilepsy syndromes.

I.7.3 Mutations of β3 Subunit

The association of GABRB3 with idiopathic generalized epilepsies was first reported in 1999 (Feucht et al., 1999). *Urak et al.* performed a mutation screening of GABRB3 of 45 CAE patients and found 13 single nucleotide polymorphisms and 4 haplotypes in the haplotype 2 region of the GABRB3 promoter. Lowered transcriptional activity of this region is highly associated with CAE (Feucht et al., 1999; Urak et al., 2006). Thus, diminished expression of the GABRB3 gene could be a possible cause for the development of CAE.

Missense mutations (P11S, S15F, and G32R) in GABRB3 were found in families with remitting CAE (Tanaka et al., 2008). P11S and S15F are heterozygous mutations in the exon 1a that encodes the signal peptide of the GABRB3. The P11S mutation was found in four affected subjects of a two-generation Mexican family and the S15F was found in

one family from Honduras. G32R is a heterozygous mutation in the exon 2 of GABRB3 found in four affected persons of a two-generation Honduran family. Further investigation revealed that G32R mutation causes a partial shift of αβ3γ2L receptors to αβ3 and β3 receptors and a reduction in macroscopic current density (Gurba et al., 2012). HEK293T cells expressing GABA-ARs with these mutations have reduced GABA-AR current density attributed to hyperglycosylation in the in vitro translation and translocation system. Results suggest that elevated glycosylation in the mutant exon 1a and exon 2 may contribute to CAE by interfering with the maturation and trafficking of GABA-ARs and affecting receptor function. Mutation screening performed in 183 French-Canadian individuals with idiopathic generalized epilepsy including 88 with CAE also found nine single nucleotide polymorphisms and the P11S missense mutation in GABRB3 (Lachance-Touchette et al., 2010). However, another study demonstrated that no mutations in the exon 1a promoter of GABRB3 were found in 780 German patients with idiopathic generalized epilepsy, including 250 with CAE (Hempelmann et al., 2007). Therefore, the association of GABRB3 with CAE is still under debate.

I.7.4 Mutations of γ2 Subunit

The γ-containing GABA-ARs are the main mediators of fast inhibitory transmission through phasic current inhibition in the synaptic sites (Sieghart and Sperk, 2002; Farrant and Nusser, 2005; Olsen and Sieghart, 2009). The γ subunit is required for the formation of the binding site for BZs. In addition, it is also important for the clustering of the GABA-AR subtypes in the postsynaptic sites (Essrich et al., 1998; Fang et al., 2006). Mutations in the gene encoding γ subunit of GABA-ARs (GABRG) have been associated with the pathogenesis of epilepsy; mostly FS and GEFS+. The first evidence linking GABA-AR subunit genes with epilepsy was reported in 2001. GABRG2 was the first identified GABA-AR subunit gene that is involved in idiopathic generalized epilepsy (Baulac et al., 2001). More evidence was subsequently discovered supporting the association between genetic epilepsies and GABA-AR subunit genes. A missense mutation in GABRG2 found in a large French family with GEFS+ phenotype is caused

by a substitution of a positively charged lysine residue for a neutral methionine (K328M) in the extracellular loop between the TM2 and TM3 transmembrane domains of GABRG2. The recombinant receptors with this mutant $\gamma2_{K328M}$ subunit expressed in *X. Laevis* oocytes have significantly lower amplitudes of GABA-evoked currents, indicating impaired receptor function (Baulac et al., 2001). Receptors with $\gamma2_{K328M}$ subunit expressed in cultured rat hippocampal neurons displayed accelerated decay time constant of mIPSCs. In addition, mutant $\gamma2_{K328M}$ receptors had decreased frequency of mIPSCs and enhanced membrane diffusion of receptors after 1-hour exposure of elevated temperatures, which was not observed in WT receptors, suggesting reduced number of functional inhibitory synapses and compromised GABAergic transmission (Bouthour et al., 2012). These could be a novel mechanism involved in the pathology of FS.

Two nonsense mutations (R136X and W429X) in GABRG2 were identified in a two-generation family with GEFS+, and one of twenty-three Chinese families with GEFS+, respectively (Sun et al., 2008; Johnston et al., 2014). The R136X mutation in the GABRG2 reduces receptor current amplitudes and surface expression with greater intracellular retention when $\gamma2_{R136X}$ subunits were heterologously expressed in HEK293T cells with the α1 and β2 subunits since the mutant $\gamma2_{R136X}$ subunit did not allow the assembly of functional receptors. No dominant negative suppression effects from the mutant $\gamma2_{R136}$ subunits on the WT receptors were noticed. The W429X is located in the extracellular loop between the TM3 and TM4 transmembrane domains of GABRG2. It generates a premature translation termination codon and is predicted to translate a truncated protein.

A novel frameshift mutation in the γ2 subunit gene (GABRG2) was also identified in a family with GEFS+ (Tian et al., 2013). A cytosine nucleotide deletion in the last exon of GABRG2 results in a $\gamma2S_{S443delC}$ subunit with a modified and elongated carboxy-terminus. $\gamma2_{S443delC}$ subunits, which are larger than WT γ2 subunits when translated, displayed higher retention in ER and lower membrane expression. Electrophysiological characterization revealed significantly decreased peak GABA-evoked currents in

HEK293T cells, showing GABRG2 haploinsufficiency.

Q390X, a nonsense mutation in the intracellular loop between the TM3 and TM4 transmembrane domains of the GABRG2 was found in GEFS+, FS, and DS patients. This mutation introduces a premature stop codon at Q390 in the immature protein. *X. Laevis* oocytes expressing recombinant receptors with mutant $\gamma2_{Q390X}$ subunit showed diminished response to GABA and retention in the intracellular compartment, which are also found in HEK293T cells expressing receptors with mutant $\gamma2_{R136X}$ subunit (Harkin et al., 2002). Mutant $\gamma2_{R136X}$ subunits accumulated and formed high-molecular-mass aggregation rapidly and showed longer half-life and slower degradation compare to WT subunits in several cell lines including HEK293T, COS-7, and Hela cells, and cultured rat cortical neurons (Kang et al., 2010). The accumulation and aggregation of misfolded or truncated proteins are commonly observed in neurodegenerative diseases. However, Kang et al. showed that the aggregates are also associated with genetic epilepsies. The *Gabrg2*$^{+/Q390X}$ knock-in mouse, developed as an animal model for severe human genetic epileptic encephalopathy, displayed spontaneous generalized tonic-clonic seizures and reduced viability. In addition, impaired inhibitory neurotransmission including reduced amplitude and frequency of GABAergic mIPSCs and accumulation of mutant $\gamma2_{Q390X}$ subunits were also found in this mouse. The aggregation of mutant $\gamma2_{Q390X}$ subunits initiated caspase 3 activation and cell death in the mouse cerebral cortex (Kang et al., 2015). Their results revealed that genetic epilepsies and neurodegenerative diseases may share relevant pathological pathways and therapies.

A missense mutation (R82Q) in the GABRG2 was found in an Australian family and results in an autosomal dominant inherited form of CAE and FS (Hancili et al., 2014; Wallace et al., 2001). Arginine 82, located in the high-affinity BZ-binding region, abolishes diazepam-potentiated currents in recombinant receptors expressed in X. Laevis oocytes, but does not affect Zn^{2+} sensitivity. Receptors with the mutant $\gamma2$ subunit ($\alpha3\beta3\gamma2_{R82Q}$) expressed in COS-7 cells display impaired receptor trafficking, and reduced membrane expression due to impaired assembly into pentamers. Furthermore, ER

retention and degradation causes abnormal receptor function when $\alpha1\beta2\gamma2_{R82Q}$ receptors were expressed in HEK293T cells (Wallace., et al., 2001; Kang and Macdonald, 2004; Frugier et al., 2007; Huang et al., 2014). $\gamma2_{R82Q}$ receptors expressed in cultured rat hippocampal neurons and COS-7 cells show increased clathrin-mediated dynamin-dependent endocytosis, hindering their detection on the cell membrane (Chaumont et al., 2013). Animal studies revealed $\gamma2S_{R82Q}$ mice displayed enhanced cortical spontaneous single-cell activity, membrane potential shift, and variance of stimulus evoked cortical responses after pentylenetetrazol (PTZ) injection, supporting the focus on the cortical region in the pathology of absence epilepsy (Tan et al., 2007; Witsch et al., 2015). A splice-site mutation in intron 6 of the GABRG2 was also found in patients with idiopathic absence epilepsies, CAE, and FS. This mutation is predicted to translate a nonfunctinal protein and may be involved in the pathophysiology of CAE and FS (Kananura et al., 2002).

A missense mutation (R177G) in the GABRG2 was reported in patients with FS, GEFS+, and CAE (Audenaert et al., 2006). The mutation, located in the BZ allosteric site, substitutes a highly conserved arginine with glycine at position 177 in the immature peptide. Receptors with mutant $\gamma2L_{R177G}$ subunit expressed in HEK293T cells conferred faster current desensitization and decreased sensitivity to diazepam. The disruption of the BZ-binding site could be the reason for the diminished response to BZ drugs and abnormal receptor function and may contribute to the disinhibition of the brain. $\gamma2L_{R177G}$ has been demonstrated to have decreased GABA sensitivity and surface expression due to the retention of receptors in the ER. $\gamma2L_{R177G}$ subunits also showed impaired subunit folding and/or oligomerization and could interrupt intra-subunit salt bridges, and thereby, have destabilized secondary and tertiary structure (Todd et al., 2014).

A missense mutation (P83S) in the GABRG2 was found in patients with idiopathic generalized epilepsies in a French Canadian family (Lachance-Touchette et al., 2011). The mutation, which showed high degree of penetrance, is caused by the change of the proline 83 residue of the immature protein to a serine in a region which affects BZ

binding on the extracellular ligand-binding domain. Unlike other missense mutations found in the GABRG2 gene, functional analysis of the receptors revealed that $\gamma2_{P83S}$ expressed in HEK293 cells does not alter the surface expression or the receptor sensitivity to Zn^{2+} or BZ when co-expressed with α1 and β2 subunits. Further experiments are needed to elucidate whether an appreciable phenotype can be observed in the receptors with this mutant when assembling with other subunits.

A nonsense mutation (Q40X) in the GABRG2 was found in dizygotic twin girls with DS and their phenotypically healthy father in a Japanese family (Ishii et al., 2014). The mutation causes premature termination codons at position 40 of the GABRG2 molecule. The inward currents and current density of receptors with homozygous $\gamma2_{Q40X}$ mutation expressed in HEK293T cells in response to GABA were intermediate between WT and heterozygous $\alpha1\beta2\gamma2_{Q40X}$ GABA-ARs, showing the haploinsufficiency effects of mutant $\gamma2_{Q40X}$. In addition, cells expressing this mutant subunit have abnormal intracellular trafficking and impaired axonal transport of α1 and β2 subunits.

I.7.5 Mutations of δ Subunit

The δ-containing GABA-ARs primarily control the baseline neuronal network excitability through shunting and tonic inhibition. Mutations in the gene encoding δ subunit of GABA-ARs (GABRD) are thought to be involved in the pathology of epilepsy (Dibbens et al., 2004; Feng et al., 2006). To date, three point mutations (E177A, R220C, and R220H) of GABRD have been described in patients with idiopathic generalized epilepsies (a cohort study with 72 unrelated IGE, 65 unrelated GEFS+ and 66 unrelated FS). Two missense mutations, E177A and R220C, located in the extracellular N-terminus of the δ subunit were identified in a small GEFS+ family (Dibbens et al., 2004). E177 is located immediately adjacent to one of the two cysteines that form a disulfide bond, the signature feature of the cys-loop family of ligand-gated ion channels, and the R220 is positioned between the cys-loop and the first transmembrane domain. In HEK293T cells, recombinant $\alpha1\beta2S\delta$ GABA-ARs expressing E177A and R220H mutations displayed

decreased GABA sensitivity and increased neuronal excitability. Further investigation revealed that human recombinant α4β2δ GABA-ARs with E177A and R220H variants have significantly reduced receptor surface expression and altered channel gating frequency, resulting in impaired inhibitory neurotransmission. In addition, mutations in the main cytoplasmic loop of the δ subunit result in interrupted receptor trafficking and decreased surface expression in recombinant HEK 293 cells (Bracamontes et al., 2014). Since δ-containing GABA-ARs localize exclusively to extrasynaptic membranes and control tonic inhibition by continuously regulating the basal tone of inhibition when activated by GABA, alteration of features such as gating frequency or GABA sensitivity caused by mutations in δ subunit genes may contribute to the idiopathic generalized epilepsies.

I.7.6 Other GABA Receptor Subunit Mutations

A mutation in GABRA6 (R46W) was found in a patient with CAE (Dibbens et al., 2009; Hernandez et al., 2011). This mutation, caused by the substitution of arginine to tryptophan at position 46, is located in the N-terminal extracellular domain of the α6 subunit. Notably, R46 is a highly conserved residue identified from humans to *D. melanogaster* and *C. elegans*. R46W impaired receptor assembly/trafficking and gating in both $\alpha6_{R46W}\beta2\gamma2L$ and $\alpha6_{R46W}\beta2\delta$ recombinant receptors expressed in *X. Laevis* oocytes. Surface expression of δ subunits was also decreased in R46W, showing a similar trend with a study reported early that a dramatic decrease of cerebellar δ subunit protein in α6 knockout mice (Jones et al., 1997). These results suggest that mutations in GABRA6 could lead to disinhibition and elevated susceptibility to genetic epilepsies due to compromised receptor function and membrane expression.

In the past decades, no genetic studies demonstrated that mutations in GABRB2 are associated with genetic epilepsies. Until recently, Srivastava and colleagues reported a case study in which a de novo heterozygous missense mutation of GABRB2 was found in a girl with intellectual disability and epilepsy (Srivastava et al., 2014). Their finding

suggests the need for further investigation into the role of GABRB2 in the pathology of epilepsy and other neurological disorders.

I.8 Insights from Transgenic Models on Tonic Inhibition

In order to elucidate the distinctive pharmacological and functional properties and the role of the δ subunit in brain disorders, a strain of mice globally lacking the δ subunit (δKO) of GABA-ARs was introduced in 1999 (Mihalek et al., 1999). Initial pharmacological and behavioral characterizations revealed the δKO mice have significantly lower binding affinity for muscimol, a GABA binding agonist with high affinity to δ-containing GABA-ARs, and faster decay of mIPSCs and inhibitory postsynaptic potentials than that of WTs. In addition, δKO mice show significantly decreased sleep time in response to alphaxolone, a neurosteroid and general anesthetic, diminished sensitivity to anxiolytic drugs examined by elevated plus-maze assay, diminished GX facilitated exacerbation of PTZ-induced absence seizure, and higher vulnerability to the chemoconvulsants seizures caused by GABA-AR antagonists. Their results suggest that deficiency of the δ subunit of the GABA-ARs leads to a significant attenuation in the sensitivity to behavioral actions of neurosteroids, which may contribute to a higher degree of seizure susceptibility (Mihalek et al., 1999; Spigelman et al., 2002; Porcello et al., 2003; Spigelman et al., 2003; Chandra et al., 2010).

The δ-specific selectivity for neurosteroid modulation is further confirmed by electrophysiological studies demonstrating suppressed responses to THDOC modulation such as decreased spontaneous IPSCs in cerebellar granule cells and decreased tonic conductance in DGGCs in the δKO mouse model (Vicini et al., 2002; Wohlfarth et al., 2002; Stell et al., 2003). In addition, attenuated response to AP potentiation of GABAergic and tonic currents is also evident in mice bearing a targeted deletion of the δ subunit, underscoring the role of δ-containing GABA-ARs for neurosteroid activity (Carver et al., 2014; Carver and Reddy, 2016). Reduced response to gaboxadol-induced hypnotic activity is also reported in δ-deficient mice, suggesting the requirement of δ-

containing GABA-ARs in the action of gaboxadol, a preferential agonist of δ-containing GABA-ARs at low concentrations (Boehm et al., 2006; Meera et al., 2011).

In the composition of the receptor subunits, deletion of the δ subunit accompanied the decreased expression of the α4 subunit and the increased expression of the γ2 subunit in brain regions that normally contained the δ subunit such as hippocampus and thalamus (Korpi et al., 2002; Peng et al., 2002). The results from electrophysiology, animal knockout models, and immunohistochemistry specific to DGGCs indicate that α4β2δ GABA-ARs are the major receptors located in extrasynaptic sites and responsible for tonic current inhibition in DGGCs (Sun et al., 2004; Chandra et al., 2006; Herd et al., 2008). The α5 subunit contributes to the remaining tonic currents in DGGCs (Glykys et al., 2008; Carver and Reddy, 2013). The δ-containing GABA-ARs are highly sensitive to Zn^{2+} and the Zn^{2+}-reduced decay time and amplitude of evoked IPSCs in DGGCs from WT is lacking in δKO mice. Recently, we have uncovered that Zn^{2+} showed a concentration-dependent blockade of AP-potentiated tonic currents in DGGCs. Moreover, Zn^{2+} inhibition of AP-sensitive tonic currents is absent in δKO mice (Wei et al., 2003; Carver et al., 2016). Animal studies further revealed that Zn^{2+} prevents the antiseizure activity of AP in epileptic mice, suggesting that Zn^{2+} blockade of neurosteroid-sensitive, extrasynaptic δ-containing GABA-ARs in the hippocampus possesses implications in a variety of neuronal hyperexcitability disorders like SE and epilepsy.

I.9 Therapeutic Insights of Tonic Inhibition in Epilepsy

Extrasynaptic GABA-ARs are involved in the pathophysiology of certain brain conditions, such as catamenial epilepsy, SE, and other neuroendocrine disorders (Belelli and Lambert 2005; Brickley and Mody, 2012; Reddy, 2013ab; 2016a). Consequently, these receptors are emerging as novel targets for excitability disorders (Reddy and Estes, 2016). Substantial evidence suggests that neurosteroid-sensitive, extrasynaptic GABA-ARs play a critical role in the pathophysiology of catamenial epilepsy, a menstrual cycle-related seizure clustering in women with epilepsy (Reddy, 2009a; 2014; 2016ab; Reddy

and Rogawski, 2001; 2012; Reddy et al., 2001; 2012; Wu et al., 2013). Although this condition has been documented for millennia, there is currently no effective treatment for catamenial seizures, leaving many women and their families desperate for answers. Recently, a catamenial-like seizure exacerbation has been clearly demonstrated in mice with targeted ablation of extrasynaptic δGABA-ARs in the brain (Clossen and Reddy, 2017). This has substantially bolstered the role of tonic inhibition in catamenial epilepsy (Reddy, 2016a). In essence, extrasynaptic δGABA-ARs are strikingly upregulated during perimenstrual-like neuroendocrine milieu (Gangisetty and Reddy, 2010; Carver et al., 2014). Consequently, there is greater antiseizure efficacy of neurosteroids in catamenial models because δGABA-ARs confer enhanced neurosteroid sensitivity and greater seizure protection. Therefore, this molecular mechanism of tonic inhibition as the major regulator of the catamenial seizures is providing a strong platform for "neurosteroid replacement therapy," a pulse therapy with low doses of synthetic neurosteroid agents that may effectively control catamenial seizures without hormonal side effects (Reddy and Rogawski, 2009).

Neurosteroid levels are reduced during SE, a neurological emergency characterized by continuous seizure activity or multiple seizures without regaining consciousness for more than 30 minutes (Meletti et al., 2017). BZs such as lorazepam and MDZ are the primary anticonvulsants for SE, but some patients do not respond to these treatments, a condition referred as refractory SE (Reddy and Reddy, 2015). BZs target synaptic GABA-ARs, but have little effect on extrasynaptic isoforms which are responsible for tonic inhibition (Reddy et al., 2015). There are many theories but functional inactivation of synaptic GABA-ARs via active internalization appears a lead physiological mechanism by which BZ resistance emerges in SE (Naylor et al., 2005; Reddy and Reddy, 2015). Therefore, neurosteroid agents such as AP and its synthetic analogs, which potentiate both phasic and tonic current, have been proposed as better anticonvulsants for SE (Briyal and Reddy, 2008; Reddy, 2009b; Rogawski et al., 2013). Clinical evaluation of AP is in progress to test this therapeutic premise (Rosenthal et al., 2017; Vaitkevicius et al., 2017).

Synthetic neurosteroids are proposed as novel anticonvulsant antidotes for chemical intoxication caused by organophosphate (OP) pesticides and nerve agents like sarin and soman (Reddy, 2016c). BZs, such as diazepam, are the current anticonvulsants of choice for controlling nerve agent–induced seizures, SE, and brain injury. BZs can control acute seizures when given early, but they are ineffective for delayed treatment of SE after nerve agent exposure (Reddy and Reddy, 2015). Neurosteroid-sensitive extrasynaptic GABA-ARs are minimally impacted by OP intoxication. Thus, anticonvulsant neurosteroids may produce more effective protection than BZs against a broad spectrum of chemical agents, even when given late after nerve agent exposure, because neurosteroids can activate both synaptic and extrasynaptic GABA-ARs and thereby can produce maximal inhibition (Carver and Reddy, 2016). An intramuscular GX product is being developed as anticonvulsant antidote for nerve agents (patent #WO2016036724A1). A neurosteroid therapy with a synthetic neurosteroid such as GX has been found to more protective than MDZ for controlling persistent SE and neuronal damage caused by OP pesticides and nerve agents (Reddy, 2016c). Although neurosteroids show great promise in the treatment of SE, none are currently approved by the FDA for clinical use.

Some endogenous neurosteroids, such as dehydroepiandrosterone sulfate (DHEAS), are negative modulators of GABA-ARs and can cause proconvulsant actions (Majewska et al., 1990; Reddy and Kulkarni, 1998). It is likely that such actions have clinical implications in certain physiological and pathological conditions (Galimberti et al., 2005; Reddy, 2006; 2009; Pack et al., 2011). It is hypothesized that the increase in the frequency of onset of seizures during the process of adrenarche, which is associated with a massive increase in DHEAS production, is caused by DHEAS's ability to block GABA-ARs. However, it remains unclear if DHEAS can negatively modulate extrasynaptic GABA-ARs in the brain. In addition, there are developmental changes in hippocampal extrasynaptic GABA-ARs during puberty with significant impact on cognitive function (Shen et al., 2010; Reddy, 2014).

CHAPTER II

AIMS AND OBJECTIVES[†‡]

The main objective of this dissertation is to investigate the molecular, cell-specific, and phosphorylation-dependent mechanisms of action of the synthetic neurosteroid GX and related neurosteroid agents at extrasynaptic δGABA-ARs. We use a combination of pharmacological, electrophysiological, and behavioral approaches to address the proposed questions. In addition, structure-activity relationships of synthetic analogs are tested in native neurons. This study also aims to examine the influence of protein kinase activity on the neurosteroid mechanism of action in native neurons. We also explore the physiological interaction between neurosteroids and Zn^{2+} at extrasynaptic δGABA-ARs as well as the combination potential of GX with other AEDs for epilepsy.

II.1 Specific Aim 1

The first specific aim investigates the mechanisms of action and structure-activity relationships of GX and related neurosteroid analogs on extrasynaptic δGABA-AR-mediated tonic inhibition and seizure protection.

The GABA-ARs regulate fast inhibitory transmission in the brain. These chloride channels are composed of a pentamer of subunits, of which there are 19 subtypes (α1-6, β1-3, γ1-3, δ, ε, θ, π, ρ1-3). There are two classes of GABA-ARs in the hippocampus, categorized based on their localization (Chuang and Reddy, 2018a). Synaptic receptors (γ-containing) are responsible for phasic inhibition via synaptic neurotransmission,

---

[†] Reprinted (adapted) with permission from "3β-methyl-neurosteroid analogs are preferential positive allosteric modulators and direct activators of extrasynaptic δ-subunit γ-aminobutyric acid type A receptors in the hippocampus dentate gyrus subfield." by S-H Chuang and DS Reddy, 2018. T*he journal of pharmacology and experimental therapeutics*, 365(3): 583–601, Copyright © 2018 by The American Society for Pharmacology and Experimental Therapeutics. All rights reserved.

[‡] Reprinted (adapted) with permission from "Zinc reduces antiseizure activity of neurosteroids by selective blockade of extrasynaptic GABA-A receptor-mediated tonic inhibition in the hippocampus" by S-H Chuang and DS Reddy, 2019. *Neuropharmacology*, 148: 244–256, Copyright © 2018 Elsevier Ltd. All rights reserved.

whereas extrasynaptic receptors (α4/δ-containing in dentate gyrus, α5/γ2-containing in CA1) mediate tonic inhibition through high affinity and low-efficacy binding of ambient GABA. Endogenous neurosteroids are potent allosteric agonists of GABA-ARs. AP is an endogenous neurosteroid with potent antiseizure effects mediated by GABA-ARs (Reddy et al., 2014; Clossen and Reddy, 2017a). Neurosteroids have a greater sensitivity for δGABA-ARs, which are highly expressed in the dentate gyrus (Brown et al., 2002; Bianchi and Macdonald, 2003; Carver and Reddy, 2013). Natural neurosteroids have several limitations for therapeutic use, including low bioavailability, ultra-short t1/2, and hormonal side effects due to steroid metabolites (Rupprecht et al., 1993). Therefore, synthetic analogs have been prepared to surpass these limitations (Reddy and Estes, 2016). GX is the 3β-methylated analog of AP, first characterized in 1997 with recombinant α1β1γ2L receptors expressed in *Xenopus* oocytes (Carter et al., 1997). GX was shown to have comparable modulatory activity to that of AP. The synthetic 3β-substitution provides a more favorable pharmacokinetic profile as an AED, overcoming the limitations of lower bioavailability and short t1/2 by preventing the oxidation of the 3α-hydroxyl group (Carter et al., 1997). GX has broad-spectrum anticonvulsant activity in animal seizure models, and is currently being evaluated in clinical trials for the treatment of epilepsy including partial-onset seizures, infantile spasms, catamenial epilepsy, genetic seizure conditions, and chemical neurotoxicity (Kerrigan et al., 2000; Laxer et al., 2000; Nohria and Giller, 2007; Pieribone et al., 2007; Reddy and Rogawski, 2012; Bialer et al., 2015; Braat et al., 2015; Reddy, 2016a; Clossen and Reddy, 2017b; Sperling et al., 2017; Younus and Reddy, 2018). Surprisingly, there is limited literature investigating the mechanism of action of GX in the brain.

Phosphorylation status of GABA-ARs influences surface expression, chloride conductance, and sensitivity to neurosteroids. Several GABA-AR subunits contain residues that can be phosphorylated by protein kinases (Moss and Smart, 1996; Brandon et al., 2000; Chuang and Reddy, 2018a). Conserved serine residues (Ser-409 or Ser-410) of the β subunits are phosphorylated by PKC, PKA, CaMKII, and cGMP-dependent

protein kinase. Two additional serine residues of the β subunits (Ser-408 and Ser-383) are phosphorylated by PKA and CaMKII, respectively (McDonald et al., 1998; Saliba et al., 2012). Additionally, the serine residues (Ser-443) within the intracellular domain of the α4 subunit, and the Ser-408 and Ser-409 in β3 subunits are phosphorylated by PKC (Leidenheimer and Chapell, 1997; Fancsik et al., 2000; Harney et al., 2003; Abramian et al., 2010; Abramian et al., 2014; Adams et al., 2015). However, the extent of functional impact of PKC activity on the neurosteroid potentiation of extrasynaptic GABA-AR-mediated tonic inhibition remains unclear.

In this aim, we investigate the molecular mechanisms of GX modulation of synaptic and extrasynaptic GABA-ARs in a cell-specific and phosphorylation-dependent pathway as well as the structure-activity relationships of GX and related neurosteroid analogs on extrasynaptic δGABA-AR-mediated tonic inhibition and seizure protection.

II.2 Specific Aim 2

The second specific aim investigates the influence of Zn^{2+} on neurosteroid activation of extrasynaptic δGABA-AR-mediated tonic inhibition and seizure protection.

The hippocampus is a key region associated with the pathophysiology of epilepsy (Jutila et al., 2002). There are two distinct categories of GABA-ARs in the hippocampus. Synaptic receptors and extrasynaptic receptors exhibit different characteristics in their affinity and efficacy to GABA, desensitization rate, and drug sensitivity (Bianchi and Macdonald, 2002; 2003; Brown et al., 2002; Wohlfarth et al., 2002; Mortensen et al., 2011). Synaptic receptors, mainly γ-containing receptors, produce rapid and transient phasic currents in response to presynaptic release of GABA (~1 mM), whereas extrasynaptic receptors, mostly δ-containing receptors in dentate gyrus and α5β3γ2 receptors in CA1, generate persistent, non-desensitizing tonic currents by ambient GABA (~0.3 – 2 μM) (Mody et al., 1994; Brickley et al., 1996; Farrant and Nusser, 2005). Tonic currents contribute to the overall basal tone and shunting inhibition via continuous

channel conductance in neurons expressing δ-containing receptors. Hippocampus dentate gyrus granule cells (DGGCs), which express high density of δ subunit-containing extrasynaptic receptors, promote tonic inhibition and thereby regulate network excitability (Coulter and Carlson, 2007; Glykys et al., 2008). GABA-ARs are modulated by many compounds including BZs, neurosteroids, and Zn^{2+}.

Zn^{2+} is the second most abundant trace metal in many cells and neurons in the brain. It regulates cellular functions such as gene expression, epigenetic enzymatic activity, protein structural stability, and neuronal plasticity. Zn^{2+} is particularly abundant in the cortex and limbic system, including hippocampus and amygdala (Frederickson, 1989; Frederickson et al., 2000; 2005; Gower-Winter and Levenson, 2012; Szewczyk, 2013). Zn^{2+} homeostasis in the brain is tightly controlled and primarily regulated by Zn^{2+} transporters and binding proteins. High level of "chelatable" Zn^{2+} is sequestered in the synaptic vesicles of glutamatergic neurons through Zn^{2+} transporter protein ZnT3. Other transporters like ZIP proteins promote the efflux of vesicular Zn^{2+} and increase the concentration of cytoplasmic Zn^{2+} (Cole et al., 1999; Kambe et al., 2004; Lee et al., 2011). Zn^{2+} is synaptically co-released with glutamate from presynaptic vesicles of the hippocampal mossy fibers, the axons of DGGCs (Frederickson et al., 1983; Assaf and Chung, 1984; Molnar and Nadler, 2001; Paoletti et al., 2009). Zn^{2+} has been shown to modulate both excitatory and inhibitory transmission (Westbrook and Mayer, 1987; Harrison and Gibbons, 1994; Vogt et al., 2000). Zn^{2+} inhibits GABA-ARs and has distinct sensitivities at different receptor subtypes partly due to the accessibility of Zn^{2+} binding sites (Smart et al., 1991; Barberis et al., 2000; Ruiz et al., 2004). The δ-containing extrasynaptic receptors exhibit greater sensitivity to Zn^{2+} blockade than γ-containing synaptic receptors (Hosie et al., 2003). Alterations in Zn^{2+} homeostasis have implications in several neurological disorders (Frederickson et al., 2005; Bitanihirwe and Cunningham, 2009; Qian et al., 2011; Szewczyk, 2013; Prakash et al., 2015). Aberrant Zn^{2+}-rich mossy fiber sprouting is a classical feature in limbic epileptogenesis (Cavazos et al., 1991). Excessive release of Zn^{2+} drastically alters the excitability of hippocampal

circuits and plays an important role in the pathophysiology of epilepsy (Takeda et al., 1999; Coulter, 2000; Foresti et al., 2008; Elsas et al., 2009).

AP and related neurosteroids are endogenous modulators of neuronal excitability and seizure susceptibility (Chuang and Reddy, 2018ab; Younus and Reddy, 2018). Neurosteroids modulate GABA-ARs primarily via allosteric potentiation of GABA at nanomolar concentrations and through direct activation of the channel at micromolar concentrations (Hosie et al., 2007). AP has powerful antiseizure activity (Kokate et al., 1996; Kaminski et al., 2003; Kaminski et al., 2004; Carver et al., 2016; Reddy and Estes, 2016). GX, a synthetic analog of AP, is designed to treat epilepsy and related seizure conditions. GX produces robust positive allosteric modulation of GABA-ARs, with preferential sensitivity at δ subunit-containing extrasynaptic receptors (Chuang and Reddy, 2018b). GX has a more favorable biopharmaceutical profile than AP due to its higher bioavailability and less hormonal side effects (Carter et al., 1997; Reddy and Woodward, 2004; Carver and Reddy, 2016). GX produces powerful antiseizure activity in a wide range of experimental models, and is being evaluated in clinical trials for epilepsy (Kerrigan et al., 2000; Laxer et al., 2000; Nohria and Giller, 2007; Pieribone et al., 2007; Reddy and Rogawski, 2012; Bialer et al., 2015; Braat et al., 2015; Sperling et al., 2017). Recently, Zn^{2+} has been shown to selectively block neurosteroid-sensitive, extrasynaptic δGABA-ARs in the hippocampus (Carver et al, 2016). Therefore, it is likely that Zn^{2+} may exert antagonistic effects on GX modulation of tonic inhibition and seizure protection.

In this aim, we investigate the pharmacodynamic interactions of Zn^{2+} and GX at extrasynaptic δGABA-ARs and its functional relevance on the anticonvulsant activity of GX in the kindling model. Our results demonstrate that Zn^{2+} diminishes the antiseizure effects of GX by selectively blocking the extrasynaptic δGABA-ARs in the hippocampus.

II.3 Specific Aim 3

The third specific aim investigates the combination efficacy of neurosteroids AP and GX with the GABA-reuptake inhibitor tiagabine (TG) or the benzodiazepine midazolam (MDZ) on tonic inhibition in dentate gyrus granule cells (DGGCs) and seizure protection in the hippocampus kindling and 6-Hz seizure models.

Antiepileptic drugs (AEDs) are the mainstay for the treatment of epilepsy, a chronic neurological disorder that affects nearly 65 million people worldwide (Thurman et al., 2011; Hesdorffer et al., 2013). AEDs are the most effective interventions to suppress the occurrence of seizures; however, approximately 30% of epilepsy patients are unresponsive to current AEDs when used in monotherapy. Consequently, a polypharmacy with combination of two or more AEDs is used to improve seizure control in persons with refractory epilepsy. Drugs given in combination may produce effects that are additive or synergistic that is estimated using isobolograms (Tallarida, 2006), including select AED combinations (Luszczki and Czuczwar, 2004; Kwan and Brodie, 2006; Luszczki, 2008a; b). Neurosteroids are developed as novel AEDs for epilepsy (Reddy and Estes, 2016). Combination of a neurosteroid with GABAergic AED may enhance seizure control in refractory epilepsy.

GABA-ARs are the prime targets of AEDs such as benzodiazepines, neurosteroids and TG. There are two subtypes of GABA-ARs in the brain, namely synaptic and extrasynaptic receptors (Chuang and Reddy, 2018a). Synaptic GABA-ARs generate transient inhibitory postsynaptic current, whereas extrasynaptic GABA-ARs generate a tonic inhibitory current that regulates neuronal network excitability. Extrasynaptic GABA-ARs typically contain either δ or α5 subunits, in combination with β2 or β3 subunits and elicit the basal inhibitory tone referred as tonic inhibition (Bianchi and Macdonald, 2003; Coulter and Carlson, 2007; Glykys et al., 2008). Extrasynaptic δGABA-ARs are expressed in a cell-type specific fashion in key brain areas such as hippocampus, thalamus, cerebellum, and amygdala. Among these brain regions,

hippocampus is linked to epilepsy pathology (Jutila et al., 2002; Mortensen et al., 2011). Tonic inhibition plays a critical role in epilepsy (Carver et al., 2014; Reddy, 2018). Neurosteroids such as AP are potent allosteric agonists of GABA-ARs, especially extrasynaptic δGABA-ARs (Chuang and Reddy, 2018a). AP has been shown to have robust anticonvulsant activity (Rupprecht, 2003; Belelli and Lambert, 2005; Carver and Reddy, 2013; Brown et al., 2015; Porcu et al., 2016; Chuang and Reddy, 2018b). GX, a synthetic analog of AP, is a broad-spectrum anticonvulsant agent with greater bioavailability and reduced side effects compared to AP. Like AP, GX is a powerful allosteric modulator of synaptic and extrasynaptic GABA-ARs (Carter et al., 1997; Chuang and Reddy, 2018b). GX is undergoing clinical trials for refractory epilepsy, pediatric genetic epilepsies, and status epilepticus (Nohria and Giller, 2007; Pieribone et al., 2007; Reddy and Rogawski, 2010; 2012; Porcu et al., 2016; Ligsay et al., 2017). However, the antiepileptic potential of GX or other neurosteroids in combination with current AEDs has not yet been investigated. It is postulated that a combination therapy utilizing pair compounds with distinct GABAergic mechanisms might provide additive or synergistic therapeutic efficacy at doses that would minimize or eliminate unwanted side effects.

TG is an adjunct AED for partial seizures (Goldenberg, 2010). TG, a GABA-reuptake inhibitor, increases GABA level in the synaptic cleft by selective blockade of the GABA transporter GAT-1 (Adkins and Noble, 1998; Meldrum and Chapman, 1999). The major limitations of TG include lack of robust antiseizure efficacy and adverse effects such dizziness nervousness, seizures, and tremors. It is suggested that a combination treatment of TG with neurosteroids might be a rational strategy to design a robust anticonvulsant drug regimen. To evaluate the effect of neurosteroids and TG combinations, we utilized the isobolographic analysis, a well-accepted approach for the assessment of drug interactions (Grabovsky and Tallarida, 2004; Luszczki, 2008a; b). It typically includes two types: type I is used to evaluate drugs that are fully active, while type II is used when one of the drugs tested has no effects (Berenbaum 1989). Drug combination analysis with isobologram is a valuable strategy to differentiate the exact type of interactions among

drugs tested as synergistic, additive or antagonistic (Grabovsky and Tallarida 2004; Tallarida 2006; 2007).

In this aim, we sought to investigate the combination interactions between neurosteroids and TG or neurosteroid and MDZ on extrasynaptic tonic inhibition in the hippocampus and seizure protection in the hippocampus kindling and 6-Hz seizure models. Our isobolographic studies demonstrate a synergistic anticonvulsant effect of neurosteroid – TG combinations, and as well as neurosteroid – MDZ regimens, indicating a role for tonically activated extrasynaptic GABA-ARs in the clinical action of AED combination regimens.

CHAPTER III

MATERIALS AND METHODS[§,**]

III.1 Experimental Animals

Young adult (2 – 3 months-old) male C57BL/6 mice were used in the study. Experiments were conducted in wildtype (WT) and GABA-AR δ subunit knockout (*Gabrd*$^{-/-}$, δKO) mice (Mihalek et al., 1999) that were maintained on a hybrid C57BL/6-129SV genetic background. Four mice were housed per cage under standard laboratory conditions with a 12 h light/dark cycle. The animals were cared for in compliance with the guidelines in the National Institutes of Health *Guide for the Care and Use of Laboratory Animals.* Animal procedures were conducted in compliance with a protocol approved by the Texas A&M Institutional Animal Care and Use Committee.

III.2 Electrophysiology Studies

III.2.1 Hippocampal Slice Preparation

Patch-clamp electrophysiological studies were conducted in acutely dissociated neurons and slices using established methods as described previously (Reddy and Jian, 2010; Carver and Reddy, 2016). Adult male mouse was anesthetized with isoflurane and the brain was rapidly removed and placed in ice-cold artificial cerebrospinal fluid (aCSF) buffer. Transverse slices (320 μm thickness) of the hippocampus were obtained with a Vibratome in 3.5˚C aCSF (model 1500 with 900 Refrigeration System; Leica

---

[§] Reprinted (adapted) with permission from "3β-methyl-neurosteroid analogs are preferential positive allosteric modulators and direct activators of extrasynaptic δ-subunit γ-aminobutyric acid type A receptors in the hippocampus dentate gyrus subfield." by S-H Chuang and DS Reddy, 2018. T*he journal of pharmacology and experimental therapeutics*, 365(3): 583–601, Copyright © 2018 by The American Society for Pharmacology and Experimental Therapeutics. All rights reserved.

[**] Reprinted (adapted) with permission from "Zinc reduces antiseizure activity of neurosteroids by selective blockade of extrasynaptic GABA-A receptor-mediated tonic inhibition in the hippocampus" by S-H Chuang and DS Reddy, 2019. *Neuropharmacology*, 148: 244–256, Copyright © 2018 Elsevier Ltd. All rights reserved.

Microsystems, Inc., Bannockburn, IL). The aCSF buffer for slice cutting was composed of (in mM): 0.3 kynurenic acid (Tocris Bioscience, Bristol, UK), 126 NaCl, 3 KCl, 0.5 $CaCl_2$, 5 $MgCl_2$, 26 $NaHCO_3$, 1.25 NaH_2PO_4, 11 glucose (pH adjusted to 7.35 – 7.40 with 95% O_2 – 5% CO_2, 305 – 315 mOsm/kg).

III.2.2 Dissociation of Neurons

Hippocampus CA1 and DG neurons were acutely dissociated by the standard enzymatic technique as described previously (Kay and Wong, 1986; Reddy and Jian, 2010). The hippocampal CA1 or DG region was microdissected under a microscope (model SMZ 647; Nikon, Tokyo, Japan) and incubated in aCSF for 1 h at 28℃. The isolated CA1 and DG slices were transferred into an enzymatic solution containing aCSF with protease XXIII (3 mg/ml, Sigma-Aldrich, St. Louis, MO). Next, the slices were incubated for precisely 23 to 25 min at 28℃, rinsed twice with aCSF, and gently triturated through three fire-polished Pasteur pipettes to yield single cells. For each batch, slices were triturated six to eight times with each pipette in approximately 1 ml of aCSF. Then, the solution was allowed to settle for 1 min, and the suspension of freshly isolated cells was plated onto the recording chamber (Warner Instruments, Hamden, CT).

III.2.3 Recording of GABA-Gated Currents

Whole-cell patch-clamp configuration was used for electrophysiological recordings in dissociated cells (Reddy and Jian, 2010). Experiments were performed at room temperature (22 – 24 ℃). The recording chamber was fixed into the stage of an inverted microscope with phase-contrast and differential interference contrast optics (model IX71; Olympus, Tokyo, Japan). The physiological bath solution for the recording of dissociated neurons was composed of (in mM): 140 NaCl, 3 KCl, 10 HEPES, 2 $MgCl_2$, 2 $CaCl_2$, and 16 glucose (pH adjusted to 7.4 with NaOH, osmolarity, 315 – 325 mOsm/kg). Cells were visualized and images were acquired through video camera CCD-100 (Dage-MTI, Michigan City, IN) with FlashBus Spectrim 1.2 software (Pelco, Clovis, CA). Recording

pipettes were pulled from capillary glass tubes (King Precision Glass, Claremont, CA) using a P-97 Flaming-Brown horizontal puller (Sutter Instrument Company, Novato, CA). The pipette tip resistances were 4 to 6 MΩ for recording. The recording pipettes were filled with a cesium pipette solution containing (in mM): 124 CsCl, 20 tetraethylammonium, 2 $MgCl_2$, 10 EGTA, 10 HEPES, 0.1 GTP, 4 ATP (pH adjust to 7.2 with CsOH, osmolarity, 295 – 305 mOsm/kg). Currents were recorded using an Axopatch 200B amplifier (Molecular Devices, Sunnyvale, CA). The membrane capacitance, series resistance, and input resistance of the recordings were monitored by applying a 5-mV (100-ms) depolarizing voltage step from a holding potential of −70 mV for dissociated cells. Signals were low-pass filtered at 2 kHz and digitized at 10 kHz with Digidata 1440A system. The current values were normalized to cell capacitance (an index of cell size) and expressed as current density (pA/pF). Fractional potentiation generated by allosteric modulator was expressed as I_A/I_{GABA}, where I_{GABA} is the GABA peak current amplitude and I_A is the peak current response of the co-application of GABA and the allosteric drug (0.05 to 1 μM). GABA at 3 μM produced 10% of the maximal current (EC_{10}), as described previously in dissociated murine CA1PCs (Reddy and Jian, 2010) and DGGCs (Wu et al., 2013; Carver and Reddy, 2016). The concentration-response relationship was fitted by the nonlinear Hill function to derive the $EC_{50,}$ which is the concentration of test drug required to generate 50% of maximal efficacy. For whole cell current from isolated single cells, current response was expressed as the percentage of potentiation produced by GABA or GABA + GX. For fast application of test drugs, the perfusion pipette was positioned < 200 μm away from the cell in the chamber. GABA, GX, and Zn^{2+} (1 – 30 μM) were applied using a multi-channel perfusion system (Automate Scientific, Berkeley, CA). A two-minute wash with bath solution was instituted after each drug trial in order to prevent receptor desensitization.

III.2.4 Slice Patch-Clamp Electrophysiology

Electrophysiological recordings in hippocampal slices were performed in the whole-cell patch-clamp configuration (Wu et al., 2013; Carver et al., 2014; Carver and Reddy, 2016).

Hippocampal neurons were visually identified with an Olympus BX51 microscope equipped with a 40x water-immersion objective, infrared-differential interference contrast optics, and video camera. Hippocampal slices (320 μm) were maintained in continuously oxygenated aCSF at 28℃ in a holding chamber for 60 min, and experiments were performed at room temperature (22 – 24 ℃) as described by other groups (Vicini et al., 2002; Scimemi et al., 2006; Nani et al., 2013; Gong and Smith, 2014). The physiological bath solution for whole-cell recording from slice was composed of (in mM): 124 NaCl, 3 KCl, 1.5 $MgSO_4$, 2.4 $CaCl_2$, 1.25 NaH_2PO_4, 26 $NaHCO_3$ and 10 glucose (pH adjusted to 7.4 with NaOH, osmolarity, 295 – 305 mOsm/kg). The pipette tip resistances were 5 to 7 MΩ for slice recordings, and were filled with a cesium pipette solution containing (in mM): 124 CsCl, 20 tetraethylammonium-chloride, 2 $MgCl_2$, 10 EGTA, 10 HEPES, 0.1 GTP, 4 ATP, and 5 lidocaine *N*-ethyl bromide (QX-314), (pH adjusted to 7.2 with CsOH, osmolarity, 295–305 mOsm/kg). Currents were recorded using an Axopatch 200B amplifier (Molecular Devices, Sunnyvale, CA). The membrane capacitance, series resistance, and input resistance of the recordings were monitored by applying a 5-mV (100-ms) depolarizing voltage step from a holding potential of –65 mV for slice recordings. Signals were low-pass filtered at 2 kHz and digitized at 10 kHz with Digidata 1440A system.

III.2.5 Tonic Current Recording and Analysis

Tonic and phasic currents of GABA-ARs were recorded in the presence of tetrodotoxin (TTX, 0.5 μM, Na^+ channel blocker and inhibition of action potential-evoked neurotransmitter release), D,L-2-amino-5-phosphonovaleric acid (APV, 40 μM, N-methyl-D-aspartate channel blocker), and 6,7-dinitroquinoxaline-2,3-dione (DNQX, 10 μM, non-N-methyl-D-aspartate glutamate receptor blocker). The competitive antagonist gabazine (SR-95531, 50 μM) was added to perfusion at the conclusion of slice recordings to confirm block of GABAergic currents. Drugs were delivered to the bath chamber using a multi-channel perfusion system (Automate Scientific, Berkeley, CA). Perfusion rate

was maintained at 2 ml/min. Drugs were allowed 2 – 4 min to perfuse into the bath chamber and slice before measurements were obtained. Four to six mice were used to obtain adequate sample size for recording of tonic currents.

Off-line current analysis was performed with pClamp 10.2 software (Molecular Devices, Sunnyvale CA) and in-house software. To study the tonic inhibitory currents, transient events were manually removed from the current trace, so that the recording consisted only of the holding current in the voltage-clamp mode (Wu et al., 2013). Averaged amplitude of tonic current shift in conductance and root-mean-square (RMS) noise amplitude were measured. The tonic current response was expressed as the differences in holding current before and after application of gabazine (50 μM) or Zn^{2+} (0.1 – 10 mM). I_{RMS} is the noise conductance from chloride ions passing through the opened channels and in proportion to the chloride driving force. Tonic current was measured and averaged in 100 ms per epoch with 1 sec interval between epochs for 30 epochs. The measurements were taken 30 s before and 2 – 3 min after application of a drug. I_{RMS} was studied in 50 ms each epoch with 500 ms interval between epochs for 30 epochs before and after drug application in each cell. To assess the effects of a drug on I_{RMS} in an individual neuron, the distribution of I_{RMS} in 30 epochs before the application of a drug (during the baseline period) was compared with that after drug application by a Student's independent t-test. To compare data obtained from a group of neurons, I_{RMS} values in individual epochs before and after drug application were averaged. Changes in I_{RMS} are expressed in pA of current. Currents for a single cell were normalized to membrane capacitance (pA/pF) as tonic current density. Concentration-response curves were subjected to non-linear, logistic fitting. A curve fitting was applied for concentration-responses that achieved a plateau at maximal levels.

III.2.6 Miniature Postsynaptic Current Recording and Analysis

Synaptic currents were recorded and analyzed as previously described (Carver et al., 2016). The mIPSCs were acquired for at least 2 min for each drug response and condition.

The amplitude and kinetics of mIPSCs were measured using MiniAnalysis software (Synaptosoft, NJ), with the threshold for detection set at least three times the baseline RMS noise. The characteristics of amplitude, frequency, rise time, and decay time constants of the mIPSCs were determined and compared between groups. The decay of averaged mIPSC within DGGCs was best fit with a double exponent time constant (Stell et al., 2003). Nonoverlapping events with single peaks were used to create an ensemble average mIPSC. A mean weighted decay time constant was determined from biexponential fitting function $I(t) = A_1 \times e^{(-t/\tau 1)} + A_2 \times e^{(-t/\tau 2)}$ as $\tau_w = (A_1 \times \tau_1 + A_2 \times \tau_2) / (A_1 + A_2)$.

III.3 Seizure Models

III.3.1 Hippocampus Kindling Model

A hippocampus kindling model was used in seizure experiments (Reddy and Mohan, 2011; Reddy et al., 2015). Mice were anesthetized by intraperitoneal injection of ketamine (100 mg/kg) and xylazine (10 mg/kg). A bipolar electrode fixed to a guide cannula (Plastics One) was stereotaxically implanted in the right ventral hippocampus (2.9 mm posterior, 3.0 mm lateral, and 3.0 mm below dura). After postoperative recovery, animals were subjected to kindling stimulation (Reddy and Mohan, 2011). The electrographic afterdischarge (AD) threshold was determined by application of 1 ms biphasic rectangular pulses at 60 Hz for 1 s, in increments of 25 μA using an isolated pulse stimulator (A-M Systems). AD duration was the total duration of electrographic spike activity (amplitude >2X baseline) occurring in a rhythmic pattern at a frequency > 1 Hz. Mice were stimulated at 125% AD threshold once per day until Stage 5 seizures were elicited on 3 consecutive days, considered the fully kindled state. The electrographic activity was recorded using Axoscope 8.0 software with Digidata 1322A interface (Molecular Devices) through a Grass CP511 preamplifier (Astro-Med). Behavioral seizures were rated according to Racine's scale as modified for mouse (Racine, 1972) stage 0 = no response or behavior arrest; stage 1 = chewing or facial twitches; stage 2 =

chewing and head nodding; stage 3= forelimb clonus; stage 4= bilateral forelimb clonus and rearing; stage 5= bilateral forelimb clonus/ rearing and falling. One week after kindling, $ZnCl_2$ (10 – 300 μM) was dissolved in sterile saline and microinfused in 5 μl volume directly into the hippocampus using a perfusion pump at 0.2 μl/min. Mice were monitored for seizures and electrographic activity for at least 10 min. GX (s.c.) was administered 15 min after infusion of Zn^{2+}. AP and GX were made in 20% β-cyclodextrin solution for *in vivo* study. Drugs were given subcutaneously in a volume equivalent to 1% of the body weight of the animals 15-min before kindling stimulations. Mice were scored for protection based on the behavioral motor seizures and AD duration after each kindling session.

III.3.2 Six-Hertz Seizure Model

The 6-Hz mouse model of partial seizures was used as previously described (Reddy et al., 2015). Mice were electrically stimulated via cornea for 0.2-millisecond-duration monopolar low-frequency rectangular pulses at 6-Hz for 3 seconds (World Precision Instruments, Sarasota, FL). Current value causing seizures in 50% of animals was determined by administering different current intensities in the range of 6 – 44 mA to a group of control animals. Current intensity at 38 mA was determined to elicit seizures in 100% population of male mice and delivered as the standardized intensity for the in vivo studies of combination therapy. The ocular anesthetic tetracaine (0.5%) drops were applied to each eye 10 minutes before stimulation. The corneal electrodes were wetted with 0.9% saline solution immediately prior to stimulation. Animals were manually restrained for stimulation and immediately released into a chamber for behavioral observation. Test drugs were administered 15 min before stimulation. The duration of seizure activity ranged from 20 to 60 seconds in untreated, control mice. Animals were considered to be protected if they resumed normal exploratory behavior within 10 seconds of the stimulation. Six to 8 animals were used for each dose of treatment.

III.4 Zinc Administration

Zinc doses were given acutely via intrahippocampal microinfusion in mice, as previously described (Carver et al., 2016). The sterile saline was used as a control. Apart from a bipolar electrode in the hippocampus, a 26 gauge guide cannula (Plastics One) was stereotaxically implanted into the left ventral hippocampus (2.9 mm posterior, 3.0 mm lateral, and 3.0 mm below dura). After a period of at least 1 week of recovery, dual-implanted animals were subjected to kindling. Zinc was dissolved in sterile saline. Mice received zinc doses (10 – 300 μM) by slow intrahippocampal microinfusion 10 min prior to GX administration and 25 min before kindling stimulations. The efficiency of zinc delivery was confirmed by the correct placement of the guide cannula by histology (Carver et al., 2016).

III.5 Isobolographic Analysis of Drug – Drug Interactions.

Interactions between neurosteroids and TG or MDZ against 6-Hz-induced seizures were examined using established methodology as described previously (Łuszczki 2008a, b). Briefly, the median effective dose (ED_{50}) of each drug administered alone in the 6-Hz seizure model was first determined by using log-probit linear regression analysis (Litchfield and Wilcoxon, 1949). Next, the theoretical additive $ED_{50\ add}$ values ± standard error of mean (SEM) for the mixtures of tested drugs at three fixed ratio of 1:1, 1:3, and 3:1 (the most commonly used drug-dose ratio combinations for the evaluation of drug interactions) were calculated. The $ED_{50\ add}$ value is a total additive dose of the two drugs in the mixture, exerting theoretically a 50% protection against 6-Hz-induced seizures. The $ED_{50\ mix}$ values are experimentally determined total doses of a mixture of two tested drugs administered at a fixed-ratio combination sufficient for 50% protection against 6-Hz-induced seizures and were derived from the seizure protection exerted by each mixture at 1:3, 1:1 and 3:1 (Fig. 29F; Table 9).

For the analysis of electrophysiological tonic currents, the isobologram method was adapted to study the interactions between neurosteroids and TG or MDZ on the tonic

inhibition. We utilized the $EF_{2\text{-fold}}$ values that represent the effective functional concentration of drug (nM) required to double the basal tonic response in DGGCs. Briefly, the $EF_{2\text{-fold}}$ values of tested drugs were deduced from their concentration-response curves. The theoretical $EF_{2\text{-fold}}$ ($EF_{2\text{-fold add}}$) values for mixtures were calculated and tested in DGGCs to quantify the contribution of each drug to the overall effects. The experimental $EF_{2\text{-fold}}$ ($EF_{2\text{-fold mix}}$) values were derived from the tonic current modulation of each mixture. The isobolograms were plotted and the theoretical and experimental-determined $EF_{2\text{-fold}}$ values of mixtures were compared (Fig. 27 – 28; Table 8).

In the present study, the isobolographic analysis was performed to ascertain the effect of combination, which is based on the concept of "dose equivalence". This isobologram method is the 'gold standard' for the evaluation of interactions between drugs, which allows their stratification as supra-additive (synergistic), additive, and sub-additive (antagonistic) drugs (Tallarida, 2006). In isobolography, it is accepted that half of the ED_{50} dose of a first drug plus half of the ED_{50} dose of a second drug, should be as therapeutically effective as a full dose of each drug administered separately. This concept of adding fractions of the effective doses of AEDs is the fundamental rule underlying the isobolographic analysis (Loewe, 1953; Berenbaum, 1989; Tallarida, 2000). The interaction of two or more drugs to produce a combined effect is described by the interaction index I (Berenbaum 1977).

$$I = D1/M1 + D2/M2 \quad \text{---------- (1)}$$

where, D1 and D2 are concentrations of drug 1 and 2 that produce a certain effect if applied together; M1 and M2 are the median concentrations that produce the same effect when given alone. Consequently, for deriving the 50 % seizure protection, then equation 1 can be expressed as:

$$I = D1/ED_{50,1} + D2/ED_{50,2} \quad \text{---------- (2)}$$

Here, $ED_{50,1}$ and $ED_{50,2}$ are the ED50 values of drug 1 and drug 2 alone. D1 and D2 are the doses of drug 1 and 2, respectively, which also produce 50 % protection when given together. This general method has been developed based on the analysis of each drug alone and the simulation of the combined action response, based on the Loewe additivity theory (Loewe, 1953). For drugs showing an interaction, equation (1) is adapted and advanced into defining a combination index (CI), indicating type and amount of interaction between two drugs with target experimental outcome (Chou and Talalay, 1983).

CI = D1/M1 + D2/M2 -- (3) > 1 for antagonism; = 1 for additivity; and < 1 for synergy

The CI can take values between 1 and infinity for antagonism, and runs between 0 and 1 for synergy. The interaction index underlies one of the most widely used graphical representations of drug synergism and antagonism, the isobologram (Figure 7). The isobolograph illustrates typical subadditive (antagonistic) and superadditive (synergistic) isoboles. The doses of drugs A and B give abscissa and ordinate, respectively, and the effect of drug combinations is plotted as graph (Figure 7). The effects of each drug alone (ED_{50}) can be read from the axes. The isobologram shows an effect, such as anticonvulsant ED_{50} and which drug concentration is needed to achieve this effect. Overall, to simplify the notation of interactions in isobolography, the drug doses were administered in fixed ratio combinations (1:3, 1:1, and 3:1) and reflect fractions of ED_{50} values denoted for the drugs used separately. The isobologram-based CI calculations were obtained to identify additive from synergistic interactions.

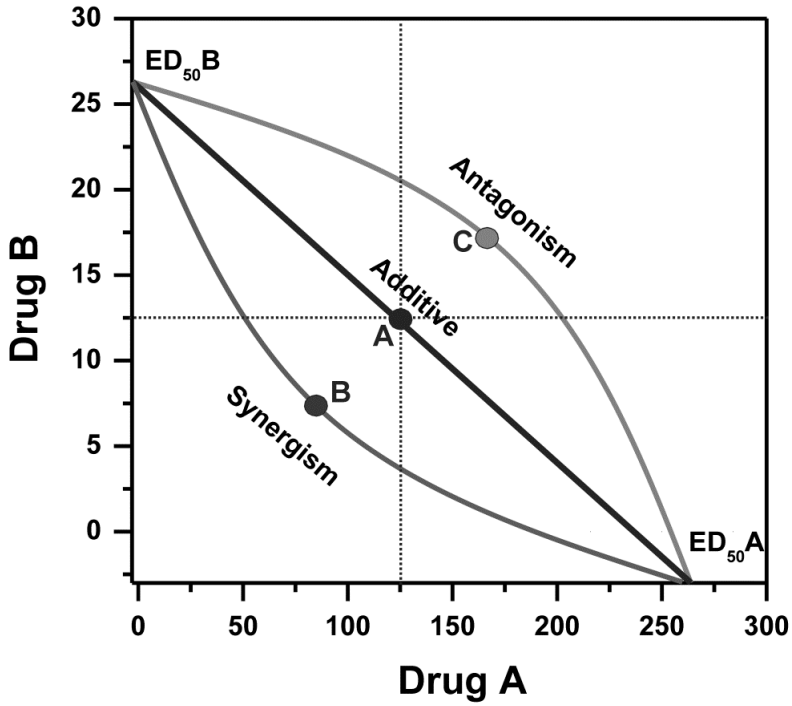

Figure 7 Isobologram-based characterization of drug combinations.

The X and Y axis units are the doses of drugs A and B. The solid black line connects doses that produce the same effect of certain examined response (ED_{50} line), such as seizure protection. From additivity (A), the combination of drug A with drug B would produce 50% protection (point A). If, 50% protection is achieved at lower doses of the two drugs, the drugs would exhibit synergism (point B). If the observed effect by the combination is less than 50%, drug A and B would interact in an antagonistic way (point C). The dashed lines are drawn to enhance the recognition of symmetry for additive isobole responses. In practical terms, fixed drug dose ratios are tested in the standard combinations (1:3, 1:1, 3:1) and ED_{50} values are determined for the mixture.

III.6 Drugs and Reagents

All chemicals utilized in electrophysiology experiments were acquired from Sigma-Aldrich unless otherwise specified. AP and GX were prepared as 2 mM stock solutions in dimethyl sulfoxide for electrophysiology experiments. Stock solutions were diluted in the external perfusion solution to the desired concentration for electrophysiological use. The concentration of dimethyl sulfoxide in final solution was less than 1%. AP was purchased from Steraloids (Newport, RI), and GX, kynurenic acid, and GF 109203X were purchased from Tocris. 21-OH-GX was synthesized in the laboratory. TTX was acquired from Calbiochem (Billerica, MA). Midazolam was purchased from Akorn (Lake Forest, IL).

III.7 Statistical Analysis

Data were expressed as the mean ± standard error of mean (SEM). In slice electrophysiology studies, concentration-response curves were subjected to non-linear, logistic fitting. A curve fitting was applied for concentration-responses that achieved a plateau at maximal levels. Comparisons of statistical significance of data were made using a Student's t-test. Comparisons of cumulative probability distributions were made using the Kolmogorov-Smirnov test. Results were considered significant if the two-tailed p values were < 0.05. In pharmacological studies, the percent protection of mice against 6-Hz-induced seizures and subsequently, dose-response relationship lines were fitted using log-probit linear regression analysis according to Litchfield and Wilcoxon (Litchfield and Wilcoxon, 1949). The ED_{50} values with their 95% confidence limits were calculated by computer-assisted log-probit analysis according to Litchfield and Wilcoxon procedure. First, the dose-response relationships of test drugs for target outcomes were subjected to the test for parallelism, an essential condition for characterizing AED interactions with isobolography. Since the dose-response relationship for GX and TG were parallel in this study, the type I isobolographic analysis for parallel dose-response relationship lines was used. Statistical evaluation of isobolographic interactions was

performed by the use of Student's t-test in order to detect the differences between the experimentally derived ($ED_{50\ mix}$) and theoretical additive ($ED_{50\ add}$) values (Tallarida, 2000; Łuszczki, 2008a, b). Comparison of the differences in seizure stage between groups was made with the nonparametric Kruskal-Wallis test followed by the Mann-Whitney U-test. The differences in means of the AD duration and the percentage inhibition of seizure stage between groups were compared with one-way analysis of variance, followed by Student's *t*-test and Wilcoxon signed ranks test, respectively. For patch-clamp data with small sample size, nonparametric tests were used to check the statistical significance especially when the data points were not normally distributed. The criterion for statistical difference was $p < 0.05$, unless otherwise specified.

CHAPTER IV
RESULTS[††‡‡]

IV.1 3β-Methyl-Neurosteroid Analogs are Preferential Positive Allosteric Modulators and Direct Activators of Extrasynaptic δGABA-ARs in the Hippocampus Dentate Gyrus Subfield

IV.1.1 Allosteric Activation of GABA-Gated Currents by GX in Acutely Dissociated Hippocampal Neurons

The chemical structures of the neurosteroid AP and its 3β-methyl analogs GX and 21-OH-GX are shown in Figure 8. To determine the modulatory effects of GX on whole-cell GABA-gated currents, we studied native neurons using patch-clamp electrophysiology. To examine the effects of subunit composition on GABA-AR function, concentration-response profiles of GX were compiled in two cell types: δ-containing dentate gyrus granule cells (DGGCs) and γ-containing CA1 pyramidal cells (CA1PCs). GABA-AR currents were recorded from acutely dissociated, voltage-clamped DGGCs or CA1PCs from adult male mice in whole-cell mode. We utilized 3 μM GABA, which was within the range of EC_{10} response for both DGGCs (Wu et al., 2013; Carver and Reddy, 2016) and CA1PCs (Reddy and Jian, 2010), to determine a baseline response and allosteric activation by tested compounds. We confirmed the EC_{10} value of GABA in DGGCs (Figure 9C). Increasing concentrations of GX were co-applied with 3 μM GABA to obtain the fractional potentiation of GABAergic currents mediated by GX. Both cell

---

[††] Reprinted with permission from "3β-methyl-neurosteroid analogs are preferential positive allosteric modulators and direct activators of extrasynaptic δ-subunit γ-aminobutyric acid type A receptors in the hippocampus dentate gyrus subfield." by S-H Chuang and DS Reddy, 2018. T*he journal of pharmacology and experimental therapeutics*, 365(3): 583–601, Figures 1 – 13, Table 1 – 2, Copyright © 2018 by The American Society for Pharmacology and Experimental Therapeutics. All rights reserved.

[‡‡] Reprinted with permission from "Zinc reduces antiseizure activity of neurosteroids by selective blockade of extrasynaptic GABA-A receptor-mediated tonic inhibition in the hippocampus" by S-H Chuang and DS Reddy, 2019. *Neuropharmacology*, 148: 244–256, Figures 1 – 7, Table 1, Copyright © 2018 Elsevier Ltd. All rights reserved.

types responded to GX in a concentration-dependent manner (Figure 9A). Concentration-response plots were generated for DGGCs and CA1PCs to determine allosteric potentiation by GX (0.05 – 1 μM) (Figure 9B). Due to the lack of a response plateau, a nonlinear curve could not be fit to the data for either DGGCs or CA1PCs. Based on previous structure-activity data, 1 μM GX-mediated current was denoted as the constrained maximum efficacy response for allosterically modulated activity. Higher micromolar concentrations of neurosteroids directly activate receptors and exhibit a biphasic modality at a separate neurosteroid binding site (Puia et al., 1990; Carver and Reddy, 2013). As shown in Figure 9B, GX (0.1 μM) potentiated GABA-gated currents significantly higher in DGGCs than CA1PCs ($n = 8 – 9$ cells per group, $p = 0.038$). GX at 0.3 and 0.5 μM concentrations also showed markedly higher GABA-gated currents in DGGCs than CA1PCs ($n = 6 – 10$ cells per group, $p = 0.05$). In maximal efficacy estimation for allosteric potentiation, GX (1 μM) displayed significantly greater GABA-gated currents in DGGCs (5-fold potentiation) than CA1PCs (2-fold potentiation; $n = 7$ cells per group, $p < 0.05$). To confirm the contributory role of the δ subunit for enhanced allosteric potentiation of GX in DGGCs, we studied GX allosteric activation of GABA-gated currents in DGGCs from δKO mice, which lack δ-containing receptors (Mihalek et al., 1999; Carver and Reddy, 2016). GX-potentiated GABAergic currents (1 μM) were significantly reduced in δKO DGGCs than WT DGGCs (Figure 8A, 8B; $n = 5 – 6$ cells per group, $p = 0.038$). These findings suggest that GX has higher sensitivity at neurons that have a high expression of δ-containing GABA-ARs, possibly driving the allosteric selectivity.

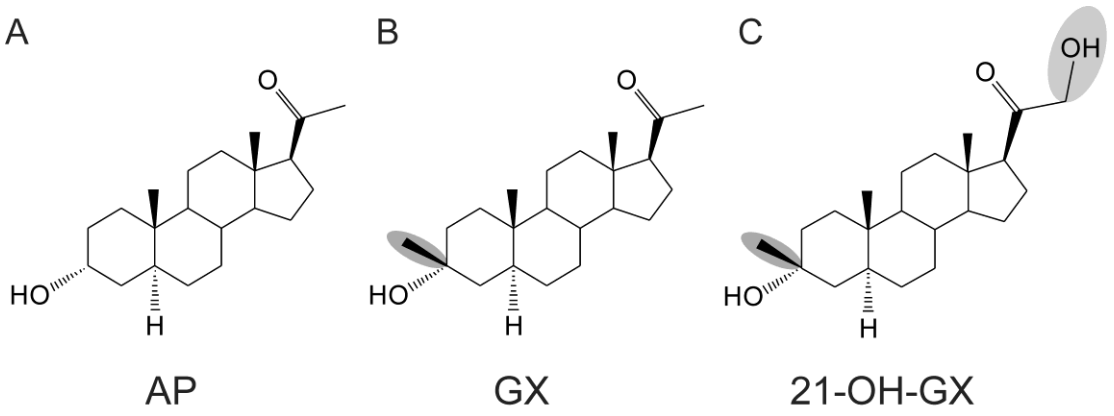

Steroid	C3 position	C5 position	C17 position	Key structure
AP	**α-OH**	**α-H**	**-$COCH_3$**	**3α-hydroxyl; 17-acetyl**
GX	**α-OH; β-CH_3**	**α-H**	**-$COCH_3$**	**3β-methyl**
21-OH-GX	**α-OH; β-CH_3**	**α-H**	**-$COCH_2OH$**	**3β-methyl; 21-hydroxyl**

Figure 8 Chemical structures of the neurosteroid AP and its 3β-methyl analogs.
(A) Allopregnanolone (AP). (B) Ganaxolone (GX). (C) 21-OH-GX.

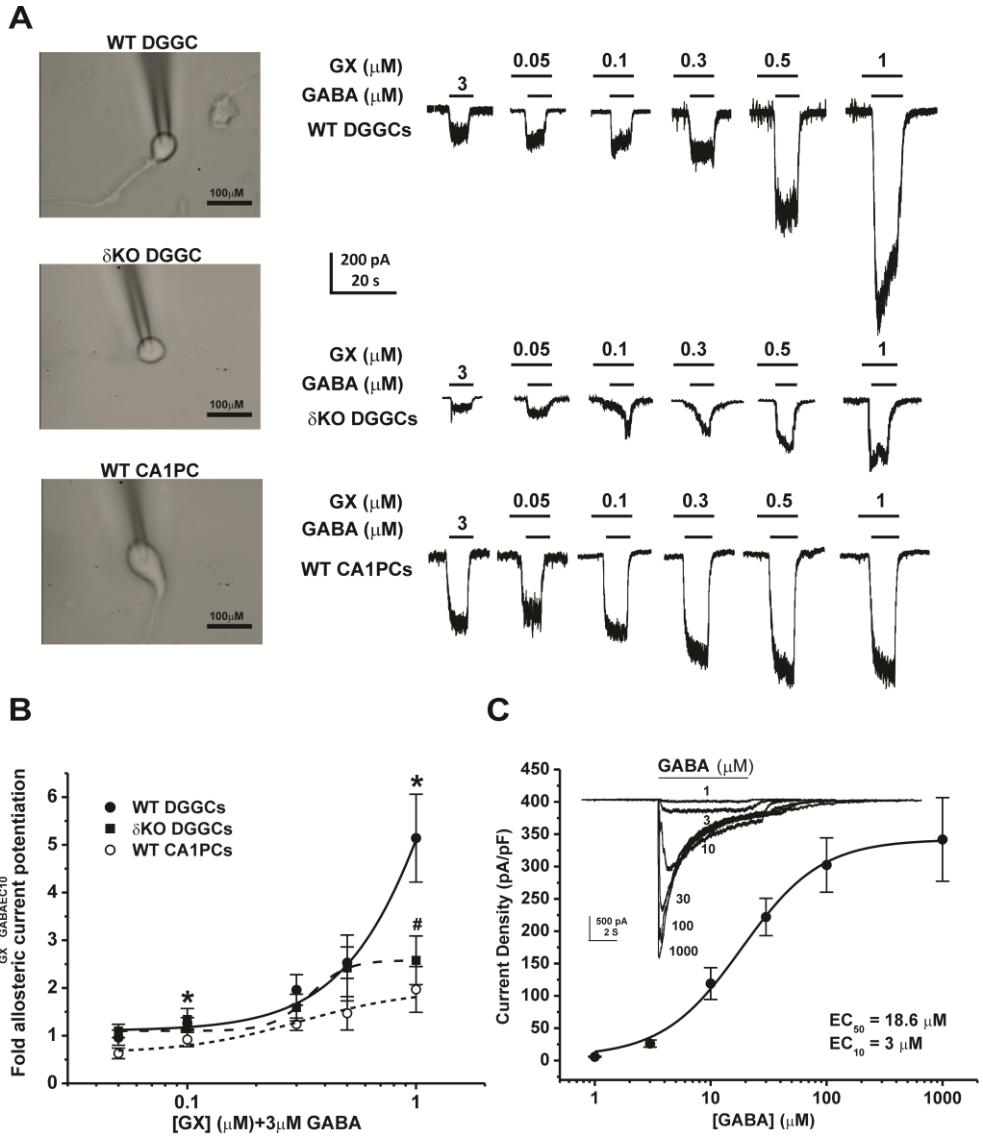

Figure 9 GX allosteric activation of GABA-gated currents in acutely dissociated neurons.

GX (1 μM) displayed significantly greater GABA-gated chloride currents in WT DGGCs (5.1 ± 0.9 fold-potentiation) than CA1PCs (2.0 ± 0.5 fold-potentiation). However, GX-potentiated GABAergic currents were significantly reduced in δKO DGGCs. (A) Representative whole-cell current recordings of DGGCs and CA1PCs. Neurons displayed concentration-dependent responses to GX potentiation of 3 μM GABA (EC_{10}). (B) Concentration-response of GX-modulated allosteric potentiation of chloride currents in DGGCs and CA1PCs from WT or δ subunit knockout (*Gabrd*$^{-/-}$, δKO) mice. (C) Concentration-response profile of GABA-potentiated current density (pA/pF). GABA EC_{10} = 3 μM. Each point represents mean ± SEM of data from 5 to 10 cells. *$p < 0.05$ vs. CA1PCs; $^{\#}p < 0.05$ vs. WT DGGCs.

IV.1.2 GX Modulation of Inhibition via GABA-ARs

To verify the target specificity of GX inhibitory activity in native DGGCs, we studied the blockade of GABAergic currents with specific GABA-AR antagonists. At 10 μM, the competitive antagonists bicuculline (BIC) or gabazine (GBZ) completely blocked whole-cell GABA-gated current potentiation by GX ($n = 4 – 5$ cells per group, $p < 0.05$; Figure 10A, 10B). When the antagonists were removed by washing, the GX-potentiated GABA-gated currents returned to the same level as before the application of antagonists. These results indicate that GX modulation of GABA-gated currents is GABA-AR-mediated.

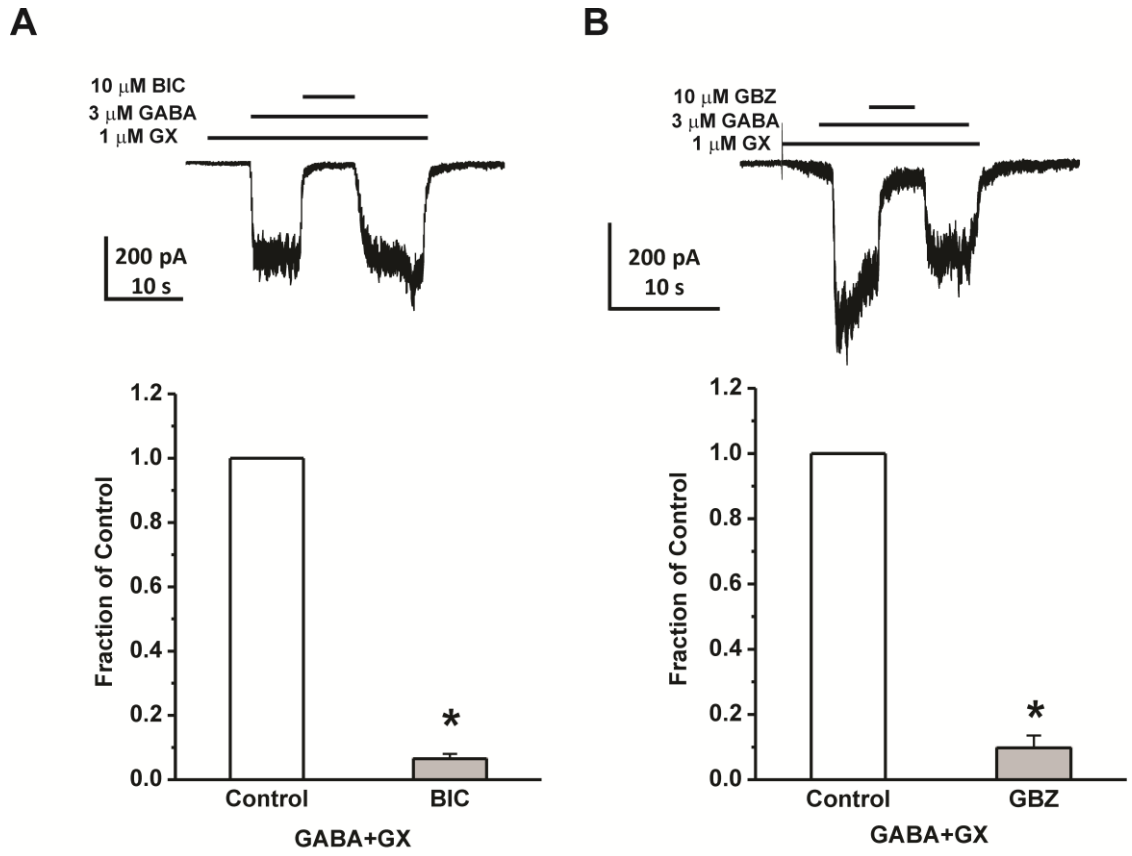

Figure 10 GX-activated chloride currents are blocked by GABA-AR antagonists.

(A) Representative recording and fractional block of currents by bicuculline (BIC, 10 μM) in DGGCs. (B) Representative recording and fractional block of currents by gabazine (GBZ, 10 μM) in DGGCs. Each bar represents mean ± SEM of data from 4 to 5 cells. *p < 0.05 vs. control.

IV.1.3 Direct Activation of GABA-Gated Currents by GX in Acutely Dissociated Hippocampal Neurons

Neurosteroids have been shown to directly activate GABA-AR chloride channels at concentrations exceeding 1 μM (Puia et al., 1990; Reddy and Rogawski, 2002). This direct activation may occur in the absence of GABA, but when GABA is present, the potentiating effects of neurosteroids are enhanced. Therefore, we examined direct activation of whole-cell GABAergic currents in acutely dissociated DGGCs and CA1PCs.

Cells were voltage-clamped in the same preparation denoted in Figure 9. Increasing concentrations of GX (1 – 100 μM, no GABA) were applied by rapid perfusion to the cell until saturation of the inward current response was observed (Figure 11A). Concentration-response curves were derived for DGGCs and CA1PCs (Figure 11B). GX evoked significantly greater inward currents in DGGCs than CA1PCs. At each concentration tested, GX potentiated-GABAergic currents were significantly higher in DGGCs (2.07 ± 0.66 fold of 3 μM GABA response at 1 μM; 3.08 ± 0.37 fold at 3 μM; 5.20 ± 0.70 fold at 10 μM; 6.01 ± 0.84 fold at 30 μM; and 6.34 ± 0. 24 fold at 100 μM) than CA1PCs (0.36 ± 0.09 fold of 3 μM GABA response at 1 μM; 0.83 ± 0.20 fold at 3 μM; 1.55 ± 0.27 fold at 10 μM; 2.05 ± 0.36 fold at 30 μM; and 2.67 ± 0. 62 fold at 100 μM). Such greater currents in response to high GX (1 – 100 μM) are mostly due to abundance of δGABA-ARs in DGGCs. Next, we compared the efficacy and potency of GX with AP for direct activation of GABAergic inward currents (Figure 11A, 11B). Table 5 shows the summary data on the efficacy and potency of GX and AP for allosteric and direct-gating effects at GABA-ARs in DGGCs. In allosteric activation, GX appears to be similar in potency and efficacy with that of AP. AP at 1 μM caused 4.3-fold potentiation ($EF_{(2\text{-fold GABA})=}$ 474 nM), which is not significantly different from GX-potentiated currents (5.1-fold; $EF_{(2\text{-fold GABA})=}$ 389 nM). In direct-gating effects, GX exhibited 1.5 to 2- fold higher efficacy than AP in DGGCs. Other parameters could not be derived because concentration responses were largely saturated at concentrations ≥ 10 μM. Overall, GX has greater efficacy than AP for direct activation of inward currents at micromolar levels (Figure 11B).

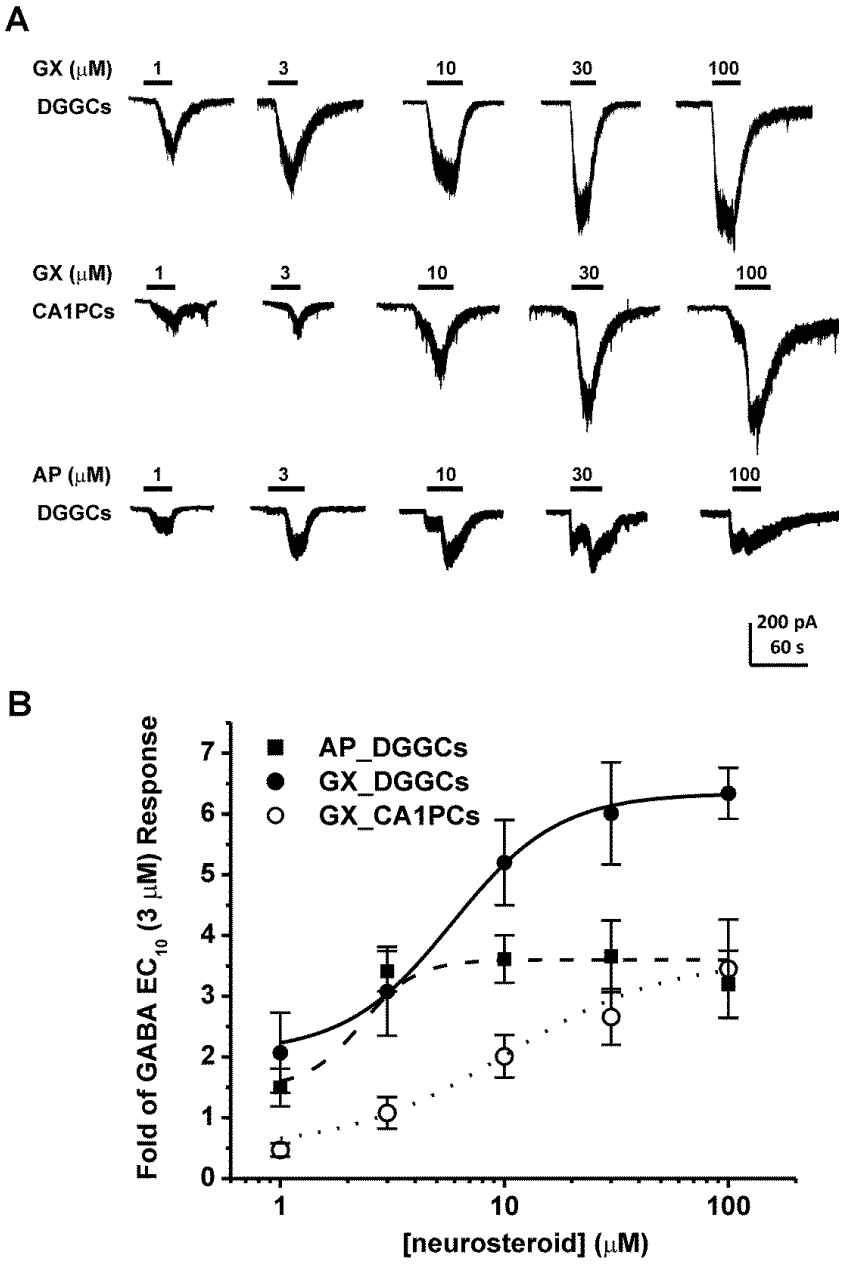

Figure 11 GX direct activation of GABA-ARs in acutely dissociated neurons.

GX and AP directly activated chloride currents in a concentration-dependent manner in hippocampal neurons. GX evoked significantly greater inward currents in DGGCs than CA1PCs. (A) Representative whole-cell current recordings of GX and AP in DGGCs and GX in CA1PCs. (B) Concentration-response curves for direct activation of inward currents by GX or AP alone in DGGCs and CA1PCs. Each point represents mean ± SEM of data from 4 to 13 cells. *$p < 0.05$ vs. CA1PCs. Other derivative parameters are listed in Table 1.

Table 5 Comparative efficacy of GX and AP for allosteric and direct-gating effect at GABA-ARs in DGGCs.

Compound	GABA-gated whole-cell current		Tonic current	
	Allosteric effect	Direct effect		
	$EF_{(2\text{-fold GABA})}$ (nM)[a]	$E_{30\ \mu M}$ (pA)[b]	$E_{1\ \mu M}$ (pA)[c]	$EF_{(2\text{-fold GABA})}$ (nM)[a]
AP	474	273.5	100.6	80
GX	389	336.1	64.0	290
GABA[d]	-	1426.3	19.6	-

[a]EF values represent the effective functional concentration of drug (nM) required to double the 3 μM GABA (EC_{10}) response.
[b]$E_{30\ \mu M}$ values represent the mean tonic current responses of drug at 30 μM concentration.
[c]$E_{1\ \mu M}$ values represent the mean tonic current responses of drug at 1 μM concentration co-applied with 1 μM GABA. GABA 1 μM tonic current response: 0.66 ± 0.22 pA/pF, 19.6 pA.
[d]GABA EC_{50}: 18.6 μM. EC_{50} values represent the concentration required to produce half of its own maximal effect.

IV.1.4 Allosteric Potentiation of Extrasynaptic δGABA-AR-Mediated Tonic Currents by GX in Hippocampus Slices

To ascertain the functional role of GX in potentiating extrasynaptic δ-containing GABA-ARs within the hippocampus, we explored the tonic current levels in WT and δKO DGGCs in slice recordings. We used voltage-clamp electrophysiology to record enhancement of GABAergic tonic currents by GX in the presence of the NMDA receptor antagonist (APV, 40 μM), the AMPA receptor antagonist (DNQX, 10 μM), and the sodium channel blocker (TTX, 0.5 μM). Baseline tonic currents were derived in a bath perfusion with 1 μM GABA. GX (0.1 – 1 μM) was co-applied with 1 μM GABA in tonic current recordings (Figure 12A, 12B). At the end of each recording, 50 μM GBZ was perfused in order to determine the total tonic current shift. Tonic current of each cell was normalized to the cell capacitance as a measure of current density (pA/pF). RMS (root-mean-square) noise was determined for each recording as previously specified (see Methods) (Figure 12C). WT DGGCs displayed concentration-dependent sensitivity to GX-mediated enhancement of tonic currents (1.08 ± 0.17 pA/pF at 0.1 μM; 1.61 ± 0.18 pA/pF at 0.3 μM; and 2.48 ± 0.49 pA/pF at 1 μM). However, the δKO DGGCs exhibited completely attenuated tonic current response at all concentrations of GX tested (0.40 ± 0.12 pA/pF at 0.1 μM; 0.16 ± 0.04 pA/pF at 0.3 μM; and 0.37 ± 0.10 pA/pF at 1 μM). WT DGGCs also showed greater concentration-dependent potentiation of GX-mediated RMS conductance than δKO neurons (Figure 12C). At 0.3 and 1 μM GX, RMS channel conductance was significantly higher in WT DGGCs compared to δKO neurons, indicating greater enhancement in chloride conductance by GX in WT DGGCs. Overall, these results indicate that the δ subunit plays an obligatory role in GX potentiation of extrasynaptic receptor-mediated tonic inhibition.

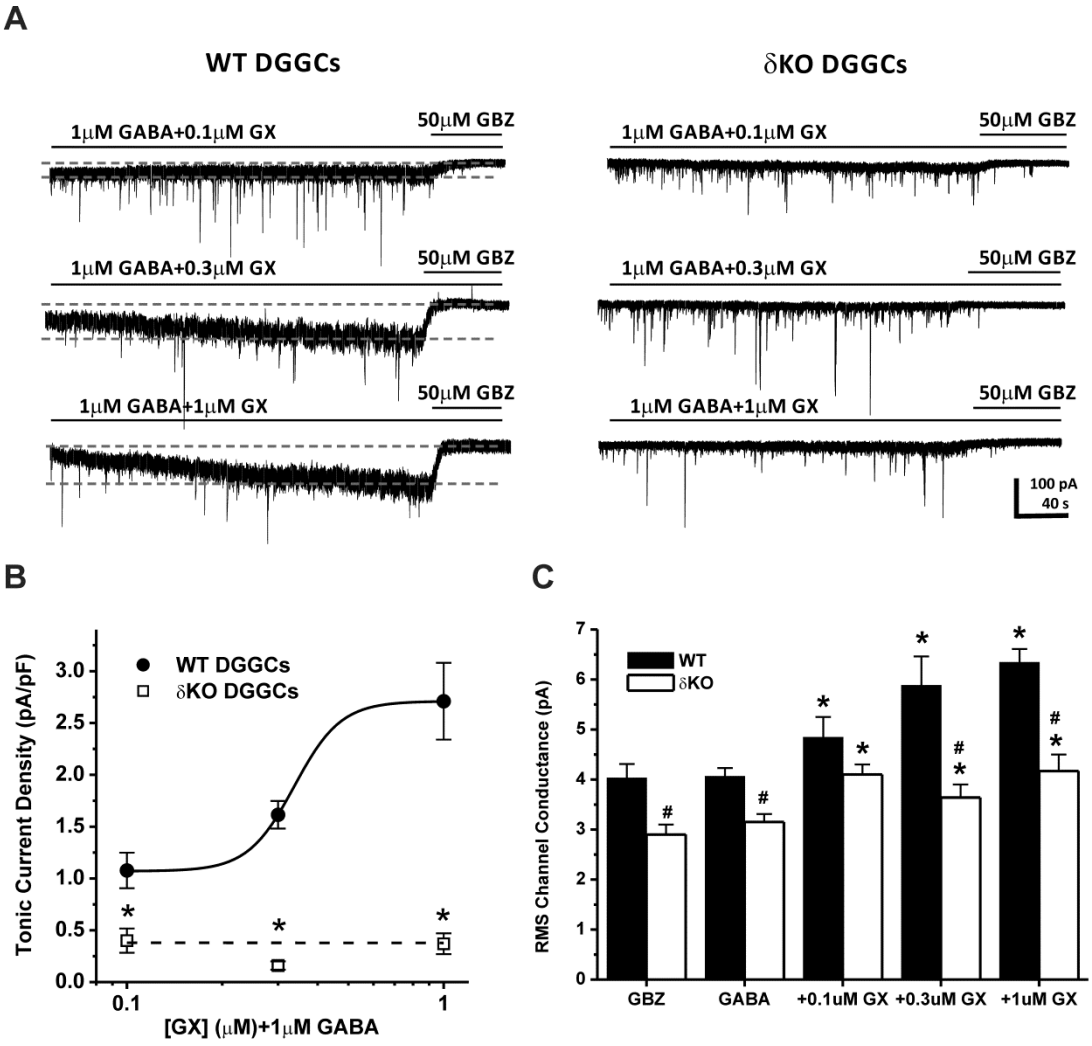

Figure 12 GX allosteric potentiation of GABA-AR-mediated tonic currents and RMS channel conductance are attenuated in DGGCs from δKO mice.

(A) Representative whole-cell current recordings of DGGCs from WT or δKO mice. Qualification of tonic current shift (between 1st and 2nd grey dashed lines) was achieved relative to complete block by gabazine (GBZ) at 50μM. (B) Concentration-response curves for allosteric activation of normalized tonic current density (pA/pF) by GX in DGGCs from WT or δKO mice. *$p < 0.05$ vs. WT. (C) I_{RMS} channel conductance (pA) of GX modulation in DGGCs from WT or δKO mice. Each point or bar represents mean ± SEM. *$p < 0.05$ vs. GABA; #$p < 0.05$ vs. WT (n = 6 – 16 cells).

IV.1.5 Direct Activation of Extrasynaptic δGABA-AR -Mediated Tonic Currents by GX in Hippocampus Slices

To further explore the functional role of the δ subunit in GX activation of GABA-ARs, we examined direct activation of extrasynaptic tonic currents in DGGCs from WT and δKO slices. Voltage-clamp electrophysiology was used to record GABA-AR-mediated potentiation of tonic currents by GX in the absence of GABA application. GX (0.1 μM – 3 μM) was applied in slice recordings (Figure 13A – 13C). 50 μM GBZ was added at the end of each recording to confirm the total tonic current shift. Current density (pA/pF) was obtained by normalizing the tonic current shift with the cell capacitance of each cell. GX (0.1 – 3 μM) directly activated GABA-AR-mediated tonic currents without exogenous GABA application in WT DGGCs in a concentration-dependent manner (0.51 ± 0.09 pA/pF at 0.1 μM; 0.54 ± 0.10 pA/pF at 0.3 μM; 1.50 ± 0.28 pA/pF at 1 μM; and 2.05 ± 0.18 pA/pF at 3 μM). However, in δKO DGGCs, GX tonic current responses were completely diminished at 0.1, 0.3, and 1 μM (0.26 ± 0.07 pA/pF at 0.1 μM; 0.31 ± 0.07 pA/pF at 0.3 μM; and 0.30 ± 0.06 pA/pF at 1 μM). At 3 μM, GX (0.82 ± 0.20 pA/pF) slightly potentiated tonic current response in δKO DGGCs, possibly eliciting a non δ-mediated response. These results demonstrate that GX potentiation of tonic currents is highly selective for δ-containing extrasynaptic GABA-ARs.

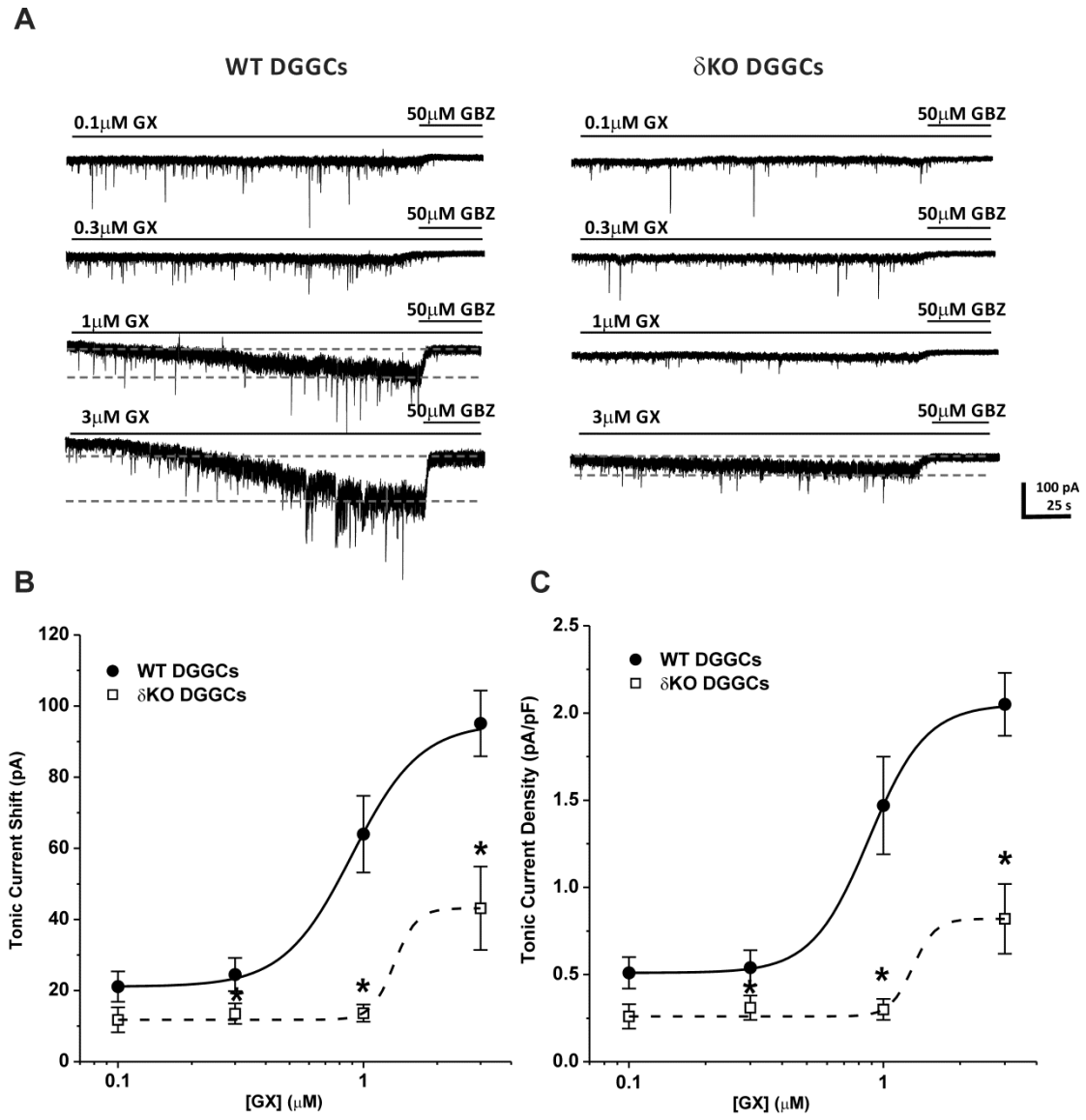

Figure 13 GX direct activation of GABA-AR-mediated tonic currents is attenuated in DGGCs from δKO mice.

(A) Representative whole-cell current recordings of DGGCs from WT or δKO mice. Qualification of tonic current shift (between 1st and 2nd grey dashed lines) was achieved relative to complete block by gabazine (GBZ) at 50 μM. Concentration-response curves for direct activation of tonic currents (pA, B) and normalized tonic current density (pA/pF, C) by GX in DGGCs from WT or δKO mice. Each point represents mean ± SEM. *$p < 0.05$ vs. WT ($n = 5 – 8$ cells).

IV.1.6 GX Modulation of Phasic Currents in DGGCs from WT and δKO Mice

The miniature inhibitory postsynaptic currents (mIPSCs) predominantly reflect the activation of synaptic GABA-ARs. To determine the effects of GX on synaptic GABA-AR-mediated phasic currents, the mIPSCs were isolated in the presence of the NMDA receptor antagonist (APV, 40 μM), the AMPA receptor antagonist (DNQX, 10 μM), and the sodium channel blocker (TTX, 0.5 μM). First, we recorded the endogenous mIPSCs of WT and δKO DGGCs. The average amplitude, frequency, 10-90% rise time, and decay time constant of mIPSCs from WT and δKO DGGCs are displayed in Figure 14. Representative traces and ensemble average mIPSCs from WT and δKO DGGCs are shown in Figure 14A, 14B. The average mIPSC from each cell was best fit with a double-exponential decay curve, depicted as τ_1 and τ_2. A mean weighted decay constant τ_w was also derived from τ_1 and τ_2 (see Materials and Methods). The average amplitude and rise time of mIPSCs were not different between WT and δKO mice (Figure 14C). However, the mean weighted decay time (τ_w) of mIPSCs in δKO neurons (n = 10, 28.2 ± 1.2 ms) was significantly faster than in WT neurons (n = 9, 34.8 ± 2.4 ms), signifying that changes in receptor subunit composition can alter the channel kinetics. Furthermore, the frequency of mIPSCs in δKO DGGCs was modestly smaller than in WT DGGCs (n = 10-12 cells per group, p = 0.06), showing a small reduction in the functional number of GABAergic synapse release sites and the rate of presynaptic release in δKO neurons (Cherubini and Conti, 2001). Overall, these findings are similar and consistent with the results reported previously in δKO mice (Spigelman et al., 2003).

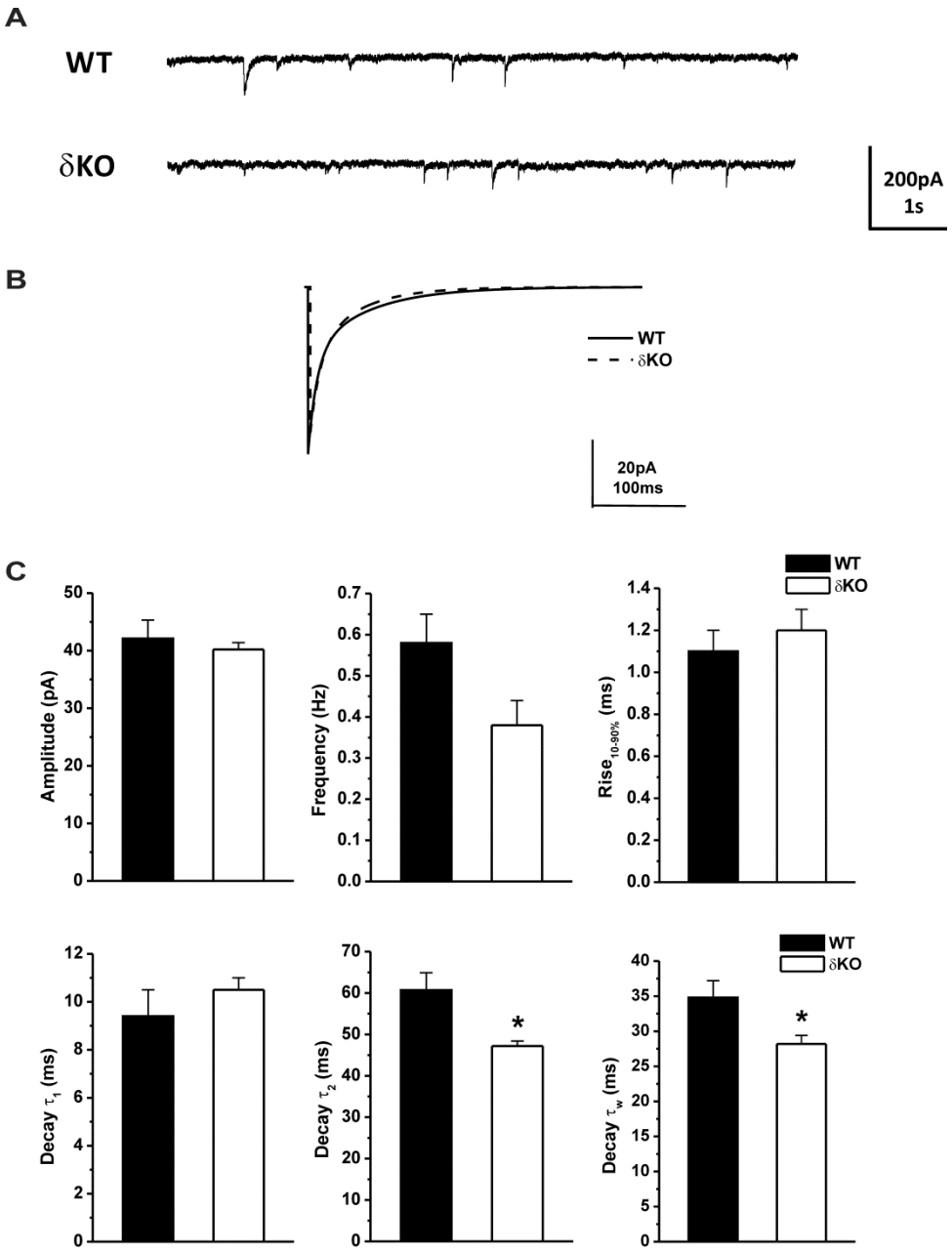

Figure 14 Alterations in mIPSCs kinetics in δKO mice.

(A) Representative traces of endogenous phasic currents by patch-clamping recording from WT or δKO DGGCs. (B) Averaged mIPSC events in the WT (solid line) or δKO (dashed line) DGGCs. (C) The bar graphs represent: amplitude, frequency, rise time (10 – 90%), decay τ_1, decay τ_2, and mean weighted decay (τ_w) of mIPSCs in DGGCs from WT or δKO mice. Each bar represents mean ± SEM. *$p < 0.05$ vs. WT ($n = 9 – 10$ cells).

Next, we analyzed the potentiation of synaptic GABA-AR-mediated mIPSCs by bath application of GX (0.1 – 1 μM) with GABA (1 μM) in WT DGGCs. To determine whether the GX-mediated changes to synaptic activity are related to δ subunit expression, we also recorded mIPSCs in DGGCs from δKO mice (Figure 15). Representative traces and ensemble average mIPSCs for each drug concentration and condition are shown in Figure 15A, 15B. GX has no significant effect on frequency or rise time of mIPSCs (Figure 15D). However, the cumulative probability of amplitude and the mean peak amplitude were strongly enhanced by GX (1 μM) in WT DGGCs but not in δKO DGGCs (Figure 15C). Concentration-dependent potentiation of amplitude of mIPSCs by GX was evident in WT neurons but not in δKO DGGCs. In addition, GX prolonged the decay time constant τ_2 and the mean weighted decay time τ_w of mIPSCs in a concentration-dependent manner in both WT and δKO neurons. However, GX prolonged τ_2 and τ_w decay time constants of mIPSCs to a significantly greater degree in WT DGGCs compared to δKO DGGCs (τ_2: $p = 0.014$ at 0.1 μM; $p = 0.015$ at 0.3 μM; and $p = 0.049$ at 1 μM; τ_w: $p = 0.007$ at 0.1 μM; $p = 0.030$ at 0.3 μM; and $p = 0.066$ at 1 μM, WT vs. δKO). These results suggest that δ-containing GABA-ARs highly contribute to GX-potentiated amplitude of mIPSCs, which reflects its influence on postsynaptic receptor density and dendritic property, and play a pivotal role in the GX-potentiated kinetics of mIPSCs and thereby to the net inhibition.

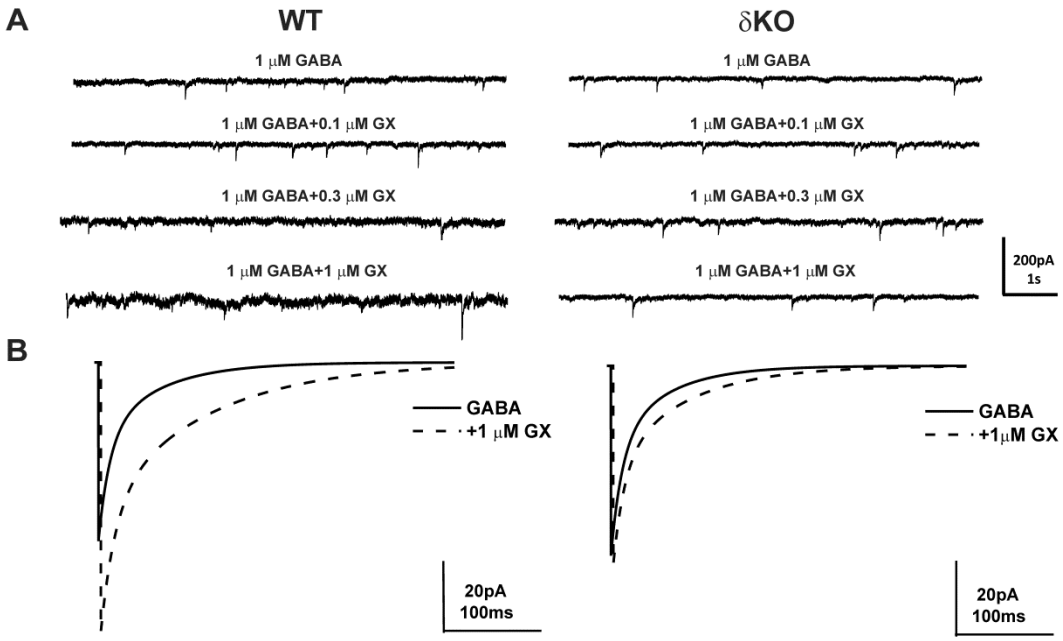

Figure 15 GX concentration-dependent potentiation of mIPSCs is attenuated in DGGCs from δKO mice.

(A) Representative traces of phasic currents by patch-clamping recording from WT or δKO DGGCs in the presence of 1 μM GABA, 1 μM GABA+0.1 μM GX, 1 μM GABA+0.3 μM GX, and 1 μM GABA+1 μM GX. (B) Averaged mIPSC events recorded from WT (B, left) or δKO (B, right) DGGCs in the presence of 1 μM GABA (solid line) or 1 μM GABA co-applied with 1 μM GX (dashed line). Cumulative probability curves for WT (C, left) or δKO (C, right) mIPSC amplitude, plotted from all events. The Kolmogorov–Smirnov test was used to compare mIPSCs before and after application of GX in DGGCs. (C, insets) Mean peak amplitude of mIPSCs in WT (left) or δKO (right) DGGCs in the presence of 1 μM GABA or 1 μM GABA co-applied with 1 μM GX. *p<0.05 vs. GABA alone (n = 14 – 19 cells per drug concentration). (D) Summary graphs of concentration-response relationship for amplitude, frequency, rise time (10-90%), decay τ_1, decay τ_2, and mean weighted decay time (τ_w) of GX modulation in DGGCs from WT or δKO mice. Each point represents mean ± SEM. *p < 0.05; **p < 0.01; ***p < 0.001 vs. GABA; $^{\#}$p < 0.05 vs. WT (n = 7 – 10 cells).

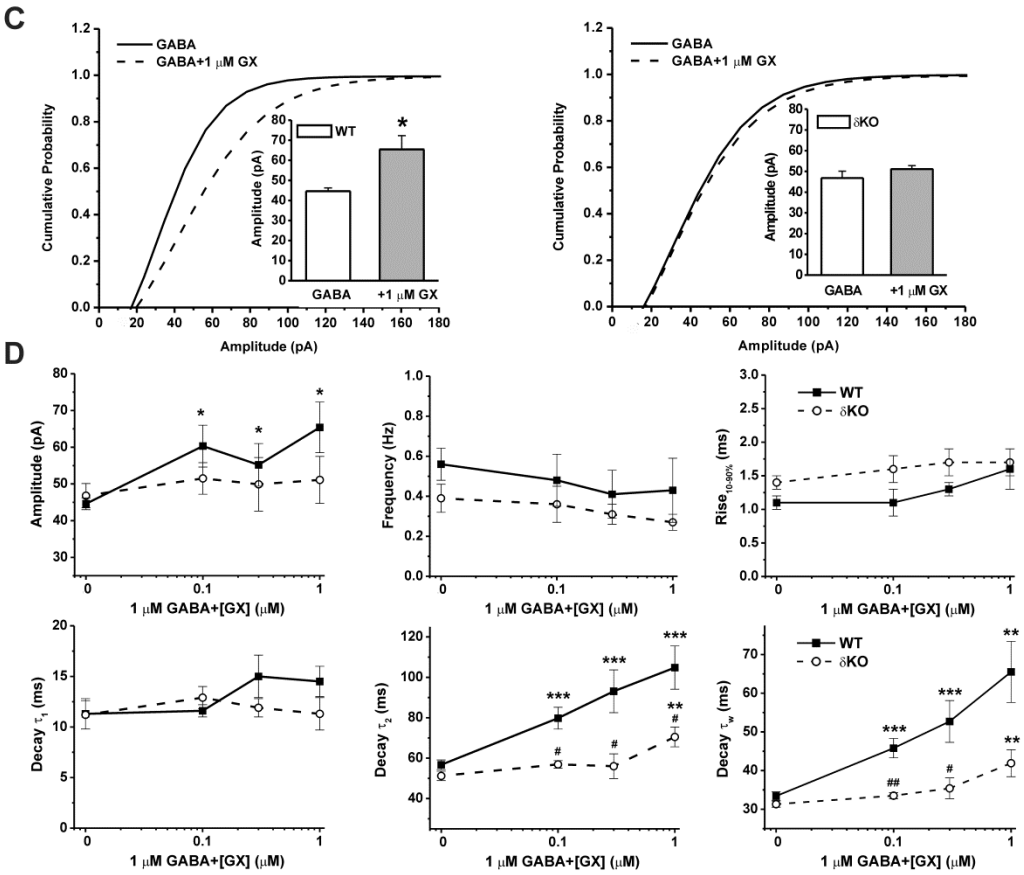

Figure 15 Continued.

IV.1.7 Inhibition of Protein Kinase C Prevents Allosteric Potentiation of Tonic Currents by GX and AP in Hippocampus Slices

Protein kinase C (PKC) activity may affect neurosteroid modulation of GABA-AR function (Fancsik et al., 2000; Harney et al., 2003; Adams et al., 2015). We hypothesize that the PKC inhibitor (PKCi) may also influence the extent of neurosteroid-potentiated tonic inhibition. To explore the effects of PKC activity on GX allosteric potentiation of tonic currents, the PKC inhibitor GF109203X (1 μM) was applied to the bath solution for 15 or 30 minutes before the perfusion of GABA and the application was continued during GABA or neurosteroid perfusion. To compare the mechanism of action of GX with AP, we also examined the influence of PKC inhibitor on AP-potentiated tonic currents. The experimental protocol is shown in Figure 16A. Pretreatment of PKC inhibitor for 15 or 30 min prior the application of GABA reduced GABA-evoked tonic current density from 0.62 ± 0.08 pA/pF to 0.11 ± 0.04 pA/pF and 0.13 ± 0.05, respectively (n = 5 cells per group; Figure 16F). The PKC inhibitor attenuated the allosteric potentiation of AP and GX in a time-dependent manner (Figure 16B – 16F). Pretreatment of PKC inhibitor for 15 or 30 min prior to the application of GABA reduced the tonic current density potentiated by AP from 1.80 ± 0.18 pA/pF to 1.07 ± 0.32 pA/pF and 0.15 ± 0.03, respectively (n = 6 – 9 cells per group, 40.6 ± 17.8% decrease, p = 0.082 and 91.9 ± 1.8% decrease, p = 0.00001, respectively; Figure 16D, 16F). Pretreatment of PKC inhibitor for 15 or 30 min prior to the application of GABA also significantly attenuated the tonic current density potentiated by GX from 1.61 ± 0.18 pA/pF to 0.66± 0.23 pA/pF and 0.49 ± 0.15 pA/pF, respectively (n = 6 – 7 cells per group, 59.2 ± 14.4% decrease, p = 0.009 and 69.8 ± 9.4% decrease, p = 0.001, respectively; Figure 16E, 16F). These results demonstrate that both AP and GX potentiation of tonic current are regulated by the extent of PKC activity in the neurons.

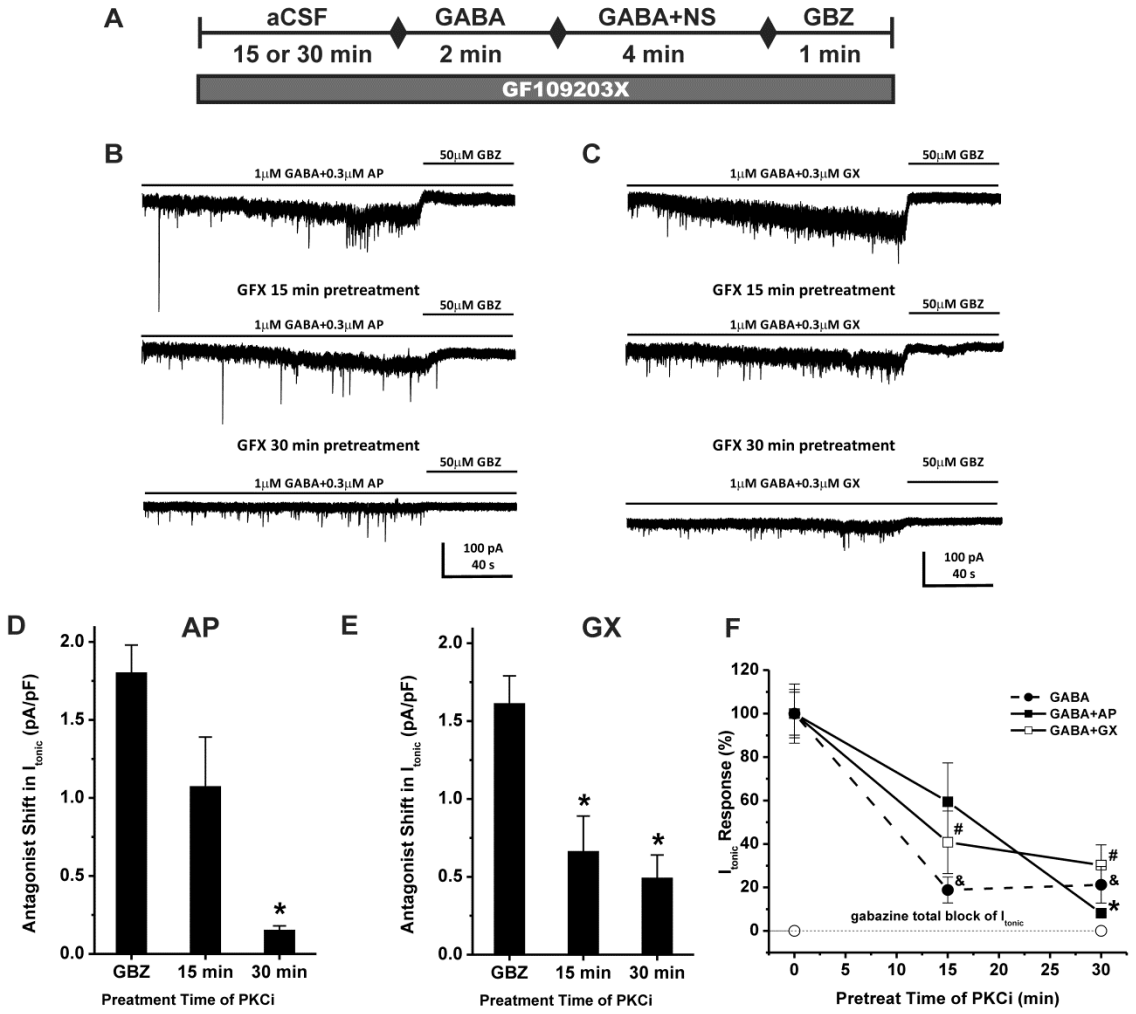

Figure 16 PKC inhibitor (PKCi) prevents neurosteroid potentiation of tonic currents in DGGCs.

(A) Scheme demonstrating experimental protocol. PKCi GX109203X (GFX, 1 μM) was applied to the bath solution for 15 or 30 minutes before the GABA application and the PKCi application was continued during GABA, neurosteroid, and gabazine (GBZ) perfusion. Representative whole-cell current recordings of DGGCs in the presence of GABA + AP (B) or GABA + GX (C) and GBZ with or without PKCi application. Qualification of tonic current shift was achieved relative to complete block by GBZ at 50 μM. (D, E) PKCi attenuation of AP- or GX- potentiated tonic current response. (F) Fractional response of GABA-, GABA + AP- or GABA + GX-modulated tonic current response due to PKCi perfusion. Each point or bar represents mean ± SEM of data from 5 to 9 cells. *$p < 0.05$ vs. GBZ or GABA + AP without PKCi group; $^{\#}p < 0.05$ vs. GABA + GX without PKCi group; $^{\$}p < 0.05$ vs. GABA without PKCi group. NS, neurosteroid.

IV.1.8 Antiseizure Activity of GX in the Hippocampus Kindling Model

To evaluate the activity of GX in protecting against hippocampus kindled seizures, fully-kindled mice were treated with various doses of GX 15 min prior to stimulation. GX produced a dose-dependent reduction of behavioral seizure activity with significant effects on both at 5 and 10 mg/kg (Figure 17A). At the highest dose tested, behavioral seizures were almost entirely inhibited. GX pretreatment markedly reduced the AD duration in a dose-dependent manner (Figure 17B). Furthermore, the overall amplitude was decreased by about 50% after 5 and 10 mg/kg GX. The estimated ED_{50} value for suppression of seizure stage and AD duration is 3.2 ± 0.7 mg/kg and 3.0 ± 0.8 mg/kg, respectively. The time courses for behavioral seizure stage and AD duration after a 10 mg/kg dose of GX are shown in Figure 17C and 17D, respectively. The seizure protective effect of GX (10 mg/kg s.c.) occurred rapidly. The protection was maximal at 15-min and reduced during the 240-min period after the administration as evident by its time-dependent decrease in seizure protection (Figure 17C) and AD duration (Figure 17D). On the day after GX treatment, all mice exhibited stage 5 seizures with AD duration (35 ± 6 s) not significantly different from the control duration (38 ± 5 s), indicating that GX suppresses the expression of behavioral seizures but does not influence the kindled state. To examine the role of δ subunit in GX protection against kindled seizures, the behavioral seizure stage and AD duration at various doses of GX in WT and δKO mice were compared. GX at 3 mg/kg displayed significantly stronger reduction in seizure stage (Figure 17E) and AD duration (Figure 17F) in WT mice compared to δKO mice, indicating that GX suppression of seizure activity is affected by the δ subunit. These results are compatible with the hypothesis that GX protection is possibly due to the potentiation of GABA-AR-mediated inhibition that occurs rapidly within a few minutes, an effect selective for δ-containing GABA-ARs.

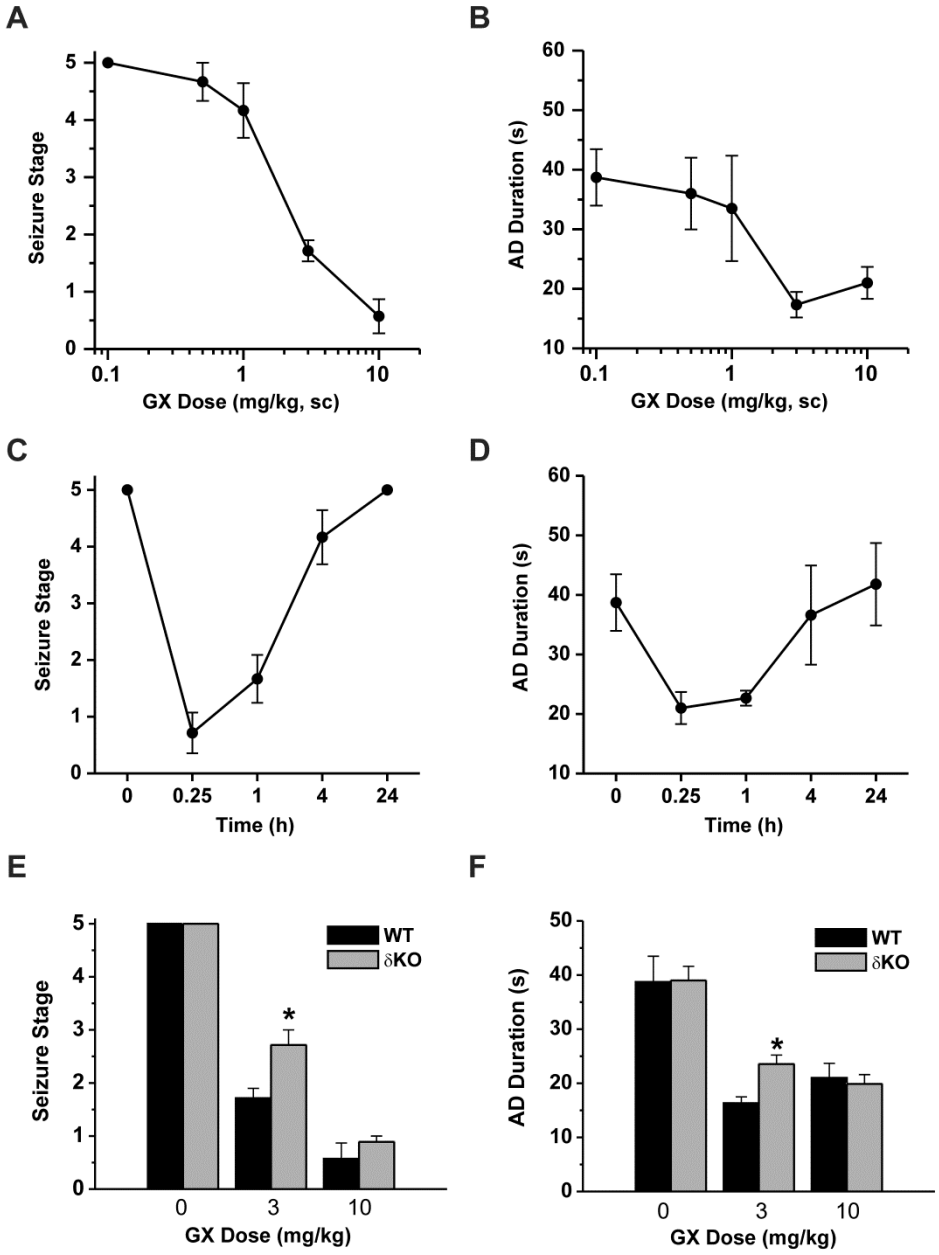

Figure 17 Antiseizure activity of GX in fully-kindled WT and δKO mice.

(A) GX dose-response curves of behavioral seizure activity and (B) afterdischarge (AD) duration. (C) Time courses for behavioral seizure stage and (D) AD duration with GX at 10 mg/kg s.c. in fully kindled mice. (E) GX dose-dependent responses of behavioral seizure activity and (F) AD duration in WT and δKO mice. Each point or bar represents mean ± SEM. *$p<0.05$ vs. WT ($n = 6 – 9$ animals per group).

IV.1.9 GX Analogs as More Selective δGABA-AR Modulators

Structure-activity relationship studies have shown the importance of the α-OH group at the C3 position in the binding affinity and potentiation of synaptic γGABA-ARs by neurosteroids (Harrison et al., 1987; Mitchell et al., 2008). Additionally, the ketone group at the C17 and C20 position and the lipophilic properties of neurosteroids are critical for the potency and efficacy of receptor modulation (Kokate et al., 1994; Upasani et al., 1997; Covey et al., 2000; Chisari et al., 2009; Reddy and Jian, 2010; Qian et al., 2014). Our structure-activity relationship studies at extrasynaptic δGABA-ARs also demonstrate the requirement of the α-OH group at the C3 position for the functional activation of extrasynaptic receptors and the influence of alternations at the C17 and C20 position in the modulation efficacy and receptor binding affinity (Carver and Reddy, 2016). To further identify key structural features of neurosteroids that are important for the functional activation of extrasynaptic δGABA-ARs, we compared the modulatory effects of GX and its analog 21-OH-GX (Figure 8) which has an additional OH group at C21 position on whole-cell GABA-gated chloride currents and extrasynaptic δGABA-AR-mediated tonic currents. We also investigated the role of δ subunit in 21-OH-GX potentiation of tonic inhibition. In dissociated DGGCs, 21-OH-GX allosterically potentiated GABA-gated currents in a concentration-dependent manner (Figure 18A). 21-OH-GX displayed significantly greater potentiation of GABA-gated chloride currents ($EF_{2\text{-fold GABA}}$ = 0.20 μM) than GX ($EF_{2\text{-fold GABA}}$ = 0.43 μM, Figure 18B). In hippocampus slices, WT DGGCs displayed concentration-dependent sensitivity to 21-OH-GX-mediated enhancement of tonic currents (0.80 ± 0.26 pA/pF at 0.1 μM; 1.44 ± 0.24 pA/pF at 0.3 μM; and 3.00 ± 0.49 pA/pF at 1 μM). The tonic current responses were not significantly different between GX and 21-OH-GX at 0.1 and 0.3 μM but were potentiated slightly more by 21-OH-GX at 1 μM (GX, 2.48 ± 0.49 pA/pF at 1 μM, $EF_{2\text{-fold GABA}}$ = 0. 29 μM; 21-OH-GX, 3.00 ± 0.49 pA/pF at 1 μM, $EF_{2\text{-fold GABA}}$ = 0. 23 μM, Figure 19A, 19B). However, 21-OH-GX potentiation of tonic inhibition at 0.3 and 1 μM was significantly attenuated in DGGCs from mice (0.39 ± 0.08 pA/pF at 0.1 μM; 0.49 ±

0.19 pA/pF at 0.3 μM; and 0.90 ± 0.15 pA/pF at 1 μM, *p<0.05 vs. WT, Figure 19C – 19E), indicating its selectivity for extrasynaptic δGABA-ARs.

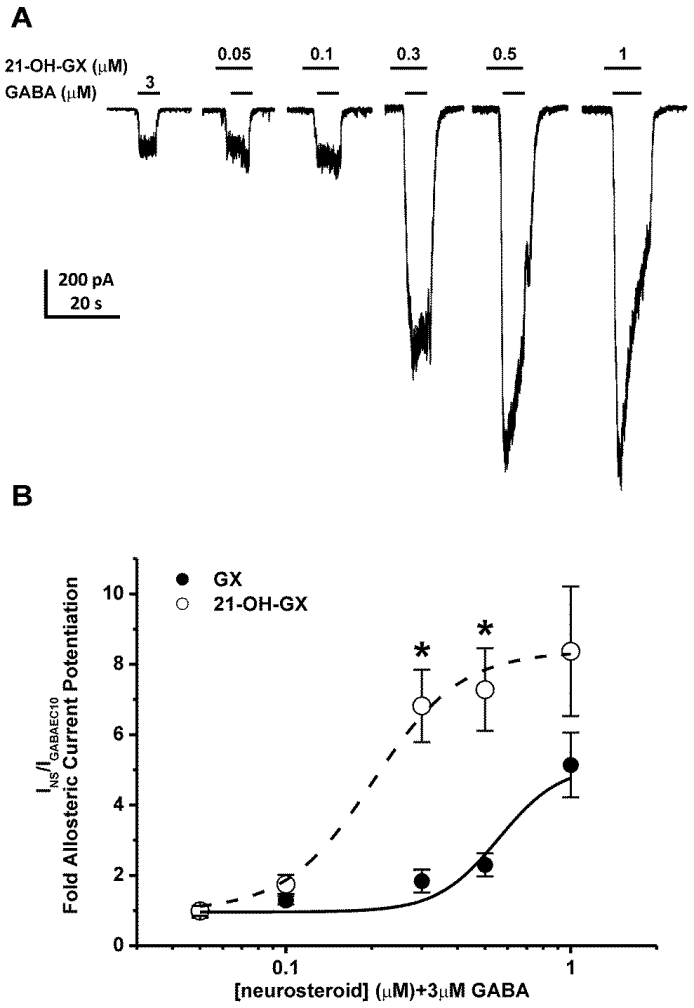

Figure 18 Comparison of allosteric modulation of GABA-gated currents by GX and 21-OH-GX in acutely dissociated DGGCs.

21-OH-GX displayed significantly greater potentiation of GABA-gated chloride currents ($EF_{2\text{-fold GABA}}$ = 0.20 μM) than GX ($EF_{2\text{-fold GABA}}$ = 0.43 μM). (A) Representative whole-cell current recordings in DGGCs. (B) Concentration-response curves of neurosteroid-modulated allosteric potentiation of chloride currents in DGGCs. Neurons displayed concentration-dependent responses to neurosteroid potentiation of 3 μM GABA (EC_{10}). Each point represents mean ± SEM. *p < 0.05 vs. GX (n = 6 – 10 cells).

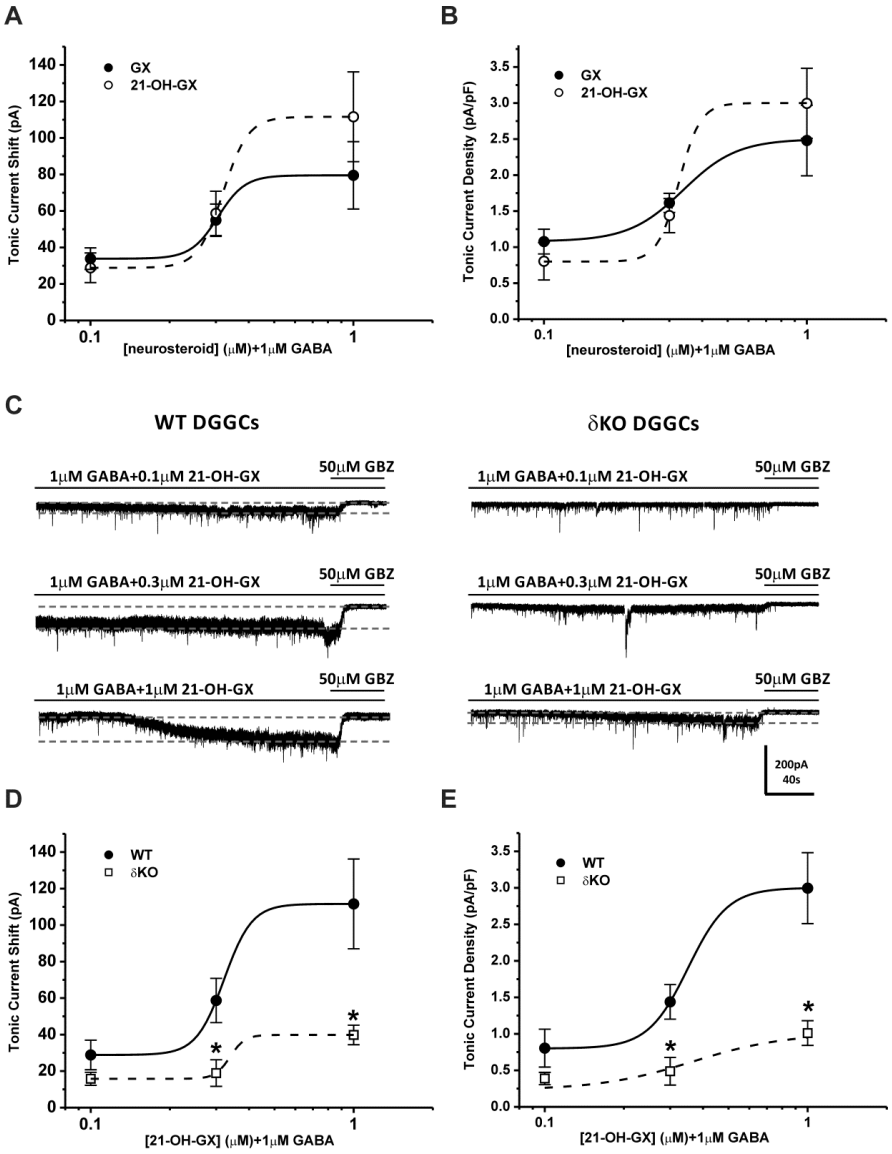

Figure 19 Comparison of allosteric modulation of tonic currents by GX and 21-OH-GX in hippocampus slices from WT and δKO mice.

21-OH-GX displayed slightly greater potentiation of tonic currents ($EF_{2\text{-fold GABA}}$ = 0. 23 μM) than GX ($EF_{2\text{-fold GABA}}$ = 0. 29 μM). 21-OH-GX potentiation of tonic inhibition at 0.3 and 1 μM was significantly diminished in DGGCs from δKO mice. Concentration-response curves for allosteric activation of tonic current (pA, A, D) and normalized tonic current density (pA/pF, B, E) by GX and 21-OH-GX in DGGCs from WT or δKO mice. (C) Representative whole-cell current recordings of DGGCs from WT or δKO mice. Qualification of tonic current response (between 1st and 2nd grey dashed lines) was achieved relative to complete block by gabazine (GBZ) at 50 μM. Each point represents mean ± SEM. *$p < 0.05$ vs. WT (n = 7 – 16 cells per drug concentration).

IV.1.10 Antiseizure Activity of GX Analogs in the Kindling Model

We compared the activity of GX and 21-OH-GX in protecting against hippocampus kindled seizures. Fully-kindled mice were treated with various doses of GX and 21-OH-GX 15 min prior to stimulation. As shown in Figure 20, both GX and 21-OH-GX produced a dose-dependent reduction of behavioral seizure activity (Figure 20A) and AD duration (Figure 20B). However, 21-OH-GX displayed greater antiseizure activity compared to GX although such effect was significant at 3 mg/kg dose (Figure 20A). Overall, the GX analog 21-OH-GX displayed stronger potentiation in GABAergic chloride currents and extrasynaptic δGABA-AR-mediated tonic inhibition; possibly conveying a stronger antiseizure effect than GX.

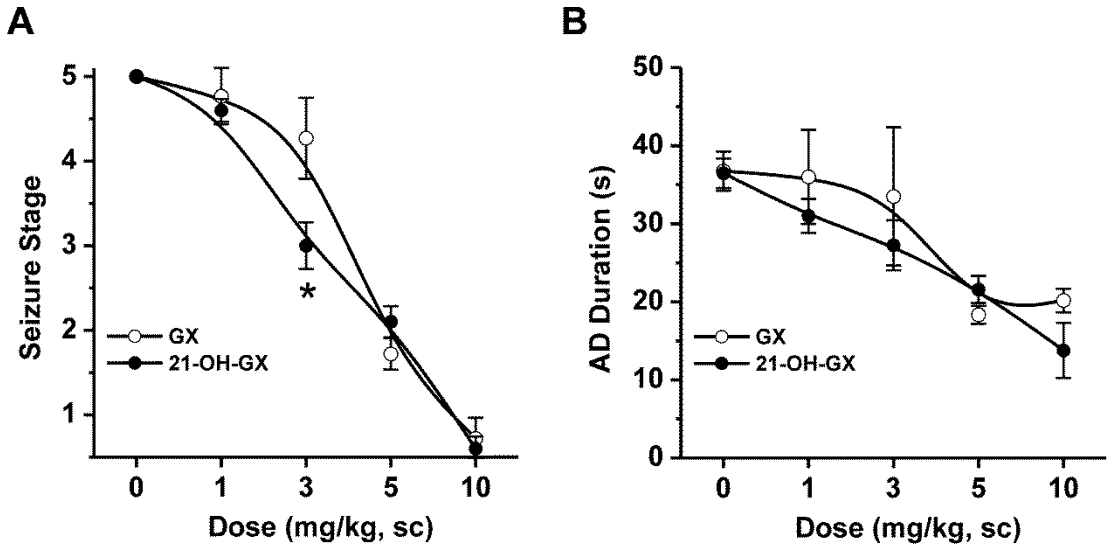

Figure 20 Comparative antiseizure effects of GX and 21-OH-GX in the hippocampus kindling model in mice.

(A) Dose-response curves of behavioral seizure activity and (B) afterdischarge (AD) duration in fully-kindled WT mice. Each point represents mean ± SEM. *$p < 0.05$ vs. GX ($n = 6 – 9$ animals per group).

IV.2 Zinc Reduces Antiseizure Activity of Neurosteroids by Selective Blockade of Extrasynaptic δGABA-AR-Mediated Tonic Inhibition in the Hippocampus

IV.2.1 Concentration-Dependent Inhibition of GX Potentiation of GABA-Gated Currents by Zn^{2+} in Hippocampal Neurons

We first examined the blockade of GABAergic chloride currents with Zn^{2+}, a negative allosteric modulator of GABA-ARs (Smart et al., 1991; Kapur and Macdonald, 1997; Barberis et al., 2000; Carver et al., 2016). To examine the effects of subunit composition on Zn^{2+} inhibition of GABA-ARs, concentration-response profiles were compiled in two cell types: δ-abundant DGGCs and δ-sparse CA1 pyramidal cells (CA1PCs). 3 μM GABA (EC_{10}) was applied for 5 seconds followed by the application of Zn^{2+} for 5 seconds (Figure 21A – 21C). GABA at 3 μM induced 249.5 ± 16.5 and 538.1 ± 34.3 pA of currents in DGGCs and CA1PCs, respectively. Zn^{2+} blocked inhibitory GABAergic chloride currents concentration-dependently in both cell types. The Zn^{2+} at 1, 3, 10, and 30 μM application blocked a mean 56.7 ± 6.9 %, 81.6 ± 6.4 %, 89.0 ± 5.7 %, and 90.4 ± 5.6 % of GABA-induced currents in DGGCs, respectively. While the Zn^{2+} at 1, 3, 10, and 30 μM blocked a mean 64.3 ± 11.4 %, 70.4 ± 12.0 %, 87.3 ± 3.6 %, and 93.1 ± 1.6 % of GABA-induced currents in γ2-containing CA1PCs, respectively. GABA-modulated currents fully returned to peak amplitude after the removal of Zn^{2+} application. The half maximal inhibitory concentrations (IC_{50}) for Zn^{2+} block of 3 μM GABA-induced currents were 0.72 and 0.70 μM in DGGCs and CA1PCs, respectively. These results show a similar concentration-dependent profile of Zn^{2+} blockade of GABA-gated chloride currents in DGGCs and CA1PCs.

Next, we studied the modulatory effects of Zn^{2+} on GX-potentiated GABA-gated currents. GX at 1 μM was co-applied with 3 μM GABA to obtain the fractional potentiation of GABAergic currents mediated by GX. Subsequent application of Zn^{2+} (1 – 30 μM) blocked whole-cell inhibitory currents in a concentration-dependent manner (Figure 22A – 22C). In δ-containing DGGCs, the IC_{50} for Zn^{2+} block of 3 μM GABA + 1 μM GX

currents was 0.44 μM. The 1 μM Zn^{2+} application blocked a mean 62.2 ± 11.6 % of whole-cell current modulation by GX. The 3 μM Zn^{2+} application blocked a mean 77.4 ± 10.5 % of whole-cell current modulation by GX. The 10 μM Zn^{2+} application blocked a mean 86.1 ± 4.8 % of whole-cell current modulation by GX. A 30 μM concentration of Zn^{2+} completely blocked GABA-AR whole-cell currents, similar to that of the competitive antagonism of channels by bicuculline and gabazine. In γ-containing CA1PCs, the sensitivity of Zn^{2+} inhibition on GX-induced currents was modestly reduced compared to that of Zn^{2+} in DGGCs (Figure 22B). The IC_{50} for Zn^{2+} block of 3 μM GABA + 1 μM GX currents was 0.93 μM, which is 2.1-fold higher than that of Zn^{2+} in DGGCs (0.44 μM). The 1 μM Zn^{2+} application blocked a mean 48.7 ± 10.7 % of whole-cell current modulation by GX. The 3 μM Zn^{2+} application blocked a mean 58.1 ± 11.9 % of whole-cell current modulation by GX. The 10 μM Zn^{2+} application blocked a mean 84.5 ± 8.7 % of whole-cell current modulation by GX. A 30 μM concentration of Zn^{2+} blocked a mean 87.3 ± 8.2 % of whole-cell currents. Overall, our results demonstrated that concentration-dependent blockade of Zn^{2+} on GX-potentiated GABA-gated chloride currents has higher sensitivity at neurons that have a higher expression of δ-containing GABA-ARs.

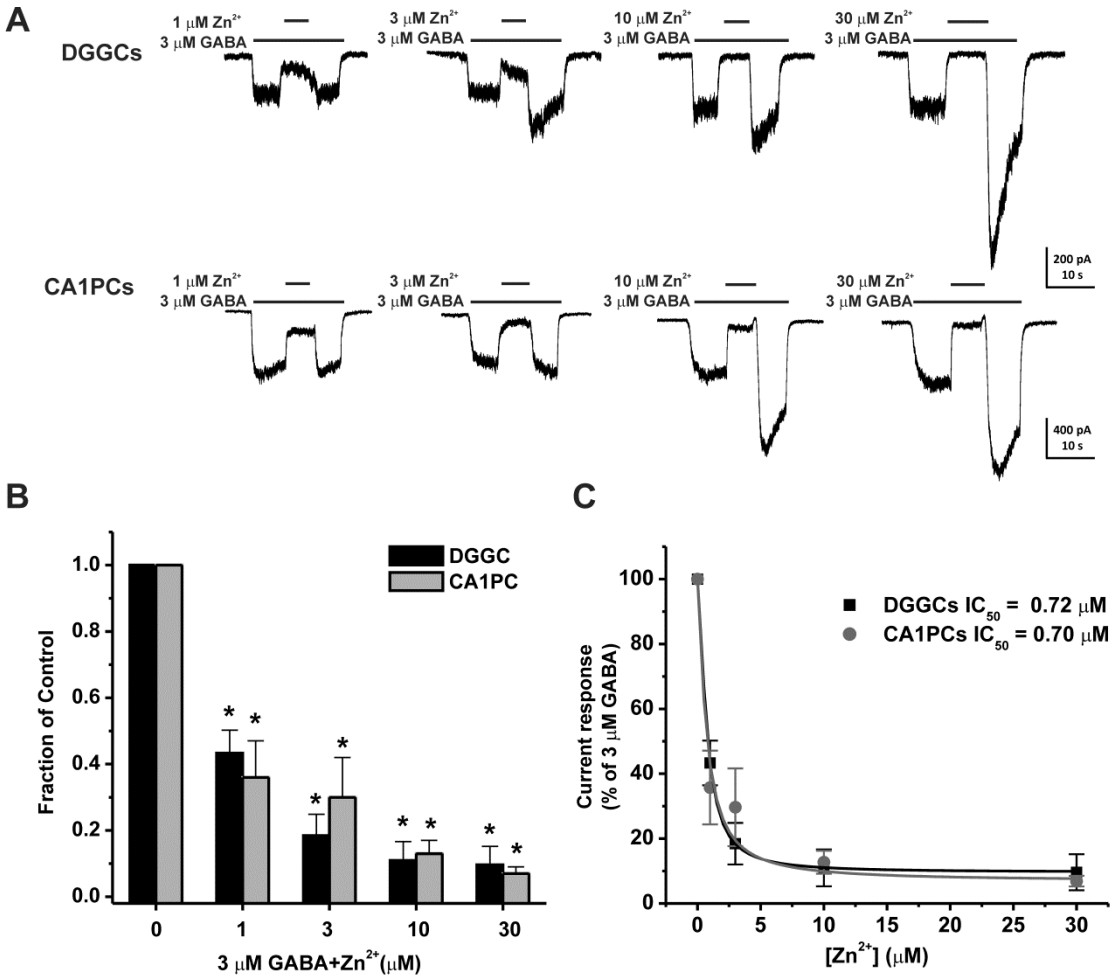

Figure 21 Zn^{2+} blockade of GABA-gated currents is concentration-dependent in dissociated DGGCs and CA1PCs.

(A) Representative whole-cell GABAergic current recordings from DGGCs and CA1PCs. Zn^{2+} (1 – 30 μM) inhibited GABA currents in a concentration-dependent fashion. (B) Fractional block of currents by Zn^{2+} (1 – 30 μM). (C) Inhibitory concentration response curves of DGGCs and CA1PCs by Zn^{2+}. DGGCs IC_{50} = 0.72 μM; CA1PCs IC_{50} = 0.70 μM. *$p < 0.05$ vs. control. Each bar represents mean ± SEM (n = 4 – 6 cells per group).

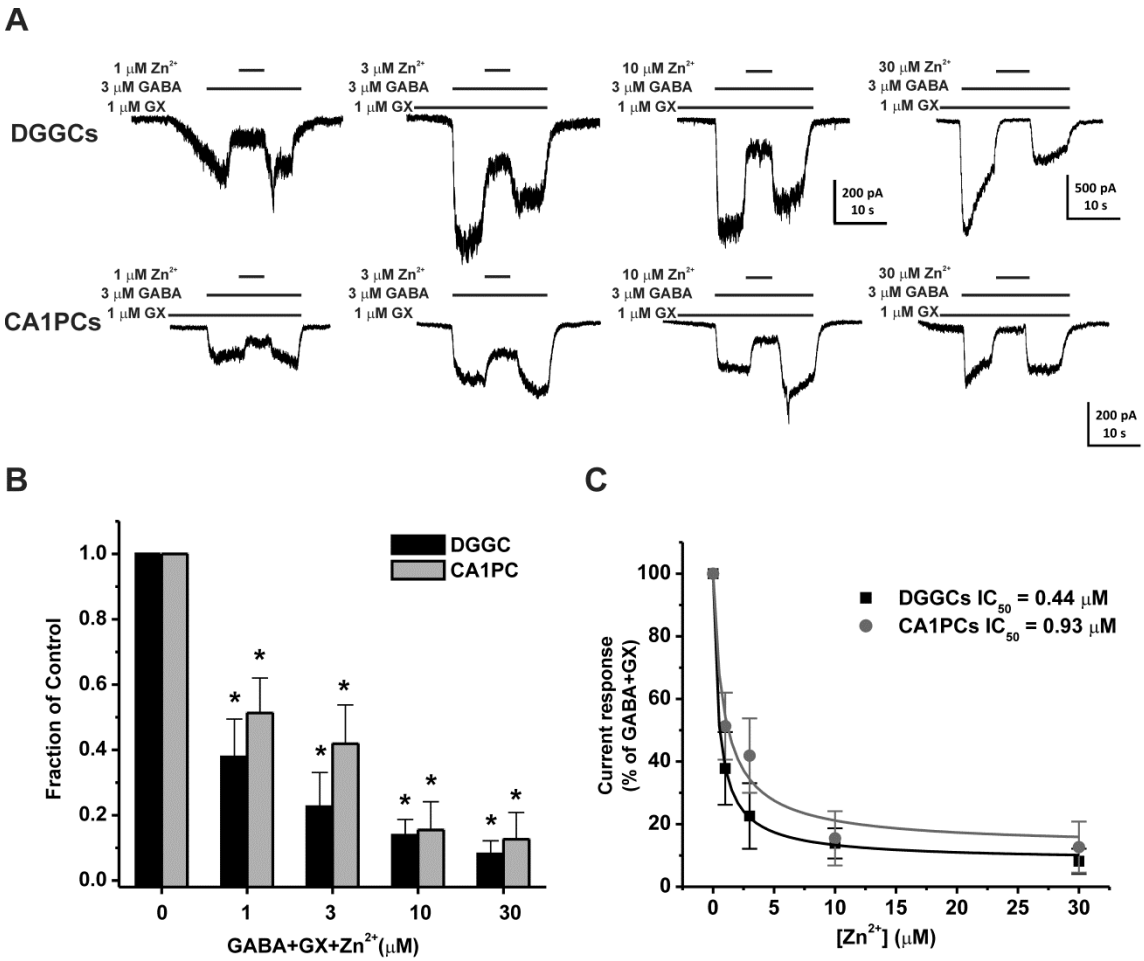

Figure 22 Zn^{2+} blockade of GX-sensitive GABA-gated currents is concentration-dependent in dissociated DGGCs and CA1PCs.

(A) Representative whole-cell GX-activated GABAergic current recordings from DGGCs and CA1PCs. Zn^{2+} (1 – 30 μM) inhibited GX-potentiated GABA currents in a concentration-dependent fashion. (B) Fractional block of currents by Zn^{2+} (1 – 30 μM). (C) Inhibitory concentration response curves of DGGCs and CA1PCs by Zn^{2+}. DGGCs IC_{50} = 0.44 μM; CA1PCs IC_{50} = 0.93 μM. *p < 0.05 vs. control. Each bar represents mean ± SEM (n = 4 – 5 cells per group).

IV.2.2 Selective Antagonism of GX Potentiation of Tonic Currents by Zn^{2+} in Hippocampal Slices

To examine the interactions of Zn^{2+} with GX at extrasynaptic δ-containing GABA-ARs, we recorded GX-activated tonic currents from DGGCs in the hippocampus slice using whole-cell voltage-clamp (-65 mV) recording. At the end of each recording, 50 μM gabazine was perfused to determine the total tonic current shift. Tonic current of each cell was normalized to the cell capacitance as a measure of current density (pA/pF). A physiological concentration of GABA (0.2 μM) was used to examine GX allosteric potentiation (Wlodarczyk et al., 2013). Our results showed that application of 0.2 μM GABA + 0.3 μM GX resulted in a negative shift in the holding current level and an increase in the RMS channel conductance (Figure 25A). However, Zn^{2+} (100 μM) perfusion positively shifted GX-potentiated tonic currents (current density: GABA + GX, 0.96 ± 0.18 pA/pF; GABA + GX + Zn^{2+}, 0.72 ± 0.11 pA/pF, n = 5 cells). To further demonstrate the pharmacological sensitivity of Zn^{2+} blockade of GX-induced tonic current potentiation, 1 μM of GABA and GX were used to record tonic responses (Figure 23A). Subsequent application of Zn^{2+} (0.1 – 10 mM) induced a concentration-dependent blockade of tonic current density, measured as positive shift of the holding currents (Figure 23B). Zn^{2+} (100 μM) wash-out reversed the holding currents to the previously enhanced level by GX. However, with the application of 1 mM Zn^{2+}, Zn^{2+} wash-out was not able to eliminate the effects induced by Zn^{2+}. The IC_{50} value for Zn^{2+} blockade of tonic currents was 0.186 mM (Figure 23C). The mean and the standard deviation (s.d.) of the tonic currents for different Zn^{2+} concentrations were plotted in Figure 23D. Higher the mean of tonic currents was accompanied with higher the s.d. of tonic currents. Zn^{2+} concentration-dependently reduced both the mean and s.d. of GX-potentiated tonic currents. Zn^{2+} at 0.1, 1, and 10 mM caused 56.2 ± 6.0 %, 60.8 ± 3.0 %, and 98.3 ± 0.7 % reduction of GX-potentiated tonic currents, respectively. Zn^{2+} also significantly reduced GX-potentiated RMS channel conductance at all concentration tested (Figure 23E). Zn^{2+} at 10 mM caused 42.0 ± 1.7 % reduction of the RMS channel conductance, similar to that

of the competitive antagonist gabazine (44.0 ± 1.8 %). Overall, these results demonstrate a concentration-dependent blockade of Zn^{2+} on GX-potentiated tonic currents.

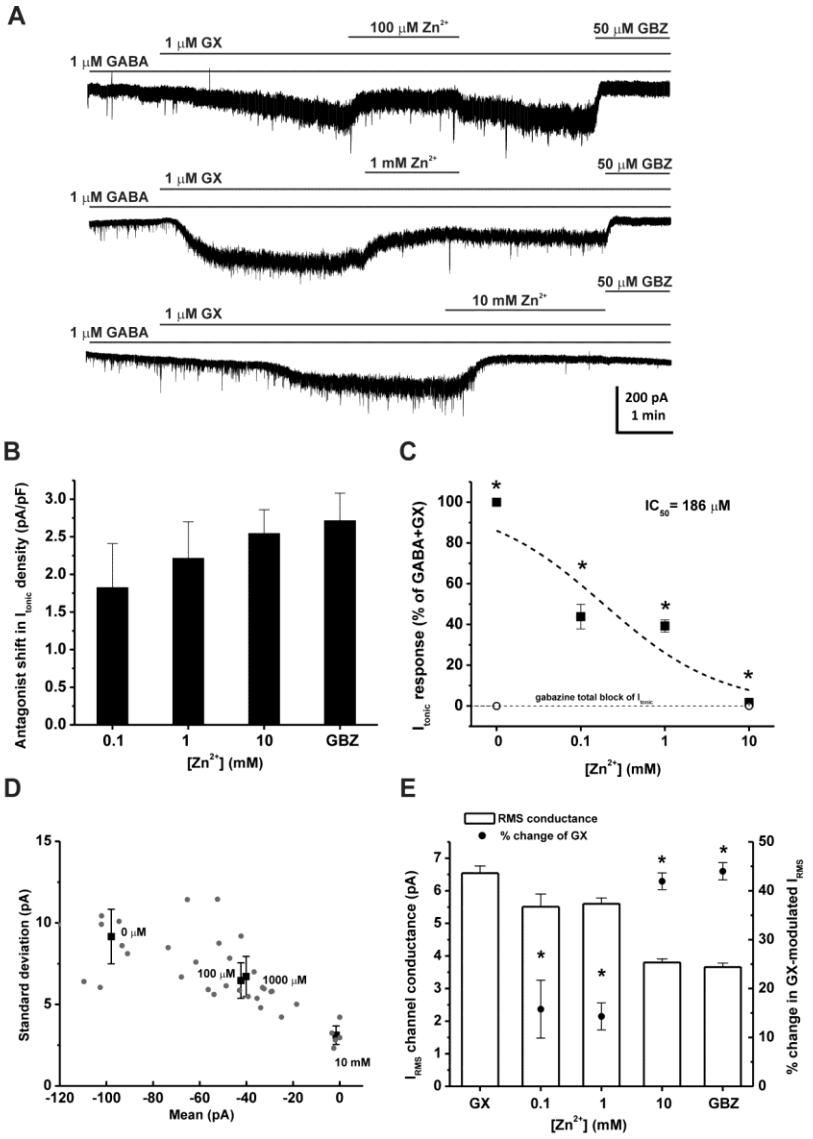

Figure 23 GX-potentiated tonic currents are sensitive to Zn^{2+} blockade in DGGCs in hippocampus slices.

(A) Representative GABAergic I_{tonic} recording from DGGCs in the presence of GABA + GX, Zn^{2+}, and 50 μM gabazine (GBZ). (B) Concentration-responses of GX-modulated, normalized I_{tonic} (pA/pF) to block by Zn^{2+} (0.1 – 10 mM). (C) Fractional responses of GX-modulated I_{tonic} due to Zn^{2+} (*$p < 0.05$ vs. maximal block due to saturating 50 μM gabazine (GBZ). (D) Zn^{2+} reduced the mean and standard deviation of GX-potentiated tonic currents in a concentration-dependent fashion. (E) I_{RMS} channel conductance (pA) and % change of Zn^{2+} blockade of GX-dependent I_{RMS}. GX denotes 1 μM GABA + 1 μM GX condition without Zn^{2+}. *$p < 0.05$ vs. GX. I_{tonic} denotes tonic currents. Each bar represents mean ± SEM (n = 6 – 21 cells per group).

IV.2.3 GX Potentiation of Phasic Currents is Insensitive to Zn^{2+} Antagonism

Next, to examine the block of Zn^{2+} on GX-potentiated phasic currents in DGGCs, we recorded GX-activated mIPSCs, which primarily reflect the activation of synaptic GABA-ARs, in the presence of the NMDA receptor antagonist (APV, 40 μM), the AMPA receptor antagonist (DNQX, 10 μM), and the sodium channel blocker (TTX, 0.5 μM) (Figure 24). Representative traces and ensemble average mIPSCs for each condition are shown in Figure 25A, 25B. The average mIPSC from each cell was best fit with a double-exponential decay curve, depicted as τ_1 and τ_2. A mean weighted decay constant τ_w was also derived from τ_1 and τ_2 (see Materials and Methods). Table 6 showed the characteristics of mIPSCs modulated by GABA, GX, or Zn^{2+}. GX significantly potentiated the amplitude, decay time τ_2, and the mean weighted decay time τ_w of mIPSCs from DGGCs (Figure 24C, 24D). However, Zn^{2+} perfusion did not change GX-modulated mean peak amplitude or decay time constant. These findings indicate that Zn^{2+} blockade of GX-induced GABAergic currents is highly selective for extrasynaptic δGABA-AR-mediated tonic currents.

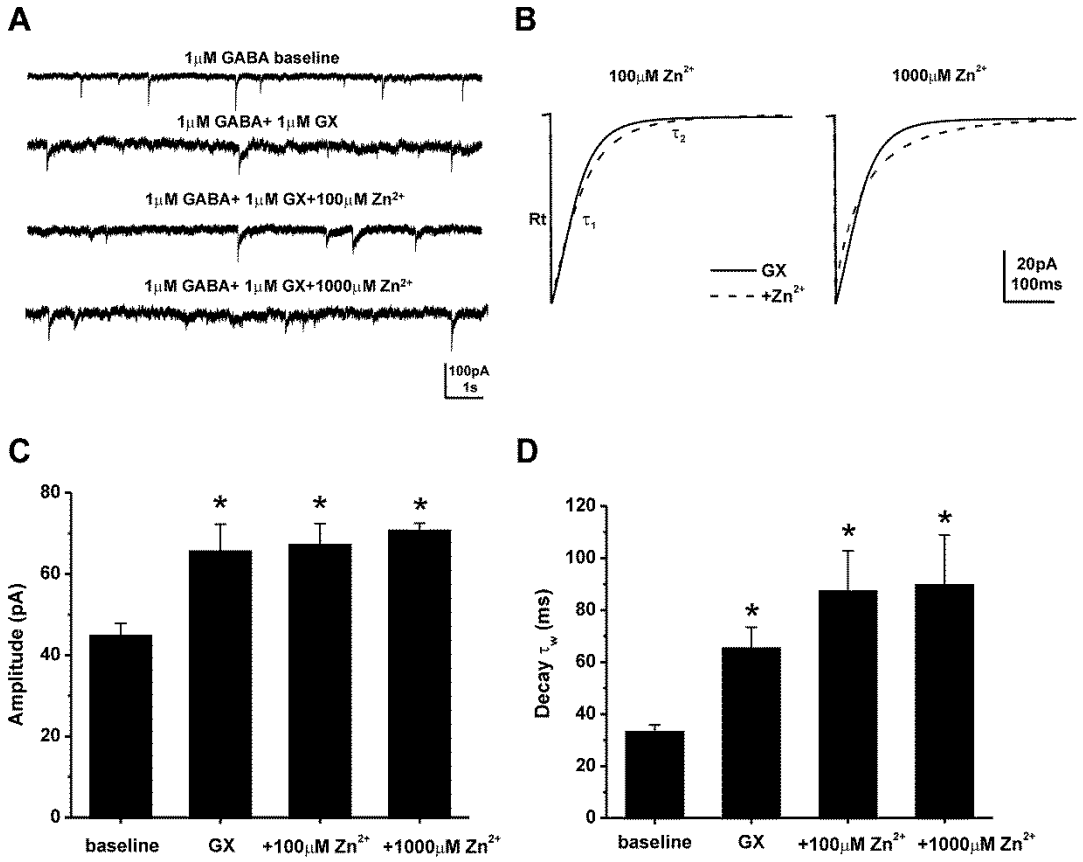

Figure 24 GX-activated mIPSCs are not sensitive to Zn^{2+} blockade.

(A) Representative traces of mIPSCs. GABA-AR mIPSC activity was isolated by using TTX, APV, and DNQX, and was completely blocked by gabazine. GX (1 μM) potentiated synaptic current but Zn^{2+} did not significantly alter the GX-potentiated mIPSCs. (B) Averaged mIPSCs in the presence of GX (solid line) and addition of Zn^{2+} (dashed line). (C) Amplitudes were not significantly different between GX and 100 μM Zn^{2+} ($p = 0.65$), or GX and 1000 μM Zn^{2+} ($p = 0.70$). (D) Zn^{2+}did not significantly alter mean weighted decay kinetics (τ_w) of GX modulation. Data bars represent mean ± SEM ($n = 4 – 9$ cells per group). *$p < 0.05$ vs. baseline. GX denotes GABA + GX; baseline denotes GABA alone; Rt denotes rise time.

Table 6 GABA-AR-mediated mIPSC characteristics in DGGCs.

Group (n)	Amplitude (pA)	Rise$_{10\text{-}90\%}$ [a] (ms)	Decay τ_1 (ms) [a]	Decay τ_2 (ms) [a]	Decay τ_w (ms)	Frequency (Hz)
1μM GABA (13)	43.1 ± 1.5	1.1 ± 0.1	10.6 ± 1.3	48.0 ± 1.9	30.2 ± 1.4	0.56 ± 0.08
GABA+1μM GX (9)	65.4 ± 6.9*	1.6 ± 0.3	14.5 ± 1.5	104.8 ± 10.7*	65.5 ± 7.9*	0.43 ± 0.16
GABA+GX+100μM Zn^{2+} (5)	67.0 ± 5.4*	1.0 ± 0.3	22.4 ± 4.7*$^{\#}$	114.1 ± 16.1*	87.4 ± 15.4*	0.30 ± 0.17
GABA+GX+1000μM Zn^{2+} (4)	70.5 ± 2.0*	1.0 ± 0.1	18.7 ± 3.9*$^{\#}$	144.9 ± 18.9*	89.9 ± 18.9*	0.10 ± 0.02*

*$p < 0.05$ vs. GABA; $^{\#}p < 0.05$ vs. GABA+GX.

IV.2.4 The Zn^{2+} Chelator TPEN Reverses Zn^{2+} Blockade of GX-Sensitive Tonic Currents

To further confirm the Zn^{2+} blockade of extrasynaptic δGABA-ARs, we investigated tonic current response in the presence of a membrane-permeable, high affinity Zn^{2+} chelator, N,N,N',N'-tetrakis(2-pyridylmethyl)ethylenediamine (TPEN). Zn^{2+} (100 μM) perfusion blocked GX-potentiated tonic currents in DGGCs, resulting in a positive shift of tonic current density (0.24 ± 0.09 pA/pF). Such blockade by Zn^{2+} was prevented when TPEN (100 μM) was added to the perfusion, and DGGCs displayed -0.27 ± 0.11 pA/pF negative shift in tonic current density (Figure 25). The differences between Zn^{2+}-antagonized and TPEN-enhanced tonic currents achieve statistical significance ($p = 0.008$, $n = 5$ cells per group). Without exogenous Zn^{2+} added to perfusion, TPEN sustained the negative shift of current density modulated by GX (-0.2 ± 0.08 pA/pF, $n = 5$ cells), indicating significant modulation of endogenous Zn^{2+} within the hippocampus.

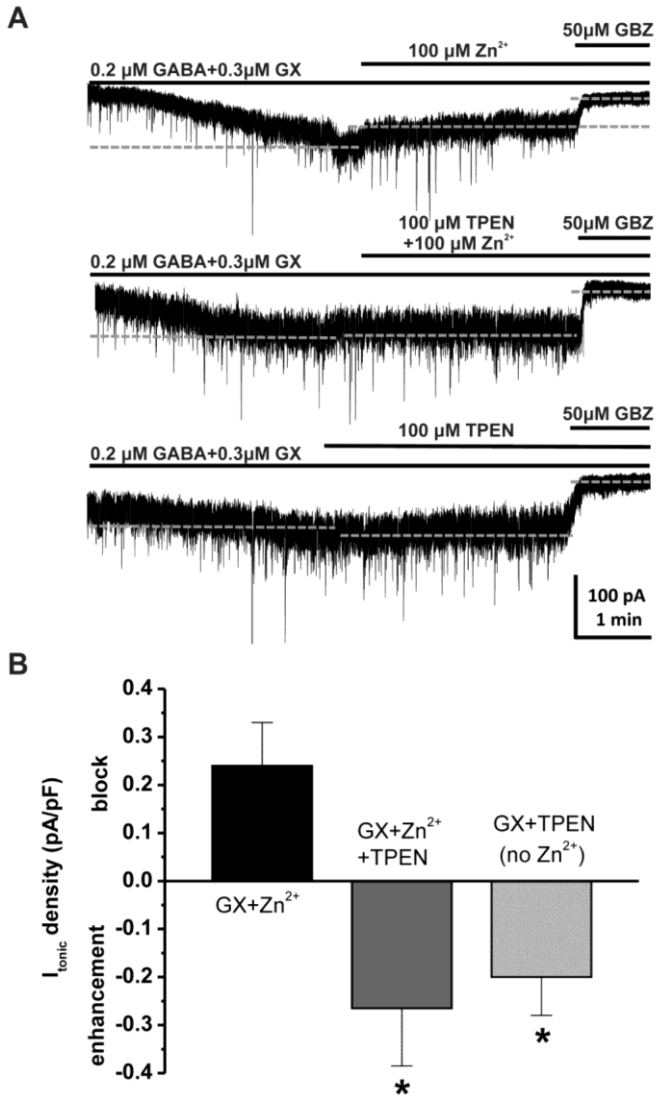

Figure 25 Zn^{2+} chelator TPEN inhibits the Zn^{2+} antagonism of GX-sensitive tonic currents.

(A) Representative GABAergic I_{tonic} recordings from DGGCs before and after the application of Zn^{2+} (100 μM) or Zn^{2+} chelator TPEN (100 μM), or in coapplication of both in modulation of 0.2 μM GABA + 0.3 μM GX. TPEN prevented Zn^{2+} blockade of GX-sensitive current, and I_{tonic} exhibited significant enhancement by TPEN in hyperpolarization of the holding current level. Quantification of I_{tonic} was achieved relative to complete block by gabazine (GBZ). Dashed lines indicate average holding current level throughout each drug application. (B) I_{tonic} density shift (pA/pF) in the presence of Zn^{2+} and/or TPEN, with positive values as block of GX-sensitive I_{tonic} and negative values as enhancement of I_{tonic}. Data bars represent mean ± SEM (n = 5 cells per group). *$p < 0.05$ vs. GX + Zn^{2+} combination (Mann-Whitney U-test).

IV.2.5 Intrahippocampal Zn^{2+} Antagonizes the Seizure Protective Effect of GX in Fully-kindled Mice

To directly investigate the interactions of Zn^{2+} and GX on hippocampal excitability and seizures, we examined the antiseizure activity of GX with or without intrahippocampal Zn^{2+} infusion in a mouse kindling model, in which the fully-kindled mice exhibit consistent, generalized stage 5 seizures. The experimental paradigm was shown in Figure 26A. Intrahippocampal Zn^{2+} (10 – 300 μM) infusion was performed 10 min before GX (10 mg/kg, s.c.) treatment followed by kindling stimulation. GX (10 mg/kg, s.c.) significantly suppressed kindling-induced seizures (Figure 26D, 26E). Zn^{2+} infusion blocked the antiseizure activity of GX dose-dependently, in which Zn^{2+} at 300 μM achieves a statistical significance. The electrograph recordings of electrically-induced, kindling afterdischarge (AD) were shown in Figure 26B. GX-treated mice (10 mg/kg, s.c.) displayed significantly reduced AD durations compared to vehicle-treated mice (Figure 26C). Despite GX treatment, 300 μM Zn^{2+}-infused mice exhibited significantly greater AD durations and higher incidence of seizures (Figure 26C – E). The reversible effect of Zn^{2+} on kindling seizures was demonstrated since all animals exhibited stage 5 seizures after 24-hr wash-out of drug. Overall, these results suggest that Zn^{2+} plays a key role in the modulation of seizure susceptibility by anticonvulsant neurosteroids like GX that are potent activators of δGABA-ARs.

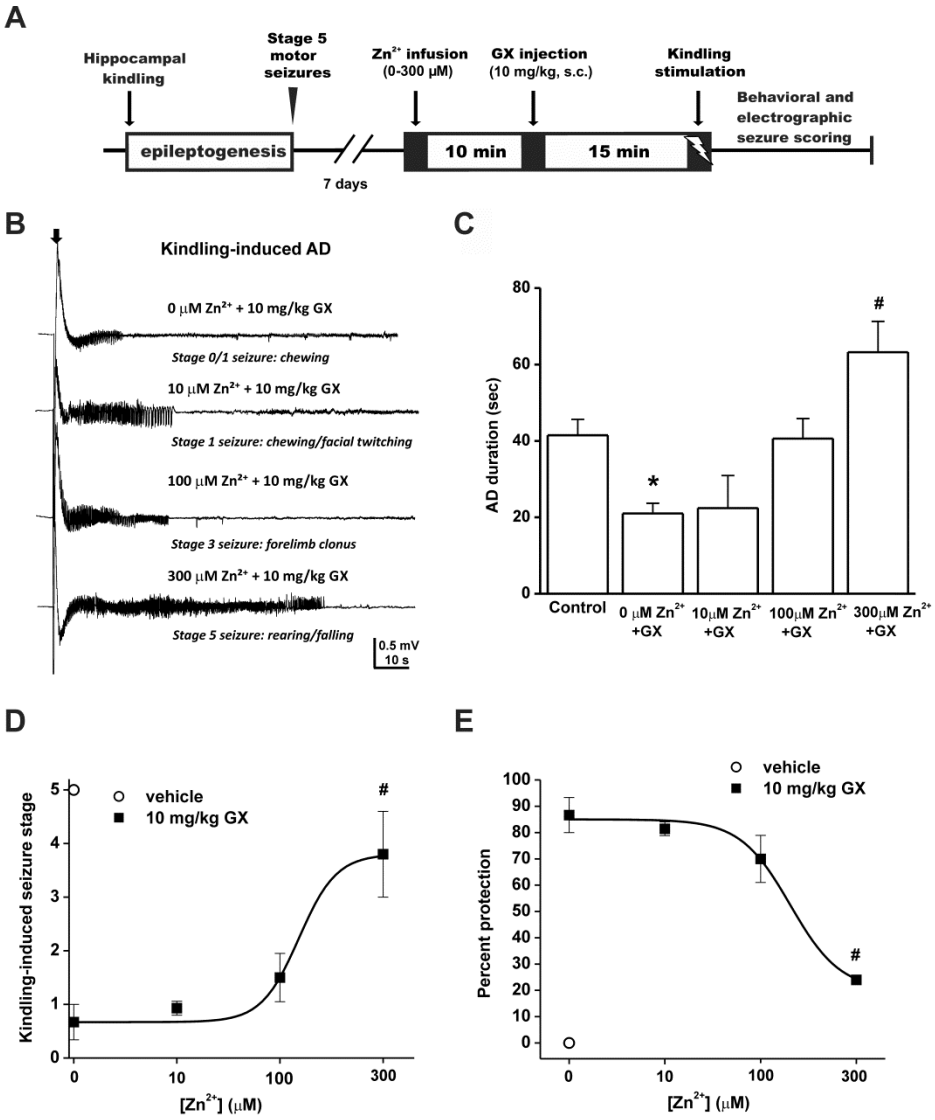

Figure 26 Intrahippocampal Zn^{2+} infusion completely prevents the antiseizure effects of the neurosteroid GX in fully-kindled mice.

(A) Experimental paradigm and infusion protocol for saline or Zn^{2+} delivery (0 – 300 μM) prior to GX (10 mg/kg, s.c.) treatment and kindling stimulation. (B) Electrograph recordings of electrically-induced, kindling afterdischarge (AD). The black arrow denotes stimulation-onset artifact. (C) AD duration of electrograph activity. Control denotes saline infusion (Zn^{2+}-free) and vehicle injection (GX-free) condition upon kindling. (D) Kindling-induced behavioral seizure score after Zn^{2+} infusion. ED_{50} = 150 μM. (E) Dose-response curve of percent seizure protection. Anticonvulsant effect of 10 mg/kg GX was inhibited by 300 μM Zn^{2+}. After 24 hr wash-out, mice displayed stage 5 seizures and similar AD duration to the control group. Data bars represent mean ± SEM (n = 5 – 6 mice per group). *$p < 0.05$ vs. control; $^{\#}p<0.05$ vs. GX without Zn^{2+} (Mann-Whitney U-test).

IV.3 Isobolographic Analysis of Extrasynaptic GABA-AR-Mediated Tonic Inhibition and Anticonvulsant Activity of Neurosteroid Combinations with TG and MDZ

IV.3.1 Synergistic Effects of GX and TG Coapplication on Extrasynaptic δGABA-AR-Mediated Tonic Inhibition in Hippocampal DGGCs

To characterize the interactions of neurosteroids with clinical GABAergic agent TG on extrasynaptic δGABA-AR-mediated tonic currents, we first recorded tonic current potentiation by AP, GX, or TG alone (0.1 – 1 μM) in DGGCs from hippocampus slices. Tonic currents were isolated in the presence of the NMDA receptor antagonist (APV, 40 μM), the AMPA receptor antagonist (DNQX, 10 μM), and the sodium channel blocker (TTX, 0.5 μM) in the bath solution by using whole-cell patch clamp electrophysiology. After application of the test drugs, a GABA-AR antagonist (gabazine, 50 μM) was perfused to determine the total GABA-AR-mediated tonic current shift. Current density (pA/pF) of each cell was obtained by normalizing the tonic current shift with the cell capacitance. The basal level of tonic currents in DGGCs was 10.8 ± 1.6 pA, 0.31 ± 0.06 pA/pF (Table 7). As shown in Figure 27A – 27C, AP (0.1 – 1 μM), and GX (0.1 – 1 μM) elicited direct tonic current activation in DGGCs in a concentration-dependent manner, as consistent with previous report (Chuang and Reddy, 2018b). The tonic current potentiation by TG (0.1 – 1 μM), in the absence of GABA, was shown in Figure 27B, 27C. We then co-applied GX (0.1 – 1 μM) with TG at 0.1 μM and recorded the combination effect of GX and TG on tonic inhibition. The potentiation of tonic currents by GX + TG was significantly greater compared to GX alone, indicating possible additive or synergistic effects of combination regimen (tonic current shift: 0.1 μM or 0.3 μM GX + 0.1 μM TG, $p = 0.018$ and 0.020, respectively; current density, 0.1 μM or 0.3 μM GX + 0.1 μM TG, $p = 0.019$ and 0.024, respectively; $n = 6 – 8$ cells per group).

To elucidate the precise interaction between GX and TG, we performed the isobolographic analysis, a commonly used method to classify drug interactions as

antagonistic, additive, or synergistic by utilizing fixed drug ratio combinations in preclinical studies (Tallarida, 2006, Wojda et al., 2009). We first examined the $EF_{2\text{-fold endogenous}}$ values that represent the effective functional concentration of drug (nM) required to double the endogenous tonic response in DGGCs (Fig. 28D – F). According to the concentration-response curves of GX and TG, we deduced the $EF_{2\text{-fold}}$ values of GX and TG as 250 nM and 220 nM, respectively (Fig. 28D – F). Fixed ratio drug combinations at 1:3, 1:1, and 3:1 were tested in DGGCs to quantify the contribution of each drug to the overall effects. The theoretical $EF_{2\text{-fold}}$ ($EF_{2\text{-fold add}}$) values for mixtures of GX and TG at three fixed ratio of 1:3, 1:1 and 3:1 are shown in Table 8. The experimental $EF_{2\text{-fold}}$ ($EF_{2\text{-fold mix}}$) values were derived from the tonic current modulation of each mixture. The tonic current shift (pA) and current density (pA/pF) exerted by each mixtures of drug combinations are shown in Table 7. The isobologram was plotted, and the theoretical and experimental $EF_{2\text{-fold}}$ of mixtures were compared (Figure 28; Table 8). In the isobologram, the $EF_{2\text{-fold}}$ for GX (250 nM) is plotted graphically on the X-axis, whereas the $EF_{2\text{-fold}}$ for TG (220 nM) is plotted graphically on the Y-axis. The distances between open-square points on the X- and Y-axes represent the 95% confidence limits (CLs) for the drugs treated alone. The straight line connecting these two $EF_{2\text{-fold}}$ values on the graph represents the theoretical line of additivity for a continuum of different fixed concentration ratios, whereas the dashed lines represent the theoretical additive 95% CLs of $EF_{2\text{-fold}}$ values. Our results showed that all three combination regimens of GX and TG were located drastically below the theoretical line of additivity (Figure 28B), indicating synergistic interactions of GX and TG coapplication on tonic current potentiation.

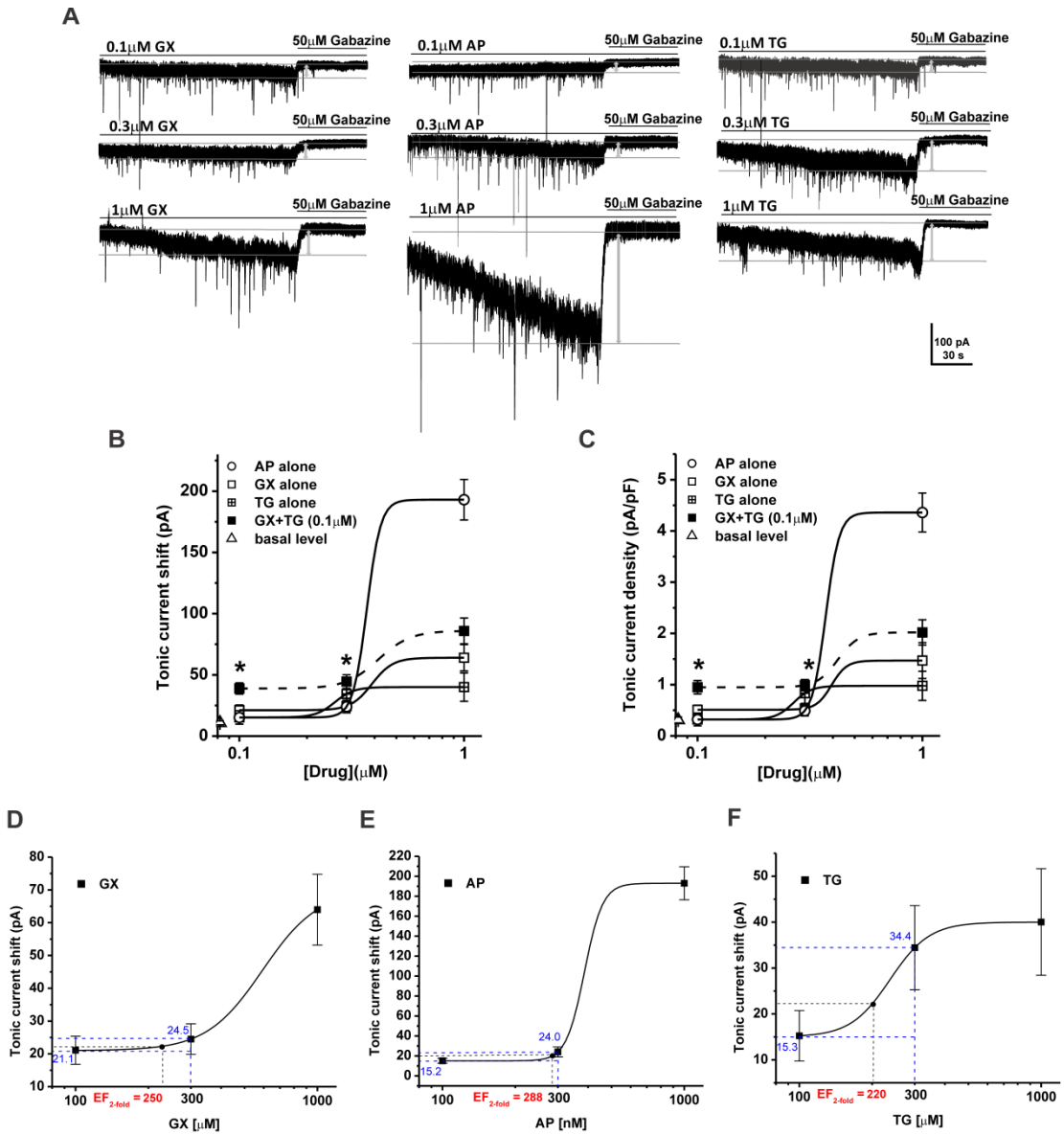

Figure 27 GX and TG combination significantly potentiates tonic currents in the hippocampal DGGCs compare to GX alone, indicating a possible synergistic interaction.

(A) Representative whole-cell, voltage-clamp recordings of tonic currents in DGGCs in response to GX, AP, or TG. Concentration responses for tonic current shift (B) and tonic current density (C) in response to GX, AP, TG, or GX+TG combination in DGGCs. (D – F) Concentration-response curves illustrating the $EF_{2\text{-fold}}$ values of GX, AP, and TG. *p < 0.05 vs. GX alone (n= 6 – 8 cells per group).

Table 7 The values of current (pA) and current density (pA/pF) potentiation by each mixtures of drug combinations.

	Current shift (pA)	Current density (pA/pF)	Sample size (n)
Endogenous	10.8 ± 1.6	0.31 ± 0.06	12
$EF_{2\text{-fold endogenous}}$	21.6 ± 3.2	0.62 ± .012	
GX:TG=1:3	59.9 ± 12.8	1.28 ± 0.25	7
GX:TG=1:1	61.3 ± 10.4	1.38 ± 0.20	7
GX:TG=3:1	30.2 ± 4.3	0.70 ± 0.09	8
AP:TG=1:3	56.5 ± 15.5	1.37 ± 0.30	6
AP:TG=1:1	51.2 ± 9.0	1.22 ± 0.17	6
AP:TG=3:1	129.5 ± 32.1	3.12 ± 0.78	6
GX:MDZ=1:3	31.5 ± 8.6	0.66 ± 0.17	6
GX: MDZ =1:1	32.0 ± 8.4	0.66 ± 0.18	6
GX: MDZ =3:1	51.1 ± 11.3	1.08 ± 0.23	6

The symbol **n** denotes cell number of each group and concentration.

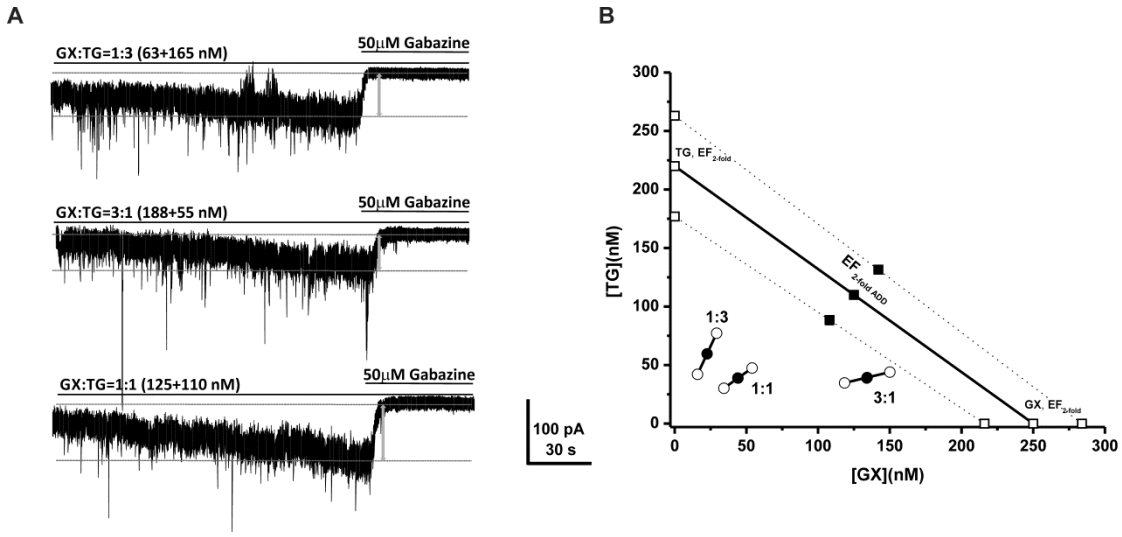

Figure 28 Synergistic interactions between GX and TG of all combinations tested on tonic current potentiation.

(A) Representative whole-cell recordings of tonic currents in DGGCs in response to combinations of GX and TG. (B) Isobologram showing interactions between GX and TG in tonic current potentiation in DGGCs. The EF_2 for GX (250 nM) is plotted graphically on the X-axis, whereas the EF_2 for TG (220 nM) is plotted graphically on the Y-axis. The distances between open-square points on the X- and Y-axes represent the 95% confidence limits (CLs) for the drugs treated alone. The straight line connecting these two EF_2 values on the graph represents the theoretical line of additivity for a continuum of different fixed concentration ratios, whereas the dashed lines represent the theoretical additive 95% CLs of EF_2 values. EF_2 denotes concentration needed to achieve 2-fold potentiation of endogenous basal tonic current (10.8 ± 1.6 pA; 0.31 ± 0.06 pA/pF). The black circles depict the experimentally derived EF_2 values (with 95% CLs as error bars) for the total concentration expressed as the proportion of GX and TG that produced 2-fold potentiation of basal tonic currents. The experimental EF_2 values of the mixture of GX+TG for the entire fixed ratio are placed below the theoretical line of additivity, indicating the tendency towards synergism.

Table 8 Isobolographic analysis showing theoretical ($EF_{2\text{-fold add}}$) and experimental determined ($EF_{2\text{-fold mix}}$) values of GX and TG combinations on tonic current potentiation in DGGCs.

AED Combination	Fixed Ratio	GX	+	TG	=	$EF_{2\text{-fold mix}}$ (nM)	n_{mix}	$EF_{2\text{-fold add}}$ (nM)	= GX	+ TG	n_{add}
GX+TG	1:3	22.6		59.6		82.2±24.2	7	227.5±40.8	62.5	165	6
GX+TG	1:1	44.1		38.8		83.0±18.5	7	235±38.5	125	110	6
GX+TG	3:1	134.3		39.4		173.6±20.5	8	242.5±36.3	187.5	55	6

n_{add} denotes total cell numbers used to calculate the theoretical line of additivity; n_{mix} denotes total cell numbers in each mixtures of drug combinations.

IV.3.2 Log-Probit Dose-Response Analysis of Anticonvulsant Effects of GX and TG in Mice

In seizure protection studies, GX and TG administered alone reduced seizures in a dose-dependent fashion in both 6-Hz and kindling seizure model in mice (Figure 29A, 29C, 29D). GX displayed a significantly faster peak response time than TG, with similar rates of disposition for each (Figure 29B). Administration of GX with TG at 0.25 mg/kg caused a leftward shift of GX dose response in the 6-Hz model; similar protection trend of reduced seizure stage and AD duration was noted in the kindling model, suggesting additive/synergistic effects of GX+TG combination in mouse seizure models (Figure 29C – D). To study the interactions of GX with TG on seizure protection, a mouse 6-Hz model of epilepsy was utilized. First, we determined the median effective dose (ED_{50}) of each drug by using log-probit linear regression analysis (Litchfield and Wilcoxon, 1949). GX was given at the increasing doses (0.5 – 10 mg/kg) and the percent protection against 6 Hz-induced seizures was calculated. The dose-response relationship for GX administered alone was determined as $y = 5.30092x + 5.30092$ [$r^2 = 0.92463$], where y denotes probit of response, x denotes logarithm of the drug dose 10, and r^2 denotes coefficient of determination (Figure 29E). The ED_{50} value for GX was 1.46 (0.74 – 2.88) mg/kg. Similarly, TG was administered at various doses (0.1 – 1 mg/kg) and the percent protection exerted by these doses was calculated. The dose-response relationship for TG

was $y = 4.71065x + 3.03345$ [$r^2 = 0.95594$]. The ED_{50} value for TG was 0.20 (0.10 – 0.39) mg/kg. The chi-square analysis revealed that the points creating the log-probit dose response relationship lines for GX and TG were not heterogeneous and thus good-to-fit as the experimentally denoted χ^2 values (GX = 2.370; TG = 1.193) were lower than the tabular χ^2 values (GX = 7.815; TG = 5.991). The parallelism test for two log-probit dose-response curves showed that the slope function ratio was lower than the factor for the slope function ratio, confirming that the lines are parallel to another.

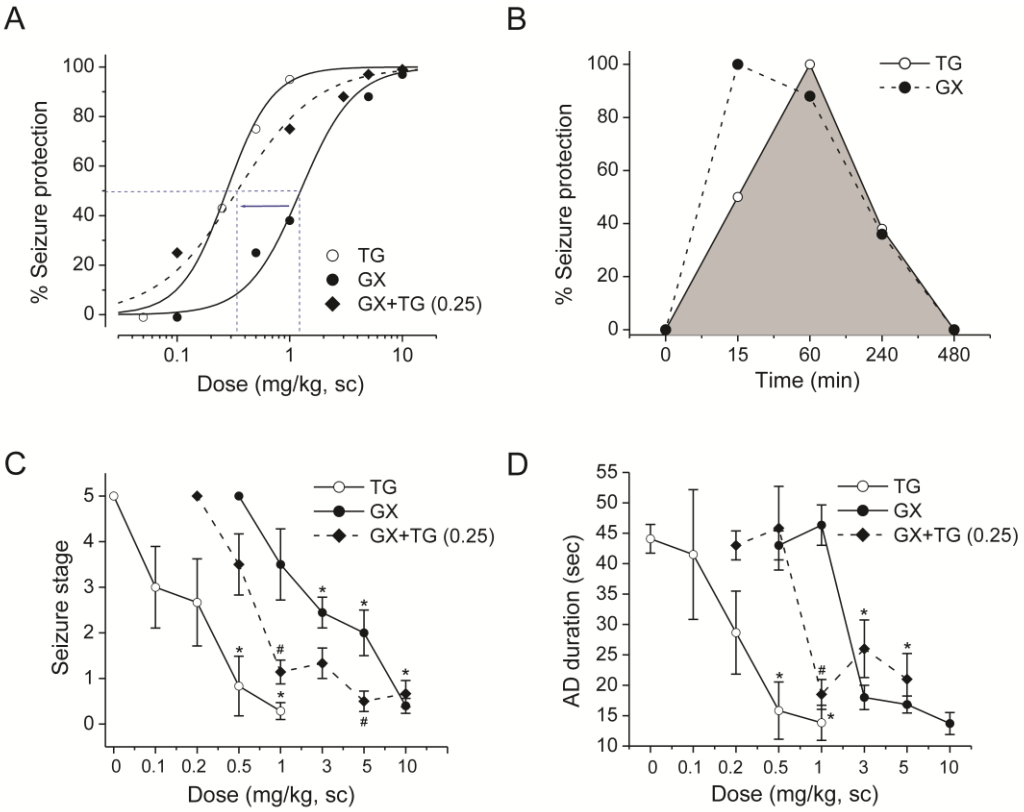

Figure 29 Additive and synergistic anticonvulsant interactions between GX and TG in acute seizure models in mice.

(A) The percentage of seizure protection by GX, TG, or GX+TG. GX and TG reduced seizures in a dose-dependent fashion in the 6-Hz model. Combination therapy of GX and TG (0.25 mg/kg) shifted the response curve of GX toward left, indicating possible synergism. (B) Efficacy timeline for GX (5 mg/kg) and TG (0.25 mg/kg) in 6-Hz model. GX displayed significantly faster peak response time than TG, with similar rates of decay for each. GX and TG reduced the seizure stage (C) and afterdischarge (AD) duration (D) in a dose-dependent fashion in fully-kindled mice. Combination therapy of GX and TG (0.25 mg/kg) shifted the dose-response curves toward left, indicating possible synergism. (E) Log-probit dose-response relationship lines for GX and TG administered alone in the 6-Hz-induced partial seizure model. (F) Isobologram showing interactions between GX and TG in the 6-Hz seizure model. The dose GX is plotted graphically on the X-axis, and the dosing for TG is plotted graphically on the Y-axis. The straight line represents the theoretical line of additivity for a continuum of different fixed concentration ratios, whereas the dashed lines represent the theoretical additive 95% CLs of ED_{50} values. ED_{50} denotes dose needed to achieve seizure protection in 50% of animals. The experimental ED_{50} values of the mixture of GX+TG for fixed ratios fall at or below the theoretical line of additivity.

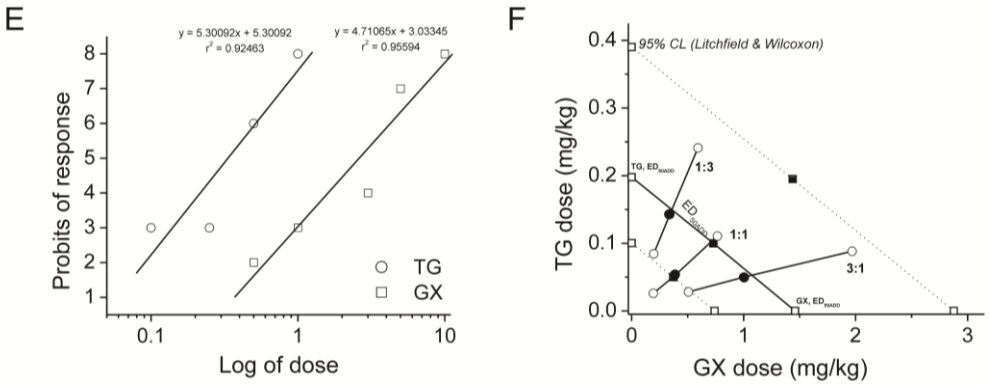

Figure 29 Continued.

IV.3.3 Synergistic Anticonvulsant Effects of GX and TG Combinations in the 6-Hz Seizure Model in Mice

In the isobolographic analysis, the theoretical $ED_{50\ add}$ values for a mixture of GX and TG at three fixed ratio of 1:3, 1:1 and 3:1 were calculated as (in mg/kg) 0.514 (0.260 – 1.012), 0.829 (0.420 – 1.634), and 1.145 (0.580 – 2.255), respectively (Figure 29, Table 9). The experimental $ED_{50\ mix}$ values were derived from the seizure protection exerted by each mixture at 1:3, 1:1 and 3:1 as 0.484 (0.282 – 0.833), 0.437 (0.219 – 0.870), and 1.049 (0.535 – 2.057), respectively. The mixture of GX and TG at the fixed-ratio of 1:1 exerted the greatest synergism (combination index, CI = .53, Table 10), whereas CI's for the mixture of GX and TG at 3:1 and 1:3 combinations were .94 and .96, respectively. In addition, combinations tested between GX and TG at 1:3 and 3:1 are plotted in the theoretical line of additivity while the combination at 1:1 is plotted below the additive line in the isobologram (Fig. 29F), indicating less synergistic (supra-additive) interactions.

Table 9 Isobolographic analysis showing theoretical ($EF_{50\ add}$) and experimental determined ($EF_{50\ mix}$) values of GX and TG combinations in the 6-Hz seizure model.

AED Combination	Fixed Ratio	GX	+ TG	= $ED_{50\ mix}$ (mg/kg)	n_{mix}	$EF_{50\ add}$ (mg/kg)	= GX	+ TG	n_{add}
GX+TG	1:3	0.341	0.143	0.484 (0.282-0.833)	32	0.514 (0.26-1.012)	0.365	0.149	32
GX+TG	1:1	0.385	0.052	0.437 (0.219-0.870)	40	0.829 (0.42-1.634)	0.73	0.099	40
GX+TG	3:1	0.999	0.05	1.049 (0.535-2.057)	32	1.145 (0.58-2.255)	1.095	0.050	32

n_{add} denotes total cell numbers used to calculate the theoretical line of additivity; n_{mix} denotes total cell numbers in each mixtures of drug combinations.

Table 10 Combination (CI) index of the combinations of GX and TG in the antiseizure activity.

ED50	GX	TG	CI	
alone	1.46	0.198		
GX+TG 1:3	0.341	0.143	0.96	addition/synergism
GX+TG 1:1	0.385	0.052	0.53	synergism
GX+TG 3:1	0.999	0.05	0.94	addition/synergism

IV.3.4 Synergistic Potentiating Effects of AP and TG Coapplication on Tonic Currents in Hippocampal DGGCs

To further characterize the combination interactions between neurosteroid and TG on tonic currents, we also examine the interactions of the endogenous neurosteroid AP and TG by using isobolographic analysis (Figure 30A – B). The $EF_{2\text{-fold endogenous}}$ value of AP was 288 nM (Fig. 27E). Fixed ratio drug combinations at 1:3, 1:1, and 3:1 were examined in DGGCs to quantify the contribution of each drug to the overall effects. The theoretical $EF_{2\text{-fold}}$ ($EF_{2\text{-fold add}}$) values for mixtures of AP and TG at three fixed ratio of 1:3, 1:1 and 3:1 were shown in Table 11. The experimental $EF_{2\text{-fold}}$ ($EF_{2\text{-fold mix}}$) values were derived from the tonic current modulation of each mixtures. In the isobologram, the $EF_{2\text{-fold}}$ for AP (288 nM) is plotted graphically on the X-axis, whereas the $EF_{2\text{-fold}}$ for TG (220 nM) is plotted graphically on the Y-axis. Like GX, all three combinations tested between AP and

TG are plotted below the theoretical line, signifying strong synergistic interactions of AP and TG on tonic current potentiation in DGGCs (Figure 30).

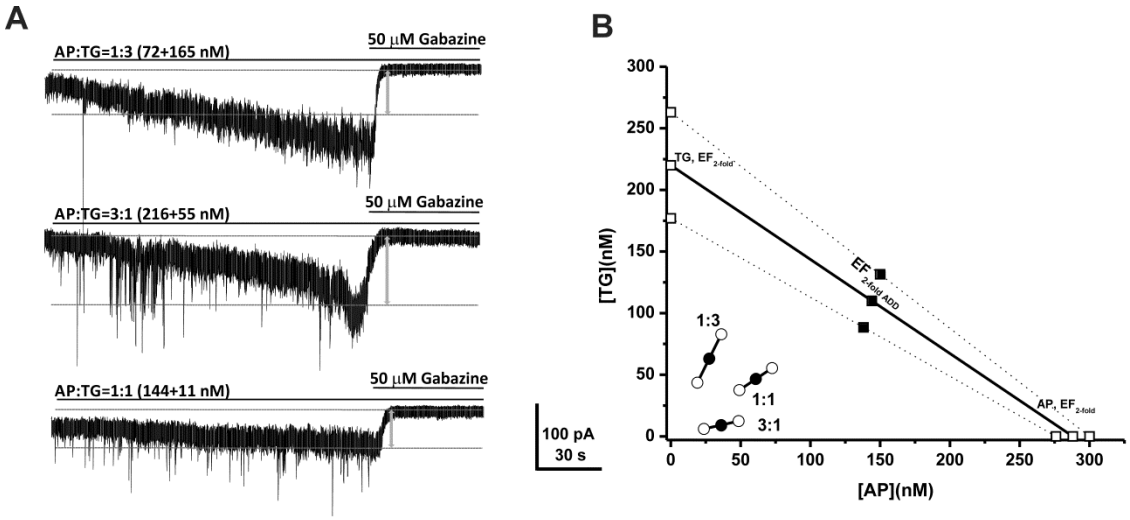

Figure 30 Synergistic interactions between AP and TG of all combinations tested in the tonic current potentiation.

(A) Representative whole-cell recordings of tonic currents in DGGCs in response to combinations of AP and TG. (B) Isobologram showing interactions between AP and TG in tonic current potentiation in DGGCs. The EF_2 for AP (288 nM) is plotted graphically on the X-axis, whereas the EF_2 for TG (220 nM) is plotted graphically on the Y-axis. The distances between open-square points on the X- and Y-axes represent the 95% confidence limits (CLs) for the drugs treated alone. The straight line connecting these two EF_2 values on the graph represents the theoretical line of additivity for a continuum of different fixed concentration ratios, whereas the dashed lines represent the theoretical additive 95% CLs of EF_2 values. EF_2 denotes concentration needed to achieve 2-fold potentiation of endogenous basal tonic current (10.8 ± 1.6 pA; 0.31 ± 0.06 pA/pF). The black circles depict the experimentally derived EF_2 values (with 95% CLs as error bars) for the total concentration expressed as the proportion of AP and TG that produced 2-fold potentiation of basal tonic currents. The experimental EF_2 values of the mixture of AP+TG in all three-fixed ratio are placed below the theoretical line of additivity, indicating the tendency towards synergism.

Table 11 Isobolographic analysis showing theoretical ($EF_{2\text{-fold add}}$) and experimental determined ($EF_{2\text{-fold mix}}$) values of AP and TG combinations on tonic current potentiation in DGGCs.

AED Combination	Fixed Ratio	AP	+	TG	=	$EF_{2\text{-fold mix}}$ (nM)	n_{mix}	$EF_{2\text{-fold add}}$ (nM)	=	AP	+	TG	n_{add}
AP+TG	1:3	27.6		63.2		90.8 ± 28.2	6	237 ± 35.3		72		165	6
AP+TG	1:1	60.8		46.5		107.3 ± 20.6	6	254 ± 27.5		144		110	6
AP+TG	3:1	36.1		9.2		45.3 ± 15.6	6	271 ± 19.8		216		55	6

n_{add} denotes total cell numbers used to calculate the theoretical line of additivity; n_{mix} denotes total cell numbers in each mixtures of drug combinations.

IV.3.5 Log-Probit Dose-Response Analysis of Anticonvulsant Effects of AP and TG in Mice

Next, we examined the interactions of AP and TG in the 6-Hz seizure model. AP was given at the increasing dosing of 1, 3, 5, and 10 mg/kg, and the percent protection against 6-Hz-induced partial seizures was 10, 38.9, 60, and 99.7, respectively. The equation of dose response relationship for AP administered alone was determined as y = 9.28311x + 1.69977 [r^2 = 0.97008], where y denotes probit of response, x denotes logarithm of the drug dose 10, and r^2 denotes coefficient of determination (Figure 31A). The ED_{50} value for AP was 4.20 (2.7 – 5.8) mg/kg. The equation for TG was y = 4.71065x + 3.03345 [r^2 = 0.95594] and the ED_{50} value for TG was 0.20 (0.1 – 0.39) mg/kg. The experimentally denoted χ^2 values (AP = 0.740; TG = 1.193) were lower than the tabular χ^2 values (AP = 7.815; TG = 5.991), signifying that the log-probit curves for AP and TG were not significantly heterogeneous and thus good-to-fit.

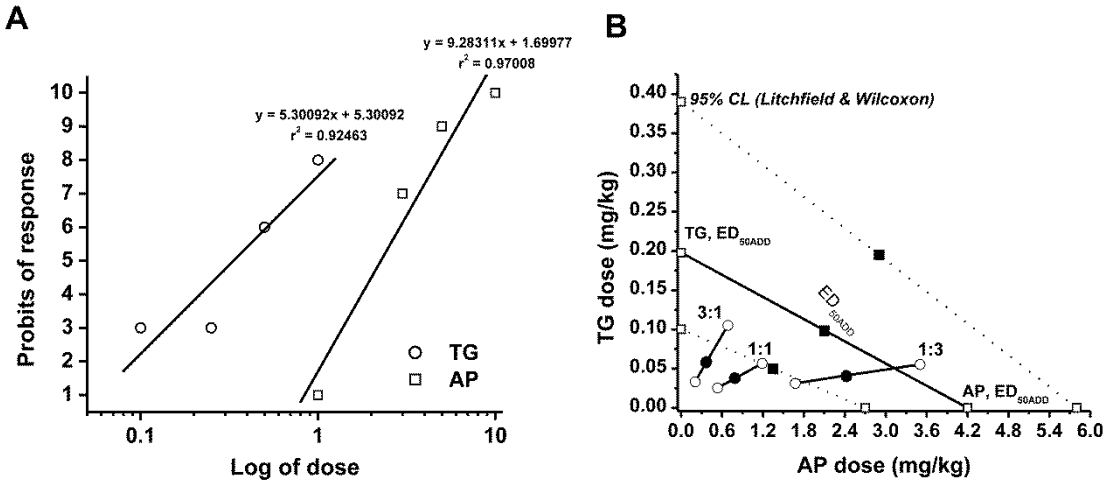

Figure 31 Synergistic anticonvulsant interactions between AP and TG in the 6-Hz test in mice.

(A) Log-probit dose-response relationship lines for AP and TG administered alone in the 6-Hz partial seizure model. (B) Isobologram showing interactions between AP and TG in the 6-Hz seizure model. The dose AP is plotted graphically on the X-axis, and the dosing for TG is plotted graphically on the Y-axis. The straight line represents the theoretical line of additivity for a continuum of different fixed concentration ratios, whereas the dashed lines represent the theoretical additive 95% CLs of ED_{50} values. ED_{50} denotes dose needed to achieve seizure protection in 50% of animals. The experimental ED_{50} values of the mixture of AP+TG for fixed ratios fall at or below the theoretical line of additivity.

IV.3.6 Synergistic Anticonvulsant Effects of AP and TG Combinations in the 6-Hz Seizure Model in Mice

In the isobolographic analysis, the theoretical $ED_{50\ add}$ values for mixtures of AP and TG at three fixed ratio of 1:3, 1:1 and 3:1 were determined as (in mg/kg) 1.199 (0.75 – 1.74), 2.199 (1.4 – 3.1), and 3.2 (2.05 – 4.45), respectively (Figure 31B, Table 12). The experimental $ED_{50\ mix}$ values were derived from the seizure protective effects exerted by each mixture at 1:3, 1:1 and 3:1 as 2.464 (1.70 – 4.06), 0.835 (0.56 – 1.25), and 0.436 (0.24 – 0.79), respectively. All combinations tested between AP and TG showed strong synergistic interactions against 6-Hz-induced seizures as the combination index (CI) of each mixture are less than 1 (CI = 0.38, 0.39, and 0.79 at 1:1, 3:1, and 1:3 ratios,

respectively, Table 13). All combination regimens of AP and TG at 1:3, 1:1 and 3:1 are all plotted below the additive line (Figure 31B), indicating synergistic anticonvulsant interactions of AP and TG.

Table 12 Isobolographic analysis showing theoretical ($EF_{50\ add}$) and experimental determined ($EF_{50\ mix}$) values of AP and TG combinations in the 6-Hz seizure model.

AED Combination	Fixed Ratio	AP	+ TG	= $ED_{50\ mix}$ (mg/kg)	n_{mix}	$EF_{50\ add}$ (mg/kg)	= AP	+ TG	n_{add}
AP+TG	1:3	2.422	0.042	2.464 (1.705-4.058)	32	1.199 (0.75-1.74)	1.05	0.149	32
AP+TG	1:1	0.797	0.038	0.835 (0.559-1.247)	32	2.199 (1.40-3.10)	2.1	0.099	32
AP+TG	3:1	0.377	0.059	0.436 (0.24-0.791)	32	3.200 (2.05-4.45)	3.15	0.050	32

n_{add} denotes total cell numbers used to calculate the theoretical line of additivity; n_{mix} denotes total cell numbers in each mixtures of drug combinations.

Table 13 Combination index (CI) of the combinations of AP and TG in the antiseizure activity.

ED50	AP	TG	CI	
alone	4.2	0.198		
AP+TG 1:3	2.422	0.042	0.79	synergism
AP+TG 1:1	0.797	0.038	0.38	synergism
AP+TG 3:1	0.377	0.059	0.39	synergism

IV.3.7 Combination Efficacy of GX and MDZ on Tonic Current Potentiation in Hippocampal DGGCs

The benzodiazepine MDZ is an allosteric agonist of synaptic GABA-ARs receptors through sites distinct from the neurosteroid binding site (Nusser et al., 1997). Therefore, it is plausible that neurosteroid+MDZ exerts a synergistic response on GABA-AR function through a mechanism involving distinct sites and thereby may be more effective for refractory seizures; however this hasn't widely investigated in seizure models. Here,

we tested if coapplication of neurosteroids with MDZ elicits additive or synergistic effects on tonic inhibition in hippocampal DGGCs (Figure 32). Like GX+TG coapplication experiments, we have simulated isobolograms for two allosteric drugs (GX and MDZ) combined. The results (Figure 32D) demonstrate that coapplication of GX and MDZ produces a curvilinear isobole; however, the curvature is less pronounced due to limited efficacy of MDZ at extrasynaptic receptors (Figure 32D). Nevertheless, combinations of GX and MDZ at three fixed ratio exerted synergistic potentiation of tonic currents as they are plotted below the theoretical line in the isobologram (Figure 32D, Table 14). These results are highly consistent with a recent study in which the potentiating effect of alfaxolone resulting from the addition of a second GABAergic drug diazepam is greater due to their distinct binding sites on the GABA-ARs (Shin et al., 2019).

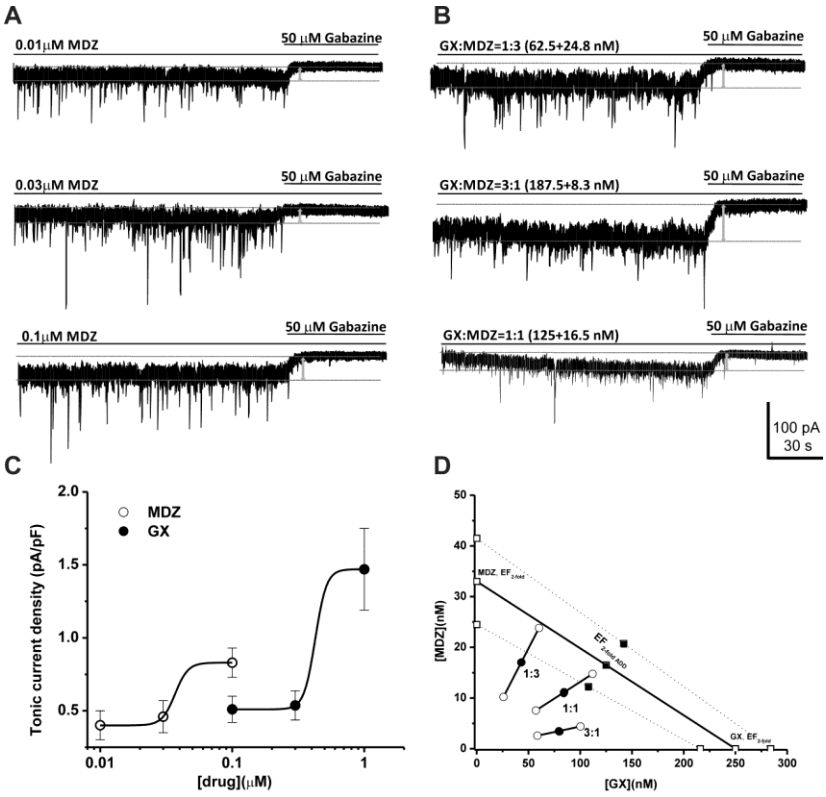

Figure 32 Synergistic interactions between GX and MDZ in the tonic current potentiation.

(A) Representative whole-cell recordings of tonic currents in DGGCs in response to MDZ (0.01 – 0.1 μM). (B) Representative whole-cell recordings of tonic currents in DGGCs in response to combinations of GX and MDZ. (C) Concentration response curves of GX and MDZ alone in the potentiation of tonic currents (pA). (D) Isobologram showing interactions between GX and MDZ in tonic current potentiation in DGGCs. The EF_2 for GX (250 nM) is plotted graphically on the X-axis, whereas the EF_2 for MDZ (33 nM) is plotted graphically on the Y-axis. The distances between open-square points on the X- and Y-axes represent the 95% confidence limits (CLs) for the drugs treated alone. The straight line connecting these two $EF_{2\text{-fold}}$ values on the graph represents the theoretical line of additivity for a continuum of different fixed concentration ratios, whereas the dashed lines represent the theoretical additive 95% CLs of EF_2 values. EF_2 denotes concentration needed to achieve 2-fold potentiation of endogenous basal tonic current (10.8 ± 1.6 pA; 0.31 ± 0.06 pA/pF). The black circles depict the experimentally derived EF_2 values (with 95% CLs as error bars) for the total concentration expressed as the proportion of GX and MDZ that produced 2-fold potentiation of basal tonic currents. The experimental EF_2 values of the mixture of GX+MDZ for the entire fixed ratio are placed fall at or below the theoretical line of additivity, indicating the tendency towards additivity.

Table 14 Isobolographic analysis showing theoretical ($EF_{2\text{-fold add}}$) and experimental determined ($EF_{2\text{-fold mix}}$) values of GX and MDZ combinations on tonic current potentiation in DGGCs.

AED Combination	Fixed Ratio	GX	+	MDZ	= $EF_{2\text{-fold mix}}$ (nM)	n_{mix}	$EF_{2\text{-fold add}}$ (nM)	= GX	+ MDZ	n_{add}
GX+MDZ	1:3	43.0		17.0	60.0±24.0	6	87.3±14.9	62.5	24.8	6
GX+MDZ	1:1	84.6		11.2	95.8±31.0	6	141.5±21.3	125	16.5	6
GX+MDZ	3:1	79.4		3.5	82.9±21.7	6	195.8±27.6	187.5	8.3	6

n_{add} denotes total cell numbers used to calculate the theoretical line of additivity; n_{mix} denotes total cell numbers in each mixtures of drug combinations.

IV.3.8 Anticonvulsant Activity of GX and MDZ Combination Regimens in the 6-Hz Seizure Model

In the 6-Hz seizure model, MDZ was given at the increasing doses (0.05 – 3 mg/kg) and the percent protection was derived from the analysis. The dose-response relationship for MDZ administered alone was determined as y = 4.69735x + 6.90629[r^2 = 0.92273], where y denotes probit of response, x denotes logarithm of the drug dose 10, and r^2 denotes coefficient of determination (Figure 33A). The ED_{50} value for MDZ was 0.40 (0.11 – 0.69) mg/kg. The equation for GX was y = 5.30092x + 5.30092 [r^2 = 0.92463] and the ED_{50} value for GX was 1.46 (0.74 – 2.88) mg/kg. The experimentally denoted χ^2 values (GX = 2.370; MDZ = 10.118) were lower than the tabular χ^2 values (GX = 7.815; MDZ = 11.07), signifying that the log-probit dose-response relationship lines for GX and MDZ were not significantly heterogeneous and thus good-to-fit. In the isobolographic analysis, the theoretical $ED_{50\ add}$ values for mixtures of GX and MDZ at three fixed ratio of 1:3, 1:1 and 3:1 were determined as (in mg/kg) 0.665 (0.268 – 1.237), 0.930 (0.624 – 1.784), and 1.195 (0.538 – 2.330), respectively (Figure 33B, Table 15). The experimental $ED_{50\ mix}$ values were derived from the seizure protective effects exerted by each mixture at 1:3, 1:1 and 3:1 as 0.910 (0.608 – 0.364), 0.550 (0.368 – 0.823), and 0.404 (0.259 – 0.631), respectively. All combinations tested between GX and MDZ showed strong synergistic interactions for seizure protection as CIs of each mixture are less than 1 (CI = 0.76, 0.59, and 0.61 at 1:1, 3:1, and 1:3 ratios, respectively, Table 16). In addition, combinations tested between GX and MDZ at 1:3, 1:1 and 3:1 are all plotted below the additive line (Figure 33B), indicating synergistic anticonvulsant interactions between GX and MDZ in the 6-Hz seizure model.

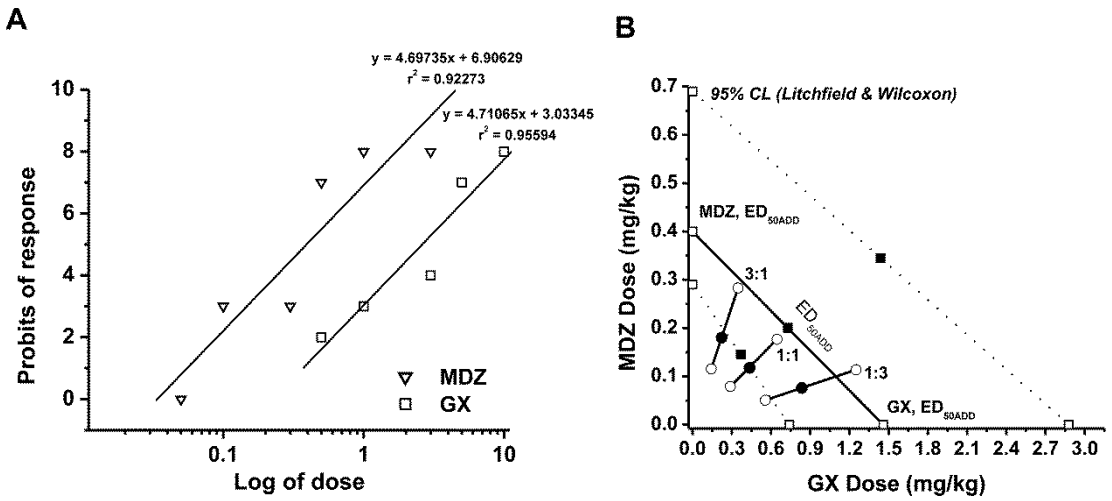

Figure 33 Synergistic anticonvulsant interactions between GX and MDZ in the 6-Hz model in mice.

(A) Log-probit dose-response relationship lines for GX and MDZ administered alone in the 6-Hz-induced partial seizure model. (B) Isobologram showing interactions between GX and MDZ in the 6-Hz seizure test. The dose GX is plotted graphically on the X-axis, and the dosing for MDZ is plotted graphically on the Y-axis. The straight line represents the theoretical line of additivity for a continuum of different fixed concentration ratios, whereas the dashed lines represent the theoretical additive 95% CLs of ED_{50} values. ED_{50} denotes dose needed to achieve seizure protection in 50% of animals. The experimental ED_{50} values of the mixture of GX+MDZ for fixed ratios fall at or below the theoretical line of additivity.

Table 15 Isobolographic analysis showing theoretical ($EF_{50\ add}$) and experimental determined ($EF_{50\ mix}$) values of GX and MDZ combinations in the 6-Hz seizure model.

AED Combination	Fixed Ratio	GX	+	MDZ	= $ED_{50\ mix}$ (mg/kg)	n_{mix}	$EF_{50\ add}$ (mg/kg)	= GX	+ MDZ	n_{add}
GX+MDZ	1:3	0.834		0.076	0.910 (0.608-0.364)	32	0.665 (0.268-1.237)	0.365	0.3	32
GX+MDZ	1:1	0.432		0.118	0.550 (0.368-0.823)	32	0.93 (0.426-1.784)	0.73	0.2	32
GX+MDZ	3:1	0.223		0.181	0.404 (0.259-0.631)	32	1.195 (0.583-2.330)	1.095	0.1	32

n_{add} denotes total cell numbers used to calculate the theoretical line of additivity; n_{mix} denotes total cell numbers in each mixtures of drug combinations.

Table 16 Combination index (CI) of the combinations of GX and MDZ in the antiseizure activity.

ED50	GX	MDZ	CI	
alone	1.46	0.4		
GX+MDZ 1:3	0.834	0.076	0.76	synergism
GX+MDZ 1:1	0.432	0.118	0.59	synergism
GX+MDZ 3:1	0.223	0.181	0.61	synergism

CHAPTER V
DISCUSSION[§§,***]

V.1 The Mechanisms of Action and Structure-Activity Relationships of GX and Related Neurosteroid Analogs on Extrasynaptic δGABA-AR-Mediated Tonic Inhibition and Seizure Protection

The principal finding of this study is the demonstration of GX and its analogs as preferential positive allosteric modulators and direct activators of extrasynaptic δGABA-ARs in the dentate gyrus that regulate network tonic inhibition and seizures. GX and its analogs are highly selective for PKC-phosphorylated extrasynaptic δGABA-AR-mediated tonic inhibition in native hippocampal neurons. In addition, GX enhancement of tonic inhibition is diminished in mice lacking δGABA-ARs. These results suggest that GX controls seizure susceptibility probably by potentiating GABA-AR-medicated synaptic and tonic inhibition though allosteric and/or direct action. Overall, these findings provide a mechanistic rationale for the clinical use of GX and its analog in seizure disorders (Reddy and Estes, 2016).

Neurosteroids are endogenous modulators of GABA-ARs acting through an allosteric binding site at submicromolar concentrations and a direct activation site at micromolar concentrations (Hosie et al., 2007). GX is a synthetic neurosteroid with robust antiseizure properties (Reddy and Woodward, 2004). Unlike its natural prototype AP, GX, with its additional methyl group at the 3β position, is not readily metabolized to hormonally active 3-keto derivative (Gee et al., 1995). Therefore, GX possesses higher bioavailability

---

[§§] Reprinted with permission from "3β-methyl-neurosteroid analogs are preferential positive allosteric modulators and direct activators of extrasynaptic δ-subunit γ-aminobutyric acid type A receptors in the hippocampus dentate gyrus subfield." by S-H Chuang and DS Reddy, 2018. T*he journal of pharmacology and experimental therapeutics*, 365(3): 583–601, Figures 1 – 13, Table 1 – 2, Copyright © 2018 by The American Society for Pharmacology and Experimental Therapeutics. All rights reserved.

[***] Reprinted with permission from "Zinc reduces antiseizure activity of neurosteroids by selective blockade of extrasynaptic GABA-A receptor-mediated tonic inhibition in the hippocampus" by S-H Chuang and DS Reddy, 2019. *Neuropharmacology*, 148: 244–256, Figures 1 – 7, Table 1, Copyright © 2018 Elsevier Ltd. All rights reserved.

and provides a more favorable pharmacokinetic profile as a promising antiepileptic drug. Although GX was previously tested in recombinant $\alpha1\beta1\gamma2_L$ GABA-ARs (Carter et al., 1997), its precise mode of action on native hippocampal neurons remained largely unclear. Here we demonstrated that GX is a potent allosteric modulator of both synaptic and extrasynaptic GABA-ARs in native hippocampal neurons. We compared the modulatory effects of GX with AP. GX and AP at 0.3 μM allosterically potentiated tonic current density to 1.61 ± 0.18 pA/pF and 1.80 ± 0.18 pA/pF, respectively (Figure 12 and 16). In seizure models including the 6-Hz test, GX exhibited improved potency compared with AP (Kaminski et al., 2004; Carver and Reddy, 2016). This may be attributed to its enhanced pharmacokinetic profile preventing its metabolism, thereby offering increased bioavailability.

Like our previous structure-activity relationship study (Carver and Reddy, 2016), we compared the potency and efficacy of GX with its analog 21-OH-GX. Our results demonstrate that, with the addition of a hydroxyl group in the C21 position, 21-OH-GX displayed higher efficacy than GX in the augmentation of GABA currents and tonic inhibition. These could be related to the plausible comparable bioavailability and higher binding affinity to GX. In addition, both GX and 21-OH-GX displayed dose-dependent reduction of seizure stage and AD duration. However, 21-OH-GX exhibited significantly greater antiseizure potency, an effect highly selective for extrasynaptic δGABA-ARs. Our studies confirm that 21-OH-GX possesses higher efficacy in potentiation of GABA currents and extrasynaptic δGABA-AR-mediated tonic inhibition, possibly contributing to its better antiseizure activity.

The δ subunit and its expressional plasticity remain key factors in understanding neurosteroid sensitivity, network excitability, and seizure susceptibility (Mihalek et al., 1999; Carver and Reddy, 2013; Whissell et al., 2015; Reddy et al., 2017; Chuang and Reddy, 2018a). Mice lacking the δ subunit display significantly decreased sleep time in response to neurosteroid alphaxolone and reduced sensitivity to GX-exerted anxiolytic response (Mihalek et al., 1999; Spigelman et al., 2002; Porcello et al., 2003; Spigelman et

al., 2003). The δ-selective effect for neurosteroid modulation is also established by electrophysiological studies. THDOC-potentiated tonic currents and spontaneous IPSCs are absent in the δKO mice (Vicini et al., 2002; Wohlfarth et al., 2002; Stell et al., 2003). AP-enhanced GABAergic currents and tonic inhibition in WT DGGCs are also attenuated in δKO mice (Carver et al., 2014; Carver and Reddy, 2016), signifying the obligatory role of the δ subunit in neurosteroid sensitivity. In the present study, we demonstrate that δ subunit plays an essential role in GX's allosteric and direct augmentation of tonic inhibition in native neurons. These findings are consistent with the emerging importance of δ-containing GABA-ARs to tonic inhibition and neurosteroid sensitivity.

The IPSCs primarily represent the activation of synaptic GABA-ARs. To elucidate the extent of GX's modulation of synaptic GABA-ARs and the role of δ subunit in such modulation, we recorded the mIPSCs from WT and δKO DGGCs. GX has a greater effect on the amplitude and the decay time of mIPSCs in WT DGGCs, an effect prevented by the deletion of δ-subunit, which indicates that δGABA-ARs mediate this effect. Previous studies have shown the effect of δ subunit on the neurosteroid-mediated phasic currents (Carver and Reddy, 2016). In cerebellar granule neurons, which have the highest expression of the δ subunit, THDOC exerts strong potentiation of spontaneous IPSCs. However, this is significantly diminished in δKO neurons (Vicini et al., 2002). In WT DGGCs, which have the second highest expression of the δ-subunit, alphaxolone strongly prolongs the decay time of mIPSCs, but not in those from δKO mice (Spigelman et al., 2003). δKO mice were observed to have a significant reduction in the expression of the α4 subunit and an increase in the γ2 subunit (Peng et al., 2002; Spigelman et al., 2003). This notion is with previous reports that α4δ-containing GABA-ARs are more sensitive to neurosteroid modulation (Brown et al., 2002; Wohlfarth et al., 2002). It is also possible that a population of perisynaptic GABA-ARs could respond to synaptic spillover of GABA, and this effect is likely to be prevented by the deletion of δ subunit

(Bianchi and Macdonald, 2002; Carver et al., 2014). However, another study reports that δ-containing receptors are less sensitive to GABA that could be present through synaptic spillover (Bright et al., 2011). Overall, these results demonstrate that δKO mice exhibit significantly attenuated responses to neurosteroid modulation of synaptic GABA-AR-mediated phasic currents, suggesting the significance of δ subunit in the neurosteroid sensitivity.

Protein kinase activity influences the surface expression of GABA-ARs and the neurosteroid sensitivity. Several GABA-AR subunits are substrates of PKC including the α4 and β subunits (Abramian et al., 2010; Adams et al., 2015). PKC activator potentiates THDOC-enhanced GABA-gated currents in recombinant receptors (Leidenheimer and Chapell, 1997), while inhibition of PKC reduces the THDOC and AP-prolonged decay time of mIPSCs in murine neurons (Fancsik et al., 2000; Harney et al., 2003). THDOC also promotes the phosphorylation of the S443 within the α4 subunit and the upregulation of α4-containing GABA-ARs in the cell membrane, leading to increased tonic inhibition (Abramian et al., 2010; Abramian et al., 2014). The δ subunit is predominately assembled with the α4 and α6 subunit (Jones et al., 1997; Peng et al., 2002; Spigelman et al., 2003). In the present study, we demonstrate that PKC activity mediates the potentiation of tonic currents by AP and GX in DGGCs. The inhibition of PKC may cause the downregulation of α4δ-containing GABA-ARs in the cell membrane through reduced phosphorylation of α4 subunits and subsequent attenuated tonic current potentiation by neurosteroids. A recent study indicates that sustained application of AP, but not GX, leads to increased phosphorylation and surface expression of the β3-containing GABA-ARs, and tonic current potentiation. These effects are prevented by the PKC inhibitor (Modgil et al., 2017). Although GX does not have a metabotropic effect on GABA-AR phosphorylation and trafficking, inhibition of PKC still dampens the potentiation of tonic inhibition by neurosteroids. This is likely because sustained application of the PKC inhibitor causes decreased phosphorylation and subsequent internalization of receptors, and therefore, reduced tonic current potentiation (Comenencia-Ortiz et al., 2014).

We confirmed that GX has potent antiseizure effect in the hippocampus kindling model of epilepsy, which is a well-accepted model of complex partial seizures (Albertson et al., 1980; Sutula, 1990; Reddy et al., 2010). The comparative protective profile of GX and AP is outlined in Table 17. Like other neurosteroids such as AP, GX is highly effective against seizures induced by a variety of triggers, including chemoconvulsants, electrical kindling and chemical kindling (Gasior et al., 2000; Kaminski et al., 2003; Reddy and Woodward, 2004; Reddy and Rogawski, 2012). GX is active in the 6-Hz model, which has been shown to be very responsive to positive modulators of GABA-ARs (Kaminski et al., 2004; Reddy et al., 2015). GX is developed as a rational analog of AP, which is a potent positive allosteric agonist of GABA-ARs (Carter et al., 1997). Since neurosteroids exhibit greater selectivity towards extrasynaptic receptors, the results from this study confirm that the antiseizure effect of GX is mostly due to its preferential interaction with δGABA-ARs besides its actions on synaptic receptors (Carver et al., 2014; Carver and Reddy, 2016). The PK-PD correlation of key outcomes from pharmacological and electrophysiological studies supports this conclusion. In animal seizure models, the ED_{50} value of GX ranges from 2 to 6 mg/kg (Table 17). Based on the GX plasma levels, the estimated threshold plasma concentration for 50% seizure protection is in the range of 510 – 750 ng/ml (1.5 – 2.3 μM) (Reddy and Rogawski, 2000). These concentrations exceed the range for GX allosteric potentiation in DGGCs (0.1 to 0.3 μM), and apparently near the range for producing direct activation (1 – 2 μM), indicating that GX potentiation of GABA-AR-mediated inhibition primarily contributes to its antiseizure activity. However, there is limited PK-PD data from clinical studies. Single oral doses of 50 – 500 mg in healthy subjects resulted in plasma concentrations of 32 – 376 ng/ml (0.01 – 1.1 μM) (Monaghan et al., 2013). Thus, GX and its analogs are powerful anticonvulsants with utility in the treatment of epilepsy and seizures in conditions with intact δGABA-ARs, including catamenial epilepsy, status epilepticus, and chemical neurotoxicity (Reddy, 2016ab).

In conclusion, these results demonstrate that GX and its analogs are preferential allosteric modulators of both synaptic and extrasynaptic GABA-ARs in native hippocampal neurons. GX potentiation of tonic inhibition is δ subunit-dependent and greatly influenced by PKC activity. These outcomes provide a strong mechanistic basis for the therapeutic use of GX in epilepsy and related seizure disorders.

Table 17 Comparative antiseizure ED_{50} values of GX and AP in mouse models of epilepsy.

	AP (mg/kg)	GX (mg/kg)	References
Kindling Models			
Hippocampus kindling	3.5	3.5	(Carver et al., 2014; Reddy et al., 2012)
Amygdala kindling	14 (8–23)	6.6 (5.1–9.7)	(Reddy and Rogawski, 2010)
Cocaine kindling	17.0 (ND)	17.0 (ND)	(Kaminski et al., 2003)
Pentylenetetrazol kindling	ND	3.5 (2.4–5.1)	(Gasior et al., 2000)
Corneal kindling	ND	4.5 (4.0–5.1)	(Carter et al., 1997)
Chemoconvulsant Models			
Pentylenetetrazol (mice)	13.7 (10.1–18.7)	3.5 (2.1–5.8)	(Carter et al., 1997; Kokate et al., 1994)
Pentylenetetrazol (rats)	2.14 (1.10–4.15)	4.3 (2.8–6.9)	(Reddy and Rogawski, 2000; 2001)
Bicuculline	12 (10–15)	4.6 (3.2–6.8)	(Carter et al., 1997)
Picrotoxin	10 (5–19)	ND	(Belelli et al., 1989)
t-Butylbicycloorthobenzoate	ND	11.7 (8.8–15.7)	(Carter et al., 1997)
Flurothyl (rats)	ND	5.0 (ND)	(Liptakova et al., 2000)
N-Methyl-D-aspartate	>40	>30	(Carter et al., 1997)
Kainic acid	>40	>30	(Carter et al., 1997)
4-Aminopyridine	>40	11.5 (8.1–16.3)	(Carter et al., 1997)
Strychnine	>40	>40	(Carter et al., 1997)
Electroshock Models			
Maximal electroshock	29 (19–44)	29.7 (25.3–34.8)	(Carter et al., 1997)
6-Hz stimulation	4.2 (2.7–5.8)	1.5 (1.3–1.7)	(Carver and Reddy, 2016)
Status Epilepticus Models			
Pilocarpine	7 (4–11)	~6	(Briyal and Reddy, 2008; Kokate et al., 1996)
Kainic acid	~20	ND	(Rogawski et al., 2013)

Values in parentheses are 95% confidence limits; ND, not determined.

V.2 The Influence of Zn^{2+} on Neurosteroid Activation of Extrasynaptic δGABA-AR-Mediated Tonic Inhibition and Seizure Protection

Zn^{2+} is an extremely abundant transition metal in the synaptic vesicles of hippocampal glutamatergic mossy fibers and remains a key factor in the modulation of neuronal plasticity (Assaf and Chung, 1984). Disruption of Zn^{2+} homeostasis is associated with many neurological disorders, including seizures, epilepsy, and conditions with compromised brain functions. Previous studies show that Zn^{2+} modulates kinetics of synaptic GABA-ARs and alters the balance of inhibition and excitation (Barberis et al., 2000; Lambert and Belelli, 2002). Zn^{2+} exhibits higher sensitivity to extrasynaptic δGABA-ARs than synaptic γGABA-ARs (Hosie et al., 2003; Wei et al., 2003). However, its inhibition on extrasynaptic receptor-mediated tonic currents and interactions with neurosteroids are not fully understood. Our current study shows that Zn^{2+} pretreatment prevents the anticonvulsant activity of neurosteroids, an effect most likely due to the Zn^{2+} blockade of neurosteroid-potentiated extrasynaptic δGABA-ARs. These receptors represent the main contributors in maintaining the tonic inhibition in the dentate gyrus, which is involved in a number of seizure and memory disorders (Carver et al., 2016).

Positive allosteric modulators targeting extrasynaptic δGABA-ARs, such as neurosteroids, are being evaluated as potential therapeutic agents for the treatment of hyperexcitable brain disorders (Reddy and Rogawski, 2001; 2010; Reddy et al., 2018; Younus and Reddy, 2018). GX is a neurosteroid analog developed as a more favorable therapeutic compound with superior bioavailability and pharmacokinetic profile compared to its prototype neurosteroid AP. Synthetic GX serves as a robust antiseizure agent as well as a powerful allosteric modulator of GABA-ARs with higher selectivity for extrasynaptic δGABA-ARs (Reddy and Rogawski, 2000; 2010; Clossen and Reddy, 2017a; 2017b; Chuang and Reddy, 2018b). Elucidating the neuroprotective effects of GX as well as its interactions with other molecules at the extrasynaptic δGABA-ARs is of critical importance for its clinical use as an antiepileptic drug. In the present study, we demonstrate that Zn^{2+} selectively blocks GX-induced tonic inhibition, but not phasic

inhibition in DGGCs. Chelation of endogenous Zn^{2+} sustains the enhancement of tonic inhibition by GX. Furthermore, intrahippocampal infusion of Zn^{2+} significantly blocked the antiseizure activity of GX in the hippocampus kindling model of epilepsy. Zn^{2+} selective antagonistic interactions with GX at the extrasynaptic δGABA-ARs in the hippocampus may contribute to the blockade of GX-induced antiseizure activity by Zn^{2+}; this drug-drug interaction provides clinical implications in the therapeutic use of GX. Overall, these findings are compatible with an excitability-facilitating and proconvulsant role of Zn^{2+} in seizure-related disorders (Cavazos et al., 1991; Buhl et al., 1996; Coulter, 2000).

Receptor subunit composition plays a critical role not only in neurosteroid sensitivity but also in Zn^{2+} inhibition on GABA-ARs (Draguhn et al., 1990; Smart et al., 1991). Although, in recombinant systems, Zn^{2+} inhibition on GABA-ARs exhibits similar sensitivity in human α4β3γ2 and α4β3δ GABA-ARs (Brown et al., 2002), Zn^{2+} significantly shortens the decay time constant of spontaneous IPSCs as well as dendritically-evoked IPSCs in wildtype δ-rich DGGCs but not δ subunit knockout DGGCs from hippocampus slices (Wei et al., 2003). The absence of sensitivity to Zn^{2+} inhibition in δ subunit knockout DGGCs may be due to the compensatory upregulation of γ2 subunits and thus the reduction of Zn^{2+} binding sites (Peng et al., 2002; Hosie et al., 2003; Carver and Reddy, 2013). In the present study, we compared the sensitivity of GABA-induced currents and GX-potentiated GABA chloride currents to Zn^{2+} inhibition in native δ-abundant DGGCs and δ-sparse CA1PCs. We found increased inhibition of neurosteroid-potentiated GABA currents by Zn^{2+} in DGGCs compared to CA1PCs, displaying the selectivity of Zn^{2+} inhibition based on receptor subunit composition. In addition, Zn^{2+} at 30 μM completely blocks GX-potentiated GABAergic chloride currents, similar to that of the competitive antagonist, bicuculline and gabazine. Due to its preferential modulation to δ-containing receptors, Zn^{2+} represents a potential noncompetitive antagonist of extrasynaptic δGABA-ARs and would aid in pharmacological investigations of extrasynaptic GABA-ARs.

In single channel studies, Zn^{2+} primarily inhibits GABA-ARs through the reduction of channel opening probability (Smart, 1992; Smart et al., 1994). In slice recordings, Zn^{2+} significantly reduces phasic mIPSC event amplitude and kinetics, as well as desensitization kinetics (Barberis et al., 2000; Ruiz et al., 2004). However, we demonstrate that GX-enhanced phasic mIPSCs were unaltered by Zn^{2+}. It could be that GX potentiation overcomes Zn^{2+} depression of synaptic receptors so that the overall effects of Zn^{2+} on GX-potentiated phasic currents were undetectable. However, in tonic current potentiation, Zn^{2+} blocks GX-potentiated tonic response concentration-dependently in δ-rich DGGCs, probably due to its greater sensitivity towards δ-containing receptors. Unexpectedly, Zn^{2+} prolonged the fast decay time constant τ1 of mIPSCs in the presence of GX. One possibility might be due to the biphasic effects of Zn^{2+} on GABA-B receptors that tonically enhance GABA-AR currents (Turgeon and Albin, 1992; Khatri et. al., 2018). In addition, receptor combinations with different subunits respond to Zn^{2+} and neurosteroids differently. Finally, Zn^{2+} may have different effects on fast-closing GABA-AR subtypes (Draguhn et al., 1990; Smart et al., 1991).

Zn^{2+} has been shown to act on multiple neurotransmission systems in the brain. In addition to its inhibitory effects on GABA-AR function (Smart et al., 1991;1994; Barberis et. al., 2000; Carver et al., 2016), Zn^{2+} also antagonizes excitatory glutamate NMDA receptor channels and decreases the activation and surface expression of NR2A-contaning NMDA receptors in hippocampal neurons (Westbrook and Mayer, 1987; Vogt et al., 2000; Zhu et al., 2012). Additionally, Zn^{2+} enhances the activity of AMPA receptors (Timofeeva and Nadler, 2006) and increases glycinergic neurotransmission. Therefore, it is possible that the excitability-facilitating and proconvulsant role of Zn^{2+} against GX-induced protective effects in the kindling seizure model may be resulted from the overall outcome of disrupted neurotransmission by Zn^{2+}. Nevertheless, we have previously shown a critical role of extrasynaptic δGABA-AR in seizure susceptibility as mice lacking δ subunit have significantly reduced tonic currents and greater seizure susceptibility (Carver et al., 2014). Thus, Zn^{2+} selective antagonistic interactions with GX

at the extrasynaptic δGABA-ARs in the hippocampus may contribute to the inhibition of GX-induced antiseizure activity by Zn^{2+}.

Zn^{2+} exhibits antagonistic activity at α4βγ- and α1βδ-containing GABA-ARs, albeit at lower sensitivities than α4βδ subtypes (Brown et al., 2002). Specific deletion of δ subunits in α1βδ-containing DG interneurons leads to the reduced GABAergic tonic inhibition and elevated firing rate of interneurons that decrease DGGC excitability and in vivo seizure susceptibility (Lee and Maguire, 2013). Therefore, Zn^{2+} may also contribute to the disinhibition of α1βδ-containing interneurons.

In the seizure model of hippocampal kindling, the composition and expression of GABA-ARs in the hippocampus have been largely altered (Nishimura et al., 2005). In hippocampus DG, the mRNA levels of δ subunit were significantly reduced with an increase in α2 subunits seven days after kindling completion. In CA3 pyramidal neurons, α2 and β3 subunits were significantly upregulated after hippocampal kindling. While in CA1 pyramidal neurons, no significant changes of GABA-AR subunits were observed. As a result, the sensitivity of each cell types to Zn^{2+} modulation may be different from animals without kindling, which may also involve in the Zn^{2+} antagonism of GX-induced seizure protection. Nevertheless, we observed the net outcome of Zn^{2+} in hippocampal kindling to be proconvulsant.

Zn^{2+} increases the permeability of blood-brain barrier and proconvulsant activity in rats (Yorulmaz et al., 2013). Severe blood-brain barrier damage is also found in pentylenetetrazol-induced epileptic seizures. The Zn^{2+} level in the brain may fluctuate due to the contribution of peripheral Zn^{2+} that penetrates the damaged blood-brain barrier. Zn^{2+} concentrations are particularly high in some brain regions including hippocampus and amygdala, which are also the most vulnerable regions for the focal point of seizures (Frederickson et al., 2005). The effective concentrations of Zn^{2+} in the inhibition of GX-potentiated tonic currents are within the levels that may occur in synaptic clefts following the Zn^{2+} release from the vesicles of presynaptic neurons during neuronal activity.

Therefore, Zn^{2+} may disrupt the neurosteroid-augmented basal inhibitory tone and hinder the balance of hippocampal neural circuits. In physiological condition, free zinc cations released from glutamatergic synapses in the hippocampus may block the inhibition of extrasynaptic activity of neurosteroids, hindering the antiseizure effects of neurosteroids. Therefore, combination therapies of neurosteroids with Zn^{2+} chelators may be potential avenues for the treatment of seizure-related disorders. We have attempted to examine the effects of Zn^{2+} chelators on the seizure activity of hippocampal kindling animals. However, a previous study shows that TPEN exerts notable toxic effects in *in vivo* animal studies, which was the reason these studies were not conducted further (Elsas et al., 2009). In Foresti et al., 2008, they used another Zn^{2+} chelator and found that pretreatment of Zn^{2+} chelator DEDTC (700 mg/kg) diminishes the duration of behavioral seizures and electrical afterdischarges, and EEG spikes, without altering seizure severity progression in a rat model of amygdala kindling, showing the antiseizure effects of the Zn^{2+} chelator (Foresti et al., 2008). Although their experiments show an antiseizure role of the zinc chelator, they cannot exclude the potential toxic effects of DEDTC. In their studies, they selected a dose that did not cause significant behavioral changes but still may be high enough to cause toxic effects in cellular and molecular levels since animals experienced severe ocular and nasal bleeding and reduced locomotor activity with the treatment of DEDTC. Future studies of Zn^{2+} chelators on the seizure activity are feasible when nontoxic Zn^{2+} chelators become available.

The schematic diagram of the antagonistic interactions of Zn^{2+} and neurosteroids (NSs) at GABA-ARs is summarized in Figure 34. Neurosteroids exhibit powerful seizure protective effects against experimental seizures probably through the potentiation of synaptic and extrasynaptic GABA-AR-mediated inhibitory currents. However, Zn^{2+} selectively hinders neurosteroid-augmented tonic inhibition but not phasic inhibition, which may partially contribute to the Zn^{2+} antagonism of neurosteroid-induced antiseizure activity. Previous studies show that Zn^{2+} blocks the frequency of mIPSCs in DGGCs from kindled but not controls (Buhl et al., 1996). Reduced Zn^{2+} sensitivity in GABA currents is found in DGGCs from rats with status epilepticus (Kapur and

Macdonald, 1997). Zn^{2+} inhibition of GABA-AR function is also decreased in pilocarpine-induced status epilepticus (Banerjee et al., 1999). Overall, Zn^{2+} greatly contributes to the balance of neuronal excitation and inhibition in both physiological and pathophysiological conditions. There are many questions that remain unclear, including whether posttranslational modifications affect Zn^{2+} sensitivity of GABA-ARs.

In conclusion, the present study demonstrates selective antagonistic interactions of Zn^{2+} and GX at extrasynaptic δGABA-ARs in the hippocampus. Zn^{2+} chelation sustains the potentiation of tonic inhibition by GX. Furthermore, intrahippocampal infusion of Zn^{2+} significantly blocks the antiseizure activity of GX in the mouse kindling model of epilepsy, indicating that Zn^{2+} reduces the antiseizure effects of neurosteroids by selective blockade of extrasynaptic δGABA-ARs. These pharmacodynamic interactions may have clinical implications in neurosteroid therapy of brain disorders susceptible to zinc fluctuations.

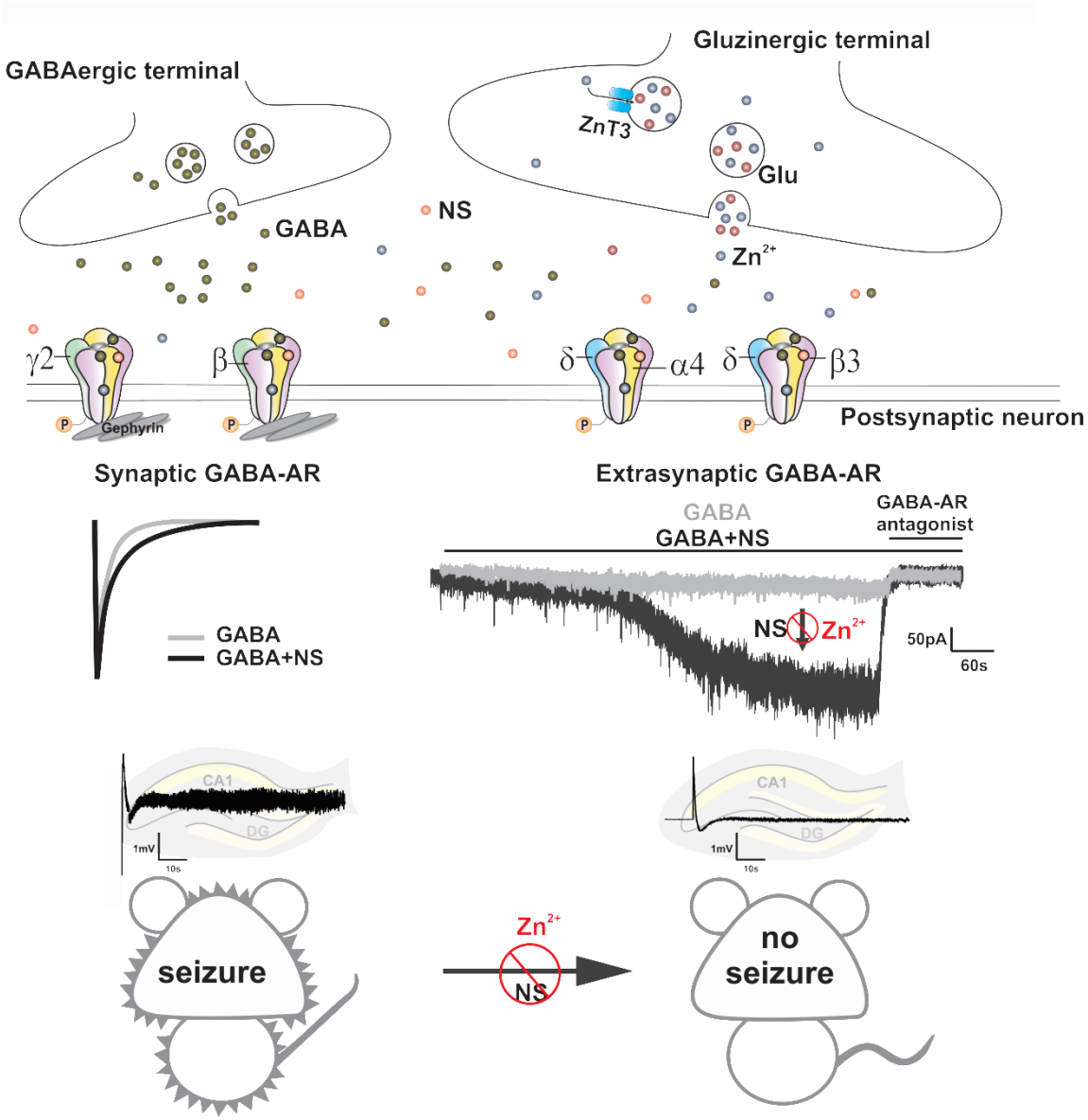

Figure 34 Schematic diagram of pharmacodynamic interactions of Zn^{2+} and neurosteroids at GABA-ARs.

Neurosteroids exhibit powerful seizure protective effects against kindling-induced limbic seizures probably through the potentiation of synaptic and more preferably extrasynaptic GABA-AR-mediated inhibitory currents. Zn^{2+} selectively hinders neurosteroid-sensitive tonic inhibition but not phasic inhibition, which may partially contribute to the Zn^{2+} antagonism of antiseizure activity of neurosteroids, including endogenous neurosteroids and their synthetic analogs such as GX. NS denotes neurosteroid.

V.3 Isobolographic Analysis of Extrasynaptic GABA-AR-Mediated Tonic Inhibition and Anticonvulsant Activity of Neurosteroid Combinations with TG and MDZ

The main finding of the present study is the demonstration of synergistic effects of neurosteroids and TG combinations in potentiating tonic inhibition in the hippocampus and protecting against acute seizures. This synergistic effect is likely due to a greater potentiation at extrasynaptic δGABA-ARs by neurosteroids through TG-induced elevated levels of extracellular GABA. The potential pharmacodynamic synergistic interaction between neurosteroids and the benzodiazepine MDZ provides better protection against acute seizures (Figure 35). Together, these findings provide valuable mechanistic rationale for synergistic therapeutic potential of neurosteroids with TG or MDZ for epilepsy therapy, with reduced doses and possibly reduced side effects.

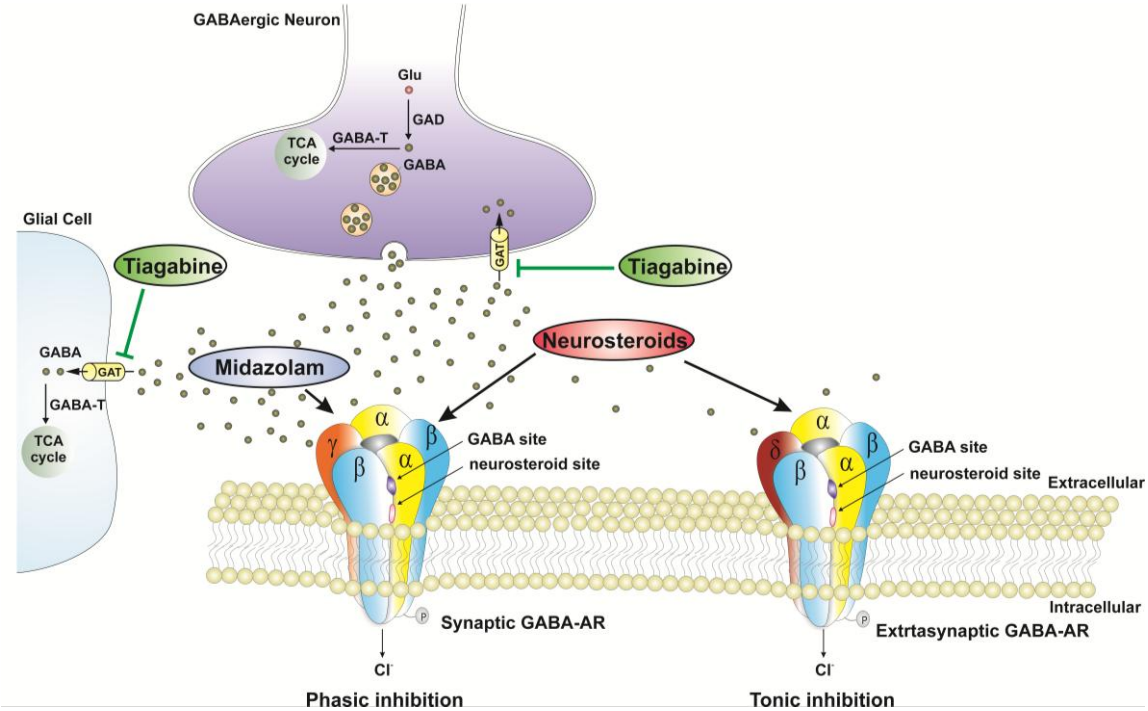

Figure 35 Molecular pathways of potential synergistic interactions between neurosteroids and the GABAergic drugs tiagabine or midazolam.

GABA-ARs are pentameric GABA-gated chloride channels formed from 19 different subunits. Channels made from different combinations of subunits produce receptor subtypes with distinct functional properties. GABA-ARs are classified into two major groups based on their location: synaptic and extrasynaptic receptors. Synaptic (γ-containing) receptors generate transient inhibitory phasic current, whereas extrasynaptic (δ-containing) receptors generate persistent inhibitory tonic currents that regulate basal neuronal excitability. The GABA reuptake inhibitor tiagabine-induced elevation in GABA levels is suggested to augment the allosteric responses of neurosteroids at synaptic and extrasynaptic GABA-ARs, possibly due to greater additivity of free energy for the open state of receptor channels. When the benzodiazepine midazolam is coadministered, a pharmacodynamic interaction is predicted to result in super-additive or synergism between neurosteroids and midazolam, possibly due to energetic additivity as they interact with distinct sites on receptor complex.

Neurosteroids can interact with other GABAergic drugs within the receptor milieu or at the receptor complex (Figure 35). The molecular mechanisms of action of neurosteroids on GABA neurotransmitter system include allosteric and direct agonism on GABA-ARs (Hosie et al., 2007). At lower nanomolar concentrations, neurosteroids bind to the allosteric site of GABA-ARs and potentiate the action of GABA; while at higher micromolar concentrations, neurosteroids can directly activate chloride channels through the binding of the orthosteric site. GX and AP potentiate phasic and tonic currents by acting at synaptic and extrasynaptic δ-rich receptors in DGGCs, respectively. GX and AP exhibit comparable allosteric and direct effects on GABA-gated chloride currents (Chuang and Reddy, 2018b, 2019). TG is a selective GABA transporter-1 inhibitor that blocks the reuptake of GABA into neurons and glial cells, resulting in the elevation of GABA concentration in the synaptic cleft and extracellular milieu (Czuczwar and Patsalos 2001). Therefore, it is predictable that combination treatment of TG and neurosteroids (AP or GX) exerts synergistic effects on extrasynaptic GABA-AR-mediated tonic inhibition in dentate gyrus since the allosteric potentiating actions of neurosteroid on GABA-ARs were GABA dependent. It would be interesting to know if the combination treatment of neurosteroids and TG also synergistically potentiate synaptic phasic currents.

The 6-Hz-induced partial seizure model is one of the most sensitive models for the evaluation of seizure protective effects of AEDs that act on GABA system (Kaminski et al., 2004; Reddy et al., 2015). Neurosteroids and benzodiazepines exhibit powerful anticonvulsant activity in the 6-Hz model. In the present study, our results show that both AP and GX have robust anticonvulsant effects in this model, supporting for that concept. Interestingly, in the combination studies, we found strong synergistic enhancement of anticonvulsant activity of AP when coadministered with TG. Both neurosteroids in combination with TG produced synergistic potentiation of tonic inhibition in the hippocampal dentate gyrus neurons. However, there are some striking differences between GX and AP. GX (ED_{50} = 1.46 mg/kg) exhibits higher anticonvulsant potency than AP (ED_{50} = 4.20 mg/kg) in the 6-Hz test. GX has greater bioavailability and fewer

side effects than AP (Carter et al, 1997). Some pharmacodynamic differences may arise due to pharmacokinetic changes between GX and TG when administered simultaneously. Another possibility is the differences in the permeability of the drugs across the blood brain barrier. TG is a lipophilic agent that effectively and competitively inhibits the GAT-1 in the brain. TG has been used in the treatment of partial seizures as an add-on drug. However, its utility is limited because of its adverse profile and limited spectrum of seizure protection. Combined treatment of neurosteroids with TG largely reduces the dosages of each drug, providing better therapeutic outcomes. Some previous studies have shown the synergistic therapeutic potentials of TG with other AEDs in other seizure models, including genetic epilepsy and Dravet syndrome, supporting the benefits of combination therapies (Luszczki and Czuczwar 2004; Madsen et al., 2009; Oakley et al., 2013).

The benzodiazepine MDZ is widely used for controlling acute seizures and status epilepticus, but it is not highly effective for delayed therapy or refractory status epilepticus. MDZ is an allosteric agonist of synaptic GABA-ARs through sites distinct from the neurosteroid binding site (Nusser et al., 1997). A previous study has shown that the combination of GX and MDZ exerts synergistic anxiolytic effects (Gunter et. al., 2016). In the present study, we found that neurosteroid exerts a synergistic response with MDZ on GABA-ARs. The interactions between neurosteroids and MDZ on GABA-AR function are complex and several possible mechanisms could explain their synergistic effects on the antiepileptic activity. MDZ is a high-affinity, preferential positive allosteric agonist of synaptic γ-containing GABA-ARs that potentiates transient phasic IPSCs. Combined with low-affinity neurosteroids whose actions mainly lie on the potentiation of extrasynaptic δ-containing GABA-AR-mediated tonic currents, the overall inhibitory GABA neurotransmitter system in the hippocampus is strongly enhanced and thus contributes to greater antiseizure activity. In addition, a recent study shows a crosstalk between phasic and tonic inhibition in DGGCs as δGABA-ARs also contribute to phasic inhibition that can effectively shunt excitatory postsynaptic potentials (Sun et al., 2018).

MDZ also interacts with TSPO, a translocator protein that plays a crucial role in the synthesis of neurosteroids (Papadopoulos et al., 2006). However, MDZ at therapeutic dosage does not influence the level of endogenous neurosteroid AP in plasma and brain (Reddy et al., 2015). Therefore, it is unlikely that the synergistic effects of GX+MDZ stem from MDZ-induced changes in neurosteroid levels in the brain.

The precise mechanisms underlying the synergic anticonvulsant response of neurosteroids are unknown. In general, the potential mechanisms underlying synergistic and additive effects on GABAergic tonic inhibition may result from a variety of pharmacodynamic effects from a combination of two drugs, including both competitive and noncompetitive interactions at the receptor sites (Earp et al., 2004). The recent analysis of GABA-AR activation by combinations of agonists acting at the same or distinct binding sites has led to an interesting premise for predicting the efficacy of GABAergic drug mixtures in combination therapy (Shin et al., 2017; 2019; Cao et al., 2018). Coapplication of two GABAergic agents typically results in potentiation of the inhibitory current response. Direct activation of the GABA-AR and potentiation of GABA-gated receptors underlie the clinical actions of neurosteroids. The extent of current potentiation and thereby the *in vivo* anticonvulsant efficacy of a neurosteroid depends on the type of co-drug (indirect acting agent or direct acting allosteric agonist that interact with the same or different sites). Combination of two agonists acting at the same sites can result in potentiation due to concentration additivity based on their individual efficacies and concentration (Shin et al., 2019). In contrast, GABAergic drug combinations where the individual drugs interact with distinct sites may produce potentiation via energetic additivity, such as coapplication of propofol with GABA or co-administration of alfaxolone with diazepam (Cao et al., 2018). Coapplication of two allosteric agonists that interact with distinct sites would result in additivity of free energies for the open state of receptor channels (Shin et al., 2017). Thus, neurosteroid combination with MDZ that interact with distinct sites may produce greater potentiation via energetic additivity and yield supra-additive or synergistic response, as evident from a curvilinear isobole (Figure 33). It has been shown previously that coapplication of the

synthetic neurosteroid alfaxalone enhances the GABAergic effects of etomidate (Li et al., 2014) and diazepam (Cao et al., 2018). In the present study, we show that GX, which acts on the same sites as alfaxolone, exhibits synergism with MDZ on tonic current potentiation (Figure 32). The indirect acting agents such as TG, an orthostatic agonist, elevate the levels of GABA. Consequently, TG is predicted to be highly synergistic when combined with the neurosteroid AP (Figure 30) or GX (Figure 28) because they interact with distinct target sites. Such agonist combinations have significant clinical implications when combination therapies are desired for refractory epilepsy, pharmacoresistant status epilepticus, and other seizure disorders. High doses of currently used AEDs exhibit notable adverse effects and drug interactions. Neurosteroids provide as viable adjuncts for combination therapy with AEDs for both increasing seizure control and reducing unwanted side effects associated with high doses of AEDs.

In conclusion, these results demonstrate robust synergistic effects of neurosteroid and TG combinations in potentiating tonic inhibition and protecting against acute seizures. This synergic efficacy is likely due to a greater allosteric agonism at extrasynaptic GABA-ARs from TG-induced increase in GABA levels, indicating a role for tonically activated extrasynaptic GABA-ARs in the clinical action of AED combination regimens. These findings provide a mechanistic rationale for clinical potential of neurosteroid – TG combination for refractory epilepsy. Similarly, the synergism between GX and MDZ offers a viable path for their combination therapy for status epilepticus, such as the benzodiazepine-refractory organophosphate nerve agent-induced status epilepticus.

CHAPTER VI
CONCLUSIONS

Epilepsy is a chronic neurological disease characterized by repeated unprovoked seizures. Antiepileptic drugs (AEDs) are the mainstay for the treatment of epilepsy that affects nearly 65 million people worldwide. AEDs are the most effective interventions to suppress the occurrence of seizures; however, approximately 30% of epilepsy patients are unresponsive to current AEDs when used in monotherapy. Neurosteroids such as AP are powerful allosteric agonists of GABA-ARs and are more efficacious on extrasynaptic δGABA-ARs that mediate tonic inhibition. There are many synthetic neurosteroids in trials. Synthetic GX is a robust antiseizure agent as well as a powerful allosteric modulator of GABA-ARs with higher bioavailability and less hormonal side effects compared to its prototype AP. Elucidating the mechanisms of action of GX as well as its interactions with other molecules at the extrasynaptic δGABA-ARs and the synergistic therapeutic potential are of critical importance for its clinical use as an AED. This work investigates the mechanisms of action of GX and related neurosteroid analogs on extrasynaptic δGABA-AR-mediated tonic inhibition and seizure protection. We also explore the physiological interactions between neurosteroids and zinc and the potential combination strategy of neurosteroids with other clinical GABAergic agents, including TG and MDZ.

In studies in aim 1, we found that GX and its analogs are positive allosteric modulators and direct activators of both synaptic and extrasynaptic δGABA-ARs in the dentate gyrus that regulate network tonic inhibition and seizures. The preferential potentiation of tonic inhibition by GX is δ subunit-dependent and greatly influenced by protein kinase C activity. In addition, GX's protection against hippocampus kindled seizures was significantly diminished in δ subunit knockout mice. These results suggest that GX controls seizure susceptibility probably by potentiating GABA-AR-medicated synaptic and tonic inhibition though allosteric and/or direct action. Overall, these findings provide a mechanistic basis for the clinical use of GX in epilepsy and related seizure disorders.

In studies in aim 2, we show that Zn^{2+} selectively blocks GX-potentiated tonic inhibition, but not phasic inhibition in DGGCs. Chelation of endogenous Zn^{2+} sustains the enhancement of tonic inhibition by GX. Furthermore, intrahippocampal infusion of Zn^{2+} significantly blocks the seizure protective activity of GX in the hippocampus kindling model of epilepsy. Zn^{2+} selective antagonistic interactions with GX at the extrasynaptic δGABA-ARs in the hippocampus may contribute to the blockade of GX-induced antiseizure activity by Zn^{2+}; this drug-drug interaction provides clinical implications in the therapeutic use of GX.

In studies in aim 3, we demonstrate strong synergistic effects of neurosteroid + TG and GX + MDZ combinations in potentiating tonic inhibition in DGGCs and protecting against acute seizures. The synergic efficacy of neurosteroid + TG is likely due to a greater allosteric agonism at extrasynaptic δGABA-ARs from TG-induced increase in GABA levels, indicating a role for tonically activated extrasynaptic δGABA-ARs in the clinical action of AED combination regimens. These findings provide a mechanistic rationale for therapeutic potential of neurosteroid + TG combination for refractory epilepsy, possibly with better efficacy and reduced side effects. Similarly, the synergism between GX and MDZ offers a viable path for their combination therapy for epilepsy therapy such as status epilepticus.

REFERENCES

Abramian AM, Comenencia-Ortiz E, Modgil A, Vien TN, Nakamura Y , Moore YE, Maguire JL, Terunuma M, Davies PA, and Moss SJ (2014) Neurosteroids promote phosphorylation and membrane insertion of extrasynaptic GABA-A receptors. *Proc Natl Acad Sci USA* **111**:7132.

Abramian AM, Comenencia-Ortiz E, Vithlani M, Tretter EV, Sieghart W, Davies PA, and Moss SJ (2010) Protein kinase C phosphorylation regulates membrane insertion of GABA-A receptor subtypes that mediate tonic inhibition. *J Biol Chem* **285**:41795.

Adams JM, Thomas P, and Smart TG (2015) Modulation of neurosteroid potentiation by protein kinases at synaptic- and extrasynaptic-type GABA-A receptors. *Neuropharmacology* **88**:63.

Adkins JC and Noble S (1998) Tiagabine. A review of its pharmacodynamic and pharmacokinetic properties and therapeutic potential in the management of epilepsy. *Drugs* **55**:437.

Albertson TE, Peterson SL, and Stark LG (1980) Anticonvulsant drugs and their antagonism of kindled amygdaloid seizures in rats. *Neuropharmacology* **19**:643.

Assaf SY and Chung SH (1984) Release of endogenous Zinc from brain tissue during activity. *Nature* **308**:734.

Audenaert D, Schwartz E, Claeys KG, Claes L, Deprez L, Suls A, Van Dyck T, Lagae L, Van Broeckhoven C, Macdonald RL, and De Jonghe P (2006) A novel GABRG2 mutation associated with febrile seizures. *Neurology* **67**:687.

Banerjee PK, Olsen RW, and Snead OC (1999) Zinc inhibition of GABA-A receptor function is decreased in the cerebral cortex during pilocarpine-induced status epilepticus. *J Pharmacol Exp Ther* **291**:361-366.

Barberis A, Cherubini E, and Mozrzymas JW (2000) Zinc inhibits miniature GABAergic currents by allosteric modulation of GABA-A receptor gating. *J Neurosci* **20**:8618-8627.

Baulac S, Huberfeld G, Gourfinkel-An I, Mitropoulou G, Beranger A, Prud'homme JF, Baulac M, Brice A, Bruzzone R, and LeGuern E (2001) First genetic evidence of GABA-A receptor dysfunction in epilepsy: a mutation in the gamma2 subunit gene. *Nat Genet* **28**:46-48.

Baulieu EE (1981) Steroid hormones in the brain: several mechanisms? In: Fuxe F, Gustafsson JA, Wetterberg L, eds. Steroid Hormone Regulation of the Brain. *Oxford: Pergamon Press*, pp-3–14.

Belelli D, Bolger MB, and Gee KW (1989) Anticonvulsant profile of the progesterone metabolite 5α-pregnan-3α-ol-20-one. *Eur J Nurosci* **166**:325-330.

Belelli D and Herd MB (2003) The contraceptive agent Provera enhances GABA-A receptor-mediated inhibitory neurotransmission in the rat hippocampus: evidence for endogenous neurosteroids? *J Neurosci* **23**:10013-10020.

Belelli D and Lambert JJ (2005) Neurosteroids: endogenous regulators of the GABA-A receptor. *Nature Rev Neurosci* **6**:565-575.

Berenbaum MC (1977) Synergy, additivism and antagonism in immunosuppression. A critical review. *Clin Exp Immunol* **28**:1-18.

Berenbaum MC (1989) What is synergy? Pharmacol Rev 41:93–141 Erratum published in (1989) *Pharmacol Rev* **41**:422

Bialer M, Johannessen SI, Levy RH, Perucca E, Tomson T, and White HS (2015) Progress report on new antiepileptic drugs: A summary of the Twelfth Eilat Conference (EILAT XII). *Epilepsy Res* **111**:85-141.

Bianchi MT and Macdonald RL (2002) Slow phases of GABA-A receptor desensitization: structural determinants and possible relevance for synaptic function. *J Physiol* **544**:3-18.

Bianchi MT and Macdonald RL (2003) Neurosteroids shift partial agonist activation of GABA-A receptor channels from low- to high-efficacy gating patterns. *J Neurosci* **23**:10934-10943.

Bitanihirwe BK and Cunningham MG (2009) Zinc: the brain's dark horse. *Synapse* **63**:1029-1049.

Blednov YA, Jung S, Alva H, Wallace D, Rosahl T, Whiting PJ, and Harris RA (2003) Deletion of the alpha1 or beta2 subunit of GABA-A receptors reduces actions of alcohol and other drugs. *J Pharmacol Exp Ther* **304**:30-36.

Boehm SL, 2nd, Homanics GE, Blednov YA, and Harris RA (2006) Delta subunit containing GABA-A receptor knockout mice are less sensitive to the actions of 4,5,6,7-tetrahydroisoxazolo-[5,4-c]pyridin-3-ol. *Eur J Pharmacol* **541**:158-162.

Bouthour W, Leroy F, Emmanuelli C, Carnaud M, Dahan M, Poncer JC, and Levi S (2012) A human mutation in GABRG2 associated with generalized epilepsy alters the membrane dynamics of GABA-A receptors. *Cerebral Cortex* **22**:1542-1553.

Braat S, D'Hulst C, Heulens I, De Rubeis S, Mientjes E, Nelson DL, Willemsen R, Bagni C, Van Dam D, De Deyn PP, and Kooy RF (2015) The GABA-A receptor is an FMRP target with therapeutic potential in fragile X syndrome. *Cell Cycle* **14**:2985-2995.

Bracamontes JR, Li P, Akk G, and Steinbach JH (2014) Mutations in the main cytoplasmic loop of the GABA-A receptor alpha4 and delta subunits have opposite effects on surface expression. *Mol Pharmacol* **86**:20-27.

Bradley CA, Taghibiglou C, Collingridge GL, and Wang YT (2008) Mechanisms involved in the reduction of GABA-A receptor alpha1 subunit expression caused

by the epilepsy mutation A322D in the trafficking-competent receptor. *J Biol Chem* **283**:22043-22050.

Brandon NJ, Delmas P, Kittler JT, McDonald BJ, Sieghart W, Brown DA, Smart TG, and Moss SJ (2000) GABA-A receptor phosphorylation and functional modulation in cortical neurons by a protein kinase C-dependent pathway. *J Biol Chem* **275**:38856-38862.

Brickley SG, Cull-Candy SG, and Farrant M (1996) Development of a tonic form of synaptic inhibition in rat cerebellar granule cells resulting from persistent activation of GABA-A receptors. *J Physiol* **497**:753-759.

Brickley SG, Cull-Candy SG, and Farrant M (1999) Single-channel properties of synaptic and extrasynaptic GABA-A receptors suggest differential targeting of receptor subtypes. *J Neurosci* **19**:2960-2973.

Brickley SG and Mody I (2012) Extrasynaptic GABA-A receptors: Their function in the CNS and implications for disease. *Neuron* **73**:23-34.

Bright DP, Renzi M, Bartram J, McGee TP, MacKenzie G, Hosie AM, Farrant M, and Brickley SG (2011) Profound desensitization by ambient GABA limits activation of delta-containing GABA-A receptors during spillover. *J Neurosci* **31**:753-763.

Briyal S and Reddy DS (2008) Neuroactive steroid therapy of status epilepticus in epilepsy rats. *Epilepsia* **49**(Suppl 7):3055.

Brown AR, Herd MB, Belelli D, and Lambert JJ (2015) Developmentally regulated neurosteroid synthesis enhances GABAergic neurotransmission in mouse thalamocortical neurones. *J Physiol* **593**:267-284.

Brown N, Kerby J, Bonnert TP, Whiting PJ, and Wafford KA (2002) Pharmacological characterization of a novel cell line expressing human alpha4beta3delta GABA-A receptors. *Br J Pharmacol* **136**:965-974.

Buhl EH, Otis TS, and Mody I (1996) Zinc-induced collapse of augmented inhibition by GABA in a temporal lobe epilepsy model. *Science* **271**:369-373.

Cao LQ, Montana MC, Germann AL, Shin DJ, Chakrabarti S, Mennerick S, Yuede CM, Wozniak DF, Evers AS, and Akk G (2018) Enhanced GABAergic actions resulting from the coapplication of the steroid 3α-hydroxy-5α-pregnane-11,20-dione (alfaxalone) with propofol or diazepam. *Sci Rep* **8**:10341.

Carter RB, Wood PL, Wieland S, Hawkinson JE, Belelli D, Lambert JJ, White HS, Wolf HH, Mirsadeghi S, Tahir SH, Bolger MB, Lan NC, and Gee KW (1997) Characterization of the anticonvulsant properties of ganaxolone (CCD 1042; 3alpha-hydroxy-3beta-methyl-5alpha-pregnan-20-one), a selective, high-affinity, steroid modulator of the gamma-aminobutyric acid A receptor. *J Pharmacol Exp Ther* **280**:1284-1295.

Carver CM, Chuang SH, and Reddy DS (2016) Zinc selectively blocks neurosteroid-sensitive extrasynaptic deltaGABA-A receptors in the hippocampus. *J Neurosci* **36**:8070-8087.

Carver CM and Reddy DS (2013) Neurosteroid interactions with synaptic and extrasynaptic GABA-A receptors: regulation of subunit plasticity, phasic and tonic inhibition, and neuronal network excitability. *Psychopharmacology (Berl)* **230**:151-188.

Carver CM and Reddy DS (2016) Neurosteroid structure-activity relationships for functional activation of extrasynaptic deltaGABA-A receptors. *J Pharmacol Exp Ther* **357**:188-204.

Carver CM, Wu X, Gangisetty O, and Reddy DS (2014) Perimenstrual-like hormonal regulation of extrasynaptic delta-containing GABA-A receptors mediating tonic inhibition and neurosteroid sensitivity. *J Neurosci* **34**:14181-14197.

Carvill GL, Weckhuysen S, McMahon JM, Hartmann C, Moller RS, Hjalgrim H, Cook J, Geraghty E, O'Roak BJ, Petrou S, Clarke A, Gill D, Sadleir LG, Muhle H, von Spiczak S, Nikanorova M, Hodgson BL, Gazina EV, Suls A, Shendure J, Dibbens LM, De Jonghe P, Helbig I, Berkovic SF, Scheffer IE, and Mefford HC (2014) GABRA1 and STXBP1: novel genetic causes of Dravet syndrome. *Neurology* **82**:1245-1253.

Cavazos JE, Golarai G, and Sutula TP (1991) Mossy fiber synaptic reorganization induced by kindling: time course of development, progression, and permanence. *J Neurosci* **11**:2795-2803.

Chandra D, Halonen LM, Linden AM, Procaccini C, Hellsten K, Homanics GE, and Korpi E (2010) Prototypic GABA-A receptor agonist muscimol acts preferentially through forebrain high-affinity binding sites. *Neuropsychopharmacology* **35**:999-1007.

Chandra D, Jia F, Liang J, Peng Z, Suryanarayanan A, Werner DF, Spigelman I, Houser CR, Olsen RW, Harrison NL, and Homanics GE (2006) GABA-A receptor alpha4 subunits mediate extrasynaptic inhibition in thalamus and dentate gyrus and the action of gaboxadol. *Proc Natl Acad Sci USA* **103**:15230-15235.

Chandra D, Korpi ER, Miralles CP, De Blas AL, and Homanics GE (2005) GABA-A receptor gamma2 subunit knockdown mice have enhanced anxiety-like behavior but unaltered hypnotic response to benzodiazepines. *BMC Neurosci* **6**:30.

Chaumont S, Andre C, Perrais D, Boue-Grabot E, Taly A, and Garret M (2013) Agonist-dependent endocytosis of GABA-A receptors revealed by a gamma2 (R43Q) epilepsy mutation. *J Biol Chem* **288**:28254-28265.

Cherubini E and Conti F (2001) Generating diversity at GABAergic synapses. *Trends in neurosciences* **24**:155-162.

Chisari M, Eisenman LN, Krishnan K, Bandyopadhyaya AK, Wang C, Taylor A, Benz A, Covey DF, Zorumski CF, and Mennerick S (2009) The influence of neuroactive steroid lipophilicity on GABA-A receptor modulation: evidence for a low-affinity interaction. *J Neurophysiol* **102**:1254-1264.

Chuang SH and Reddy DS (2018a) Genetic and molecular regulation of extrasynaptic GABA-A receptors in the brain: Therapeutic insights for epilepsy. *J Pharmacol Exp Ther* **364**:180-197

Chuang SH and Reddy DS (2018b) 3beta-methyl-neurosteroid analogs are preferential positive allosteric modulators and direct activators of extrasynaptic deltaGABA-A receptors in the hippocampus dentate gyrus subfield. *J Pharmacol Exp Ther* **365**:583-601.

Chuang SH and Reddy DS (2019) Zinc reduces antiseizure activity of neurosteroids by selective blockade of extrasynaptic GABA-A receptor-mediated tonic inhibition in the hippocampus. *Neuropharmacology* **148**:244-256

Clossen BL and Reddy DS (2017a) Catamenial-like seizure exacerbation in mice lacking extrasynaptic deltaGABA-A receptors. *J Neurosci Res* **95**:1906-1916.

Clossen BL and Reddy DS (2017b) Novel therapeutic approaches for disease-modification of epileptogenesis for curing epilepsy. *Biochim Biophys Acta* **1863**:1519-1538.

Cole TB, Wenzel HJ, Kafer KE, Schwartzkroin PA, and Palmiter RD (1999) Elimination of zinc from synaptic vesicles in the intact mouse brain by disruption of the ZnT3 gene. *Proc Natl Acad Sci USA* **96**:1716-1721.

Collinson N, Kuenzi FM, Jarolimek W, Maubach KA, Cothliff R, Sur C, Smith A, Otu FM, Howell O, Atack JR, McKernan RM, Seabrook GR, Dawson GR, Whiting PJ, and Rosahl TW (2002) Enhanced learning and memory and altered GABAergic synaptic transmission in mice lacking the alpha5 subunit of the GABA-A receptor. *J Neurosci* **22**:5572-5580.

Comenencia-Ortiz E, Moss SJ, and Davies PA (2014) Phosphorylation of GABA-A receptors influences receptor trafficking and neurosteroid actions. *Psychopharmacology (Berl)* **231**:3453-3465.

Cossette P, Liu L, Brisebois K, Dong H, Lortie A, Vanasse M, Saint-Hilaire JM, Carmant L, Verner A, Lu WY, Wang YT, and Rouleau GA (2002) Mutation of GABRA1 in an autosomal dominant form of juvenile myoclonic epilepsy. *Nat Genet* **31**:184-189.

Coulter DA (2000) Mossy fiber zinc and temporal lobe epilepsy: pathological association with altered "epileptic" gamma-aminobutyric acid A receptors in dentate granule cells. *Epilepsia* **41**(Suppl 6):96-99.

Coulter DA and Carlson GC (2007) Functional regulation of the dentate gyrus by GABA-mediated inhibition. *Prog Brain Res* **163**:235-243.

Covey DF, Nathan D, Kalkbrenner M, Nilsson KR, Hu Y, Zorumski CF, and Evers AS (2000) Enantioselectivity of pregnanolone-induced GABA-A receptor modulation and anesthesia. *J Pharmacol Exp Ther* **293**:1009-1016.

Crestani F, Keist R, Fritschy JM, Benke D, Vogt K, Prut L, Bluthmann H, Mohler H, and Rudolph U (2002) Trace fear conditioning involves hippocampal alpha5 GABA-A receptors. *Proc Natl Acad Sci USA* **99**:8980-8985.

Czuczwar SJ and Przesmycki K (2001) Felbamate, gabapentin and topiramate as adjuvant antiepileptic drugs in experimental models of epilepsy. *Pol J Pharmacol* **53**:65-68.

Dhir A and Rogawski MA (2012) Role of neurosteroids in the anticonvulsant activity of midazolam. *Br J Pharmacol* **165**:2684-2691.

Dibbens LM, Feng HJ, Richards MC, Harkin LA, Hodgson BL, Scott D, Jenkins M, Petrou S, Sutherland GR, Scheffer IE, Berkovic SF, Macdonald RL, and Mulley JC (2004) GABRD encoding a protein for extra- or peri-synaptic GABA-A receptors is a susceptibility locus for generalized epilepsies. *Human Mol Genetics* **13**:1315-1319.

Dibbens LM, Harkin LA, Richards M, Hodgson BL, Clarke AL, Petrou S, Scheffer IE, Berkovic SF, and Mulley JC (2009) The role of neuronal GABA-A receptor subunit mutations in idiopathic generalized epilepsies. *Neurosci Lett* **453**:162-165.

Ding L, Feng HJ, Macdonald RL, Botzolakis EJ, Hu N, and Gallagher MJ (2010) GABA-A receptor alpha1 subunit mutation A322D associated with autosomal dominant juvenile myoclonic epilepsy reduces the expression and alters the composition of wild type GABA-A receptors. *J Biol Chem* **285**:26390-26405.

Draguhn A, Verdorn TA, Ewert M, Seeburg PH, and Sakmann B (1990) Functional and molecular distinction between recombinant rat GABA-A receptor subtypes by Zn2+. *Neuron* **5:**781-788.

Drasbek KR and Jensen K (2006) THIP, a hypnotic and antinociceptive drug, enhances an extrasynaptic GABA-A receptor-mediated conductance in mouse neocortex. *Cerebral Cortex* **16**:1134-1141.

Elsas SM, Hazany S, Gregory WL, and Mody I (2009) Hippocampal zinc infusion delays the development of afterdischarges and seizures in a kindling model of epilepsy. *Epilepsia* **50**:870-879.

Eslami M, Ghanbari E, Sayyah M, Etemadi F, Choopani St, Soleimani M, Amiri Z, and Hadjighassem M (2016) Traumatic brain injury accelerates kindling epileptogenesis in rats. *Neurological Res* **38**:269-274.

Esmaeili A, Lynch JW, and Sah P (2009) GABA-A receptors containing gamma1 subunits contribute to inhibitory transmission in the central amygdala. *J Neurophysiol* **101**:341-349.

Essrich C, Lorez M, Benson JA, Fritschy JM, and Luscher B (1998) Postsynaptic clustering of major GABA-A receptor subtypes requires the gamma2 subunit and gephyrin. *Nat Neurosci* **1**:563-571.

Earp J, Krzyzanski W, Chakraborty A, Zamacona MK, and Jusko WJ (2004) Assessment of drug interactions relevant to pharmacodynamic indirect response models. *J Pharmacokinet Pharmacodyn* **31**:345-380.

Fáncsik A, Linn DM, and Tasker JG (2000) Neurosteroid modulation of GABA IPSCs is phosphorylation dependent. *J Neurosci* **20**:3067-3075.

Fang C, Deng L, Keller CA, Fukata M, Fukata Y, Chen G, and Luscher B (2006) GODZ-mediated palmitoylation of GABA-A receptors is required for normal assembly and function of GABAergic inhibitory synapses. *J Neurosci* **26**:12758-12768.

Farrant M and Nusser Z (2005) Variations on an inhibitory theme: phasic and tonic activation of GABA-A receptors. *Nature Rev Neurosci* **6**:215-229.

Feng HJ, Kang JQ, Song L, Dibbens L, Mulley J, and Macdonald RL (2006) Delta subunit susceptibility variants E177A and R220H associated with complex epilepsy alter channel gating and surface expression of alpha4beta2delta GABA-A receptors. *J Neurosci* **26**:1499-1506.

Feucht M, Fuchs K, Pichlbauer E, Hornik K, Scharfetter J, Goessler R, Fureder T, Cvetkovic N, Sieghart W, Kasper S, and Aschauer H (1999) Possible association between childhood absence epilepsy and the gene encoding GABRB3. *Biol Psychiatry* **46**:997-1002.

Foresti ML, Arisi GM, Fernandes A, Tilelli CQ, and Garcia-Cairasco N (2008) Chelatable zinc modulates excitability and seizure duration in the amygdala rapid kindling model. *Epilepsy Res* **79**:166-172.

Frederickson CJ (1989) Neurobiology of zinc and zinc-containing neurons. *Int Rev Neurobiol* **31**:145-238.

Frederickson CJ, Klitenick MA, Manton WI, and Kirkpatrick JB (1983) Cytoarchitectonic distribution of zinc in the hippocampus of man and the rat. *Brain Res* **273**:335-339.

Frederickson CJ, Suh SW, Silva D, Frederickson CJ, and Thompson RB (2000) Importance of zinc in the central nervous system: the zinc-containing neuron. *J Nutr* **130**:1471S-1483S.

Frederickson CJ, Koh JY, and Bush AI (2005) The neurobiology of zinc in health and disease. *Nat Rev Neurosci* **6**:449-462.

Fritschy JM and Mohler H (1995) GABA-A-receptor heterogeneity in the adult rat brain: differential regional and cellular distribution of seven major subunits. *J Comp Neurol* **359**:154-194.

Frugier G, Coussen F, Giraud MF, Odessa MF, Emerit MB, Boue-Grabot E, and Garret M (2007) A gamma2(R43Q) mutation, linked to epilepsy in humans, alters GABA-A receptor assembly and modifies subunit composition on the cell surface. *J Biol Chem* **282**:3819-3828.

Galimberti CA, Magri F, Copello F, Arbasino C, Cravello L, Casu M, Patrone V, and Murialdo G (2005) Seizure frequency and cortisol and dehydroepiandrosterone sulfate (DHEAS) levels in women with epilepsy receiving antiepileptic drug treatment. *Epilepsia* **46**:517-523.

Gallagher MJ, Ding L, Maheshwari A, and Macdonald RL (2007) The GABA-A receptor alpha1 subunit epilepsy mutation A322D inhibits transmembrane helix formation and causes proteasomal degradation. *Proc Natl Acad Sci USA* **104**:12999-13004.

Gallagher MJ, Song L, Arain F, and Macdonald RL (2004) The juvenile myoclonic epilepsy GABA-A receptor alpha1 subunit mutation A322D produces asymmetrical, subunit position-dependent reduction of heterozygous receptor currents and alpha1 subunit protein expression. *J Neurosci* **24**:5570-5578.

Gangisetty O and Reddy DS (2010) Neurosteroid withdrawal regulates GABA-A receptor alpha4 subunit expression and seizure susceptibility by activation of progesterone receptor-independent early growth response factor-3 pathway. *Neuroscience* **170**:865-880.

Gasior M, Ungard JT, Beekman M, Carter RB, and Witkin JM (2000) Acute and chronic effects of the synthetic neuroactive steroid, ganaxolone, against the convulsive and lethal effects of pentylenetetrazol in seizure-kindled mice: comparison with diazepam and valproate. *Neuropharmacology* **39**:1184-1196.

Gee KW, McCauley LD, and Lan NC (1995) A putative receptor for neurosteroids on the GABA-A receptor complex: the pharmacological properties and therapeutic potential of epalons. *Crit Rev Neurobiol* **9**:207-227.

Glykys J, Mann EO, and Mody I (2008) Which GABA-A receptor subunits are necessary for tonic inhibition in the hippocampus? *J Neurosci* **28**:1421-1426.

Glykys J and Mody I (2007) Activation of GABA-A receptors: views from outside the synaptic cleft. *Neuron* **56**:763-770.

Glykys J, Peng Z, Chandra D, Homanics GE, Houser CR, and Mody I (2007) A new naturally occurring GABA-A receptor subunit partnership with high sensitivity to ethanol. *Nat Neurosci* **10**:40-48.

Goldenberg MM (2010) Overview of drugs used for epilepsy and seizures: etiology, diagnosis, and treatment. *P T* **35**:392-415.

Gong QH and Smith SS (2014) Characterization of neurosteroid effects on hyperpolarizing current at alpha4beta2delta GABA-A receptors. *Psychopharmacology (Berl)* **231**:3525-3535.

Gower-Winter SD, and Levenson CW (2012) Zinc in the central nervous system: From molecules to behavior. *BioFactors* **38**:186-193.

Grabovsky Y and Tallarida RJ (2004) Isobolographic analysis for combinations of a full and partial agonist: curved isoboles. *J Pharmacol Exp Ther* **310**:981-986.

Greenfield LJ, Jr. (2013) Molecular mechanisms of antiseizure drug activity at GABA-A receptors. *Seizure* **22**:589-600.

Gunter BW, Jones SA, Paul IA, Platt DM, and Rowlett JK (2016) Benzodiazepine and neuroactive steroid combinations in rats: anxiolytic-like and discriminative stimulus effects. *Psychopharmacology (Berl*) **233**:3237-3247.

Gurba KN, Hernandez CC, Hu N, and Macdonald RL (2012) GABRB3 mutation, G32R, associated with childhood absence epilepsy alters alpha1beta3gamma2L GABA-A receptor expression and channel gating. *J Biol Chem* **287**:12083-12097.

Hancili S, Ö nal ZE, Ata P, Karatoprak EY, Gürbüz T, Bostancı M, Paçal Y, Nuhoglu Ç, and Ceran Ö (2014) The GABA-A receptor gamma2 subunit (R43Q) mutation in febrile seizures. *Pediatr Neurol* **50**:353-356.

Harkin LA, Bowser DN, Dibbens LM, Singh R, Phillips F, Wallace RH, Richards MC, Williams DA, Mulley JC, Berkovic SF, Scheffer IE, and Petrou S (2002) Truncation of the GABA-A-receptor gamma2 subunit in a family with generalized epilepsy with febrile seizures plus. *Am J Hum Genet* **70**:530-536.

Harney SC, Frenguelli BG, and Lambert JJ (2003) Phosphorylation influences neurosteroid modulation of synaptic GABA-A receptors in rat CA1 and dentate gyrus neurones. *Neuropharmacology* **45**:873-883.

Harrison NL and Gibbons SJ (1994) Zn2+: an endogenous modulator of ligand- and voltage-gated ion channels. *Neuropharmacology* **33**:935-952.

Hauser WA (1994) The prevalence and incidence of convulsive disorders in children. *Epilepsia* **35**(Suppl 2):1-6.

Hempelmann A, Cobilanschi J, Heils A, Muhle H, Stephani U, Weber Y, Lerche H, and Sander T (2007) Lack of evidence of an allelic association of a functional GABRB3 exon 1a promoter polymorphism with idiopathic generalized epilepsy. *Epilepsy Res* **74**:28-32.

Herd MB, Haythornthwaite AR, Rosahl TW, Wafford KA, Homanics GE, Lambert JJ, and Belelli D (2008) The expression of GABA-A beta subunit isoforms in synaptic and extrasynaptic receptor populations of mouse dentate gyrus granule cells. *J Physiol* **586**:989-1004.

Hernandez CC, Gurba KN, Hu N, and Macdonald RL (2011) The GABRA6 mutation, R46W, associated with childhood absence epilepsy, alters alpha6beta2gamma2 and alpha6beta2delta GABA-A receptor channel gating and expression. *J Physiol* **589**:5857-5878.

Herzog AG, Fowler KM, Smithson SD, Kalayjian LA, Heck CN, Sperling MR, Liporace JD, Harden CL, Dworetzky BA, Pennell PB, Massaro JM; Progesterone Trial Study Group (2012) Progesterone vs placebo therapy for women with epilepsy: A randomized clinical trial. *Neurology* **78**:1959-1966.

Hesdorffer DC, Beck V, Begley CE, Bishop ML, Cushner-Weinstein S, Holmes GL, Shafer PO, Sirven JI, and Austin JK (2013) Research implications of the Institute of Medicine Report, Epilepsy Across the Spectrum: Promoting Health and Understanding. *Epilepsia* **54**:207-216.

Hirose S (2006) A new paradigm of channelopathy in epilepsy syndromes: intracellular trafficking abnormality of channel molecules. *Epilepsy Res* **70**(Suppl 1):206-217.

Homanics GE, DeLorey TM, Firestone LL, Quinlan JJ, Handforth A, Harrison NL, Krasowski MD, Rick CE, Korpi ER, Mäkelä R, Brilliant MH, Hagiwara N, Ferguson C, Snyder K, and Olsen RW (1997) Mice devoid of gamma-aminobutyrate type A receptor beta3 subunit have epilepsy, cleft palate, and hypersensitive behavior. *Proc Natl Acad Sci USA* **94**:4143-4148.

Hosie AM, Dunne EL, Harvey RJ, and Smart TG (2003) Zinc-mediated inhibition of GABA-A receptors: discrete binding sites underlie subtype specificity. *Nat Neurosci* **6**:362-369.

Hosie AM, Wilkins ME, and Smart TG (2007) Neurosteroid binding sites on GABA-A receptors. *Pharmacol Ther* **116**:7-19.

Huang X, Hernandez CC, Hu N, and Macdonald RL (2014) Three epilepsy-associated GABRG2 missense mutations at the gamma+/beta- interface disrupt GABA-A receptor assembly and trafficking by similar mechanisms but to different extents. *Neurobiol Dis* **68**:167-179.

Ishii A, Kanaumi T, Sohda M, Misumi Y, Zhang B, Kakinuma N, Haga Y, Watanabe K, Takeda S, Okada M, Ueno S, Kaneko S, Takashima S, and Hirose S (2014) Association of nonsense mutation in GABRG2 with abnormal trafficking of GABA-A receptors in severe epilepsy. *Epilepsy Res* **108**:420-432.

Jia F, Pignataro L, and Harrison NL (2007) GABA-A receptors in the thalamus: alpha4 subunit expression and alcohol sensitivity. *Alcohol* **41**:177-185.

Jia F, Pignataro L, Schofield CM, Yue M, Harrison NL, and Goldstein PA (2005) An extrasynaptic GABA-A receptor mediates tonic inhibition in thalamic VB neurons. *J Neurophysiol* **94**:4491-4501.

Johannesen K, Marini C, Pfeffer S, Moller RS, Dorn T, Niturad CE, Gardella E, Weber Y, Søndergård M, Hjalgrim H, Nikanorova M, Becker F, Larsen LH, Dahl HA, Maier O, Mei D, Biskup S, Klein KM, Reif PS, Rosenow F, Elias AF, Hudson C, Helbig KL, Schubert-Bast S, Scordo MR, Craiu D, Djémié T, Hoffman-Zacharska D, Caglayan H, Helbig I, Serratosa J, Striano P, De Jonghe P, Weckhuysen S, Suls A, Muru K, Talvik I, Talvik T, Muhle H, Borggraefe I, Rost I, Guerrini R,

Lerche H, Lemke JR, Rubboli G, and Maljevic S (2016) Phenotypic spectrum of GABRA1: From generalized epilepsies to severe epileptic encephalopathies. *Neurology* **87**:1140-1151.

Johnston AJ, Kang JQ, Shen W, Pickrell WO, Cushion TD, Davies JS, Baer K, Mullins JGL, Hammond CL, Chung SK, Thomas RH, White C, Smith PEM, Macdonald RL, and Rees MI (2014) A novel GABRG2 mutation, p.R136*, in a family with GEFS+ and extended phenotypes. *Neurobiol Dis* **64**:131-141.

Jones A, Korpi ER, McKernan RM, Pelz R, Nusser Z, Makela R, Mellor JR, Pollard S, Bahn S, Stephenson FA, Randall AD, Sieghart W, Somogyi P, Smith AJ, and Wisden W (1997) Ligand-gated ion channel subunit partnerships: GABA-A receptor alpha6 subunit gene inactivation inhibits delta subunit expression. *J Neurosci* **17**:1350-1362.

Joshi S, Rajasekaran K, Williamson J, and Kapur J (2017) Neurosteroid-sensitive deltaGABA-A receptors: A role in epileptogenesis? *Epilepsia* **58**:494-504.

Jutila L, Immonen A, Partanen K, Partanen J, Mervaala E, Ylinen A, Alafuzoff I, Paljarvi L, Karkola K, Vapalahti M, and Pitkanen A (2002) Neurobiology of epileptogenesis in the temporal lobe. *Adv Tech Stand Neurosurg* **27**:5-22.

Jurd R, Arras M, Lambert S, Drexler B, Siegwart R, Crestani F, Zaugg M, Vogt KE, Ledermann B, Antkowiak B, and Rudolph U (2003) General anesthetic actions in vivo strongly attenuated by a point mutation in the GABA-A receptor beta3 subunit. *FASEB J* **17**:250-252.

Kambe T, Yamaguchi-Iwai Y, Sasaki R, and Nagao M (2004) Overview of mammalian zinc transporters. *Cell Mol Life Sci* **61**:49-68.

Kaminski RM, Gasior M, Carter RB, and Witkin JM (2003) Protective efficacy of neuroactive steroids against cocaine kindled-seizures in mice. *Eur J Pharmacol* **474**:217-222.

Kaminski RM, Livingood MR, and Rogawski MA (2004) Allopregnanolone analogs that positively modulate GABA receptors protect against partial seizures induced by 6-Hz electrical stimulation in mice. *Epilepsia* **45**:864-867.

Kanes S, Colquhoun H, Gunduz-Bruce H, Raines S, Arnold R, Schacterle A, Doherty J, Epperson CN, Deligiannidis KM, Riesenberg R, Hoffmann E, Rubinow D, Jonas J, Paul S, and Meltzer-Brody S (2017) Brexanolone (SAGE-547 injection) in post-partum depression: a randomised controlled trial. *Lancet* **390**:480-489.

Kananura C, Haug K, Sander T, Runge U, Gu W, Hallmann K, Rebstock J, Heils A, and Steinlein OK (2002) A splice-site mutation in GABRG2 associated with childhood absence epilepsy and febrile convulsions. *Arch Neurol* **59**:1137-1141.

Kang JQ and Macdonald RL (2004) The GABA-A receptor gamma2 subunit R43Q mutation linked to childhood absence epilepsy and febrile seizures causes

retention of alpha1beta2gamma2S receptors in the endoplasmic reticulum. *J Neurosci* **24**:8672-8677.

Kang JQ, Shen W, Lee M, Gallagher MJ, and Macdonald RL (2010) Slow degradation and aggregation in vitro of mutant GABA-A receptor gamma2(Q351X) subunits associated with epilepsy. *J Neurosci* **30**:13895-13905.

Kang JQ, Shen W, Zhou C, Xu D, and Macdonald RL (2015) The human epilepsy mutation GABRG2(Q390X) causes chronic subunit accumulation and neurodegeneration. *Nat Neurosci* **18**:988-996.

Kapur J and Macdonald RL (1997) Rapid seizure-induced reduction of benzodiazepine and Zn2+ sensitivity of hippocampal dentate granule cell GABA-A receptors. *J Neurosci* **17**:7532-7540.

Kay AR and Wong RK (1986) Isolation of neurons suitable for patch-clamping from adult mammalian central nervous systems. *J Neurosci Methods* **16**:227-238.

Khatri SN, Wu WC, and Pugh JR (2018) Enhancement of extrasynaptic GABA-A receptors by GABA-B receptors and L-type calcium channels. Program No. 200.10. 2018 Neuroscience Meeting Planner. San Diego, CA: Society for Neurosci. Online.

Kerrigan JF, Shields WD, Nelson TY, Bluestone DL, Dodson WE, Bourgeois BF, Pellock JM, Morton LD, and Monaghan EP (2000) Ganaxolone for treating intractable infantile spasms: a multicenter, open-label, add-on trial. *Epilepsy Res* **42**:133-139.

Kittler JT, Chen G, Honing S, Bogdanov Y, McAinsh K, Arancibia-Carcamo IL, Jovanovic JN, Pangalos MN, Haucke V, Yan Z, and Moss SJ (2005) Phospho-dependent binding of the clathrin AP2 adaptor complex to GABA-A receptors regulates the efficacy of inhibitory synaptic transmission. *Proc Natl Acad Sci USA* **102**:14871-14876.

Kittler JT, Chen G, Kukhtina V, Vahedi-Faridi A, Gu Z, Tretter V, Smith KR, McAinsh K, Arancibia-Carcamo IL, Saenger W, Haucke V, Yan Z, and Moss SJ (2008) Regulation of synaptic inhibition by phospho-dependent binding of the AP2 complex to a YECL motif in the GABA-A receptor gamma2 subunit. *Proc Natl Acad Sci USA* **105**:3616-3621.

Kodera H, Ohba C, Kato M, Maeda T, Araki K, Tajima D, Matsuo M, Hino-Fukuyo N, Kohashi K, Ishiyama A, Takeshita S, Motoi H, Kitamura T, Kikuchi A, Tsurusaki Y, Nakashima M, Miyake N, Sasaki M, Kure S, Haginoya K, Saitsu H, and Matsumoto N (2016) De novo GABRA1 mutations in Ohtahara and West syndromes. *Epilepsia* **57**:566-573.

Kokate TG, Cohen AL, Karp E, and Rogawski MA (1996) Neuroactive steroids protect against pilocarpine- and kainic acid-induced limbic seizures and status epilepticus in mice. *Neuropharmacology* **35**:1049-1056.

Kokate TG, Svensson BE, and Rogawski MA (1994) Anticonvulsant activity of neurosteroids: correlation with GABA-evoked chloride current potentiation. *J Pharmacol Exp Ther* **270**:1223-1229.

Korpi ER, Mihalek RM, Sinkkonen ST, Hauer B, Hevers W, Homanics GE, Sieghart W, and Luddens H (2002) Altered receptor subtypes in the forebrain of GABA-A receptor delta subunit-deficient mice: recruitment of gamma2 subunits. *Neuroscience* **109**:733-743.

Kralic JE, Wheeler M, Renzi K, Ferguson C, O'Buckley TK, Grobin AC, Morrow AL, and Homanics GE (2003) Deletion of GABA-A receptor alpha1 subunit-containing receptors alters responses to ethanol and other anesthetics. *J Pharmacol Exp Ther* **305**:600-607.

Krampfl K, Maljevic S, Cossette P, Ziegler E, Rouleau GA, Lerche H, and Bufler J (2005) Molecular analysis of the A322D mutation in the GABA receptor alpha subunit causing juvenile myoclonic epilepsy. *Eur J Nurosci* **22**:10-20.

Krishek BJ, Xie X, Blackstone C, Huganir RL, Moss SJ, and Smart TG (1994) Regulation of GABA-A receptor function by protein kinase C phosphorylation. *Neuron* **12**:1081-1095.

Kulkarni SK and Reddy DS (1995) Neurosteroids: a new class of neuromodulators. *Drugs Today* **31**:433-455.

Kwan P and Brodie MJ (2006) Combination therapy in epilepsy: when and what to use. *Drugs* **66**:1817-1829.

Lachance-Touchette P, Brown P, Meloche C, Kinirons P, Lapointe L, Lacasse H, Lortie A, Carmant L, Bedford F, Bowie D, and Cossette P (2011) Novel alpha1 and gamma2 GABA-A receptor subunit mutations in families with idiopathic generalized epilepsy. *Eur J Neurosci* **34**:237-249.

Lachance-Touchette P, Martin C, Poulin C, Gravel M, Carmant L, and Cossette P (2010) Screening of GABRB3 in French-Canadian families with idiopathic generalized epilepsy. *Epilepsia* **51**:1894-1897.

Lambert JJ and Belelli D (2002) Pharmacological characterization of a novel cell line expressing human alpha4beta3delta GABA-A receptors: commentary on Brown et al. *Br J Pharmacol* **136**:957-959.

Laxer K, Blum D, Abou-Khalil BW, Morrell MJ, Lee DA, Data JL, and Monaghan EP (2000) Assessment of ganaxolone's anticonvulsant activity using a randomized, double-blind, presurgical trial design. Ganaxolone Presurgical Study Group. *Epilepsia* **41**:1187-1194.

Lee JY, Kim JS, Byun HR, Palmiter RD, and Koh JY (2011) Dependence of the histofluorescently reactive zinc pool on zinc transporter-3 in the normal brain. *Brain Res* **1418**:12-22.

Lee V and Maguire J (2013) Impact of inhibitory constraint of interneurons on neuronal excitability. *J Neurophysiol* **110**:2520-2535.

Leidenheimer NJ and Chapell R (1997) Effects of PKC activation and receptor desensitization on neurosteroid modulation of GABA-A receptors. *Brain Res Mol Brain Res* **52**:173-181.

Li P, Bracamontes JR, Manion BD, Mennerick S, Steinbach JH, Evers AS, and Akk G (2014) The neurosteroid 5beta-pregnan-3alpha-ol-20-one enhances actions of etomidate as a positive allosteric modulator of alpha1beta2gamma2L GABA-A receptors. *Br J Pharmacol* **171**:5446-5457.

Ligsay A, Van Dijck A, Nguyen DV, Lozano R, Chen Y, Bickel ES, Hessl D, Schneider A, Angkustsiri K, Tassone F, Ceulemans B, Kooy RF, and Hagerman RJ (2017) A randomized double-blind, placebo-controlled trial of ganaxolone in children and adolescents with fragile X syndrome. *J Neurodev Disord* **9**:26

Liptakova S, Velisek L, Veliskova J, and Moshe SL (2000) Effect of ganaxolone on flurothyl seizures in developing rats. *Epilepsia* **41**:788-793.

Litchfield JT Jr and Wilcoxon F (1949) A simplified method of evaluating dose-effect experiments. *J Pharmacol Exp Ther* **96**:99-113.

Loewe S (1953) The problem of synergism and antagonism of combined drugs. *Arzneimittelforschung* **3**:285-290.

Loup F, Wieser HG, Yonekawa Y, Aguzzi A, and Fritschy JM (2000) Selective alterations in GABA-A receptor subtypes in human temporal lobe epilepsy. *J Neurosci* **20**:5401-5419.

Low K, Crestani F, Keist R, Benke D, Brunig I, Benson JA, Fritschy JM, Rulicke T, Bluethmann H, Mohler H, and Rudolph U (2000) Molecular and neuronal substrate for the selective attenuation of anxiety. *Science* **290**:131-134.

Luszczki JJ (2008a) Interactions of tiagabine with ethosuximide in the mouse pentylenetetrazole-induced seizure model: an isobolographic analysis for non-parallel dose-response relationship curves. *Naunyn Schmiedebergs Arch Pharmacol* **378**:483-492.

Łuszczki JJ (2008b) Isobolographic analysis of interaction between oxcarbazepine and valproate in pentylenetetrazole-induced seizures in mice. *J Pre Clin Clin Re.* **2**:40-45.

Luszczki JJ and Czuczwar SJ (2004) Isobolographic profile of interactions between tiagabine and gabapentin: a preclinical study. *Naunyn Schmiedebergs Arch Pharmacol* **369**:434-446.

Madsen KK, Clausen RP, Larsson OM, Krogsgaard-Larsen P, Schousboe A, and White HS (2009) Synaptic and extrasynaptic GABA transporters as targets for anti-epileptic drugs. *J Neurochem* **109**(Suppl 1):139-144.

Majewska MD, Demirgören S, Spivak CE, and London ED (1990) The neurosteroid dehydroepiandrosterone sulfate is an allosteric antagonist of the GABA-A receptor. *Brain Res* **526**:143-146.

Maljevic S, Krampfl K, Cobilanschi J, Tilgen N, Beyer S, Weber YG, Schlesinger F, Ursu D, Melzer W, Cossette P, Bufler J, Lerche H, and Heils A (2006) A mutation in the GABA-A receptor alpha1 subunit is associated with absence epilepsy. *Ann Neurol* **59**:983-987.

Marowsky A, Fritschy JM, and Vogt KE (2004) Functional mapping of GABA-A receptor subtypes in the amygdala. *Eur J Neurosci* **20**:1281-1289.

Marowsky A, Rudolph U, Fritschy JM, and Arand M (2012) Tonic inhibition in principal cells of the amygdala: a central role for alpha3 subunit-containing GABA-A receptors. *J Neurosci* **32**:8611-8619.

McDonald BJ, Amato A, Connolly CN, Benke D, Moss SJ, and Smart TG (1998) Adjacent phosphorylation sites on GABA-A receptor beta subunits determine regulation by cAMP-dependent protein kinase. *Nat Neurosci* **1**:23-28.

McKernan RM, Rosahl TW, Reynolds DS, Sur C, Wafford KA, Atack JR, Farrar S, Myers J, Cook G, Ferris P, Garrett L, Bristow L, Marshall G, Macaulay A, Brown N, Howell O, Moore KW, Carling RW, Street LJ, Castro JL, Ragan CI, Dawson GR, and Whiting PJ (2000) Sedative but not anxiolytic properties of benzodiazepines are mediated by the GABA-A receptor alpha1 subtype. *Nat Neurosci* **3**:587-592.

McKernan RM and Whiting PJ (1996) Which GABA-A receptor subtypes really occur in the brain? *Trends in neurosciences* **19**:139-143.

Meera P, Wallner M, and Otis TS (2011) Molecular basis for the high THIP/gaboxadol sensitivity of extrasynaptic GABA-A receptors. *J Neurophysiol* **106**:2057-2064.

Meldrum BS and Chapman AG (1999) Basic mechanisms of gabitril (tiagabine) and future potential developments. *Epilepsia* **40**(Suppl 9):2-6.

Meletti S, Lucchi C, Monti G, Giovannini G, Bedin R, Trenti T, Rustichelli C, and Biagini G (2017) Decreased allopregnanolone levels in cerebrospinal fluid obtained during status epilepticus. *Epilepsia* **58**:e16-20.

Mellon SH and Griffin LD (2002) Synthesis, regulation, and function of neurosteroids. *Endocr Re*s **28**:463.

Mihalek RM, Banerjee PK, Korpi ER, Quinlan JJ, Firestone LL, Mi ZP, Lagenaur C, Tretter V, Sieghart W, Anagnostaras SG, Sage JR, Fanselow MS, Guidotti A, Spigelman I, Li Z, DeLorey TM, Olsen RW, and Homanics GE (1999) Attenuated sensitivity to neuroactive steroids in GABA-A receptor delta subunit knockout mice. *Proc Natl Acad Sci USA* **96**:12905-12910.

Mitchell EA, Herd MB, Gunn BG, Lambert JJ, and Belelli D (2008) Neurosteroid modulation of GABA-A receptors: molecular determinants and significance in health and disease. *Neurochem Int* **52**:588-595.

Modgil A, Parakala ML, Ackley MA, Doherty JJ, Moss SJ, and Davies PA (2017) Endogenous and synthetic neuroactive steroids evoke sustained increases in the efficacy of GABAergic inhibition via a protein kinase C-dependent mechanism. *Neuropharmacology* **113**:314-322.

Mody I, De Koninck Y, Otis TS, and Soltesz I (1994) Bridging the cleft at GABA synapses in the brain. *Trends Neurosci* **17**:517-525.

Mohler H, Fritschy JM, and Rudolph U (2002) A new benzodiazepine pharmacology. *J Pharmacol Exp Ther* **300**:2-8.

Molnar P and Nadler JV (2001) Synaptically-released zinc inhibits N-methyl-D-aspartate receptor activation at recurrent mossy fiber synapses. *Brain Res* **910**:205-207.

Monaghan EP, Navalta LA, Shum L, Ashbrook DW, and Lee DA (1999) Initial human experience with ganaxolone, a neuroactive steroid with antiepileptic activity. *Epilepsia* **38**:1026-1031.

Mortensen M, Patel B, and Smart TG (2011) GABA Potency at GABA-A Receptors Found in Synaptic and Extrasynaptic Zones. *Front Cell Neurosci* **6**:1-12.

Moss SJ, Gorrie GH, Amato A, and Smart TG (1995) Modulation of GABA-A receptors by tyrosine phosphorylation. *Nature* **377**:344-348.

Moss SJ and Smart TG (1996) Modulation of amino acid-gated ion channels by protein phosphorylation. *Int Rev Neurobiol* **39**:1-52.

Nani F, Bright DP, Revilla-Sanchez R, Tretter V, Moss SJ, and Smart TG (2013) Tyrosine phosphorylation of GABA-A receptor gamma2-subunit regulates tonic and phasic inhibition in the thalamus. *J Neurosci* **33**:12718-12727.

Naylor DE, Liu H, and Wasterlain CG (2005) Trafficking of GABA-A receptors, loss of inhibition, and a mechanism for pharmacoresistance in status epilepticus. *J Neurosci* **25**:7724-7733

Nishimura T, Schwarzer C, Gasser E, Kato N, Vezzani A, and Sperk G (2005) Altered expression of GABA-A and GABA-B receptor subunit mRNAs in the hippocampus after kindling and electrically induced status epilepticus. *Neuroscience* **134**:691-704.

Nohria V and Giller E (2007) Ganaxolone. *Neurotherapeutics* **4**:102-105.

Nusser Z, Cull-Candy S, and Farrant M (1997) Differences in synaptic GABA-A receptor number underlie variation in GABA mini amplitude. *Neuron* **19**:697-709.

Nusser Z, Sieghart W, and Somogyi P (1998) Segregation of different GABA-A receptors to synaptic and extrasynaptic membranes of cerebellar granule cells. *J Neurosci* **18**:1693-1703.

Nutt D (2006) GABA-A receptors: subtypes, regional distribution, and function. *J Clin Sleep Med* **2**:S7-11.

Oakley JC, Cho AR, Cheah CS, Scheuer T, and Catterall WA (2013) Synergistic GABA-enhancing therapy against seizures in a mouse model of Dravet syndrome. *J Pharmacol Exp Ther* **345**:215-224.

Olmos-Serrano JL, Paluszkiewicz SM, Martin BS, Kaufmann WE, Corbin JG, and Huntsman MM (2010) Defective GABAergic neurotransmission and pharmacological rescue of neuronal hyperexcitability in the amygdala in a mouse model of fragile X syndrome. *J Neurosci* **30**:9929-9938.

Olsen RW and Sieghart W (2009) GABA-A receptors: subtypes provide diversity of function and pharmacology. *Neuropharmacology* **56**:141-148.

Pack A, Reddy DS, Duncan S, and Herzog A (2011) Neuroendocrinological aspects of epilepsy: Important issues and trends in future research. *Epilepsy Behav* **22**:94-102.

Paoletti P, Vergnano AM, Barbour B, Casado M (2009) Zinc at glutamatergic synapses. *Neuroscience* **158**:126-136.

Papadopoulos V, Baraldi M, Guilarte TR, Knudsen TB, Lacapere JJ, Lindemann P, Norenberg MD, Nutt D, Weizman A, Zhang MR, and Gavish M (2006) Translocator protein (18kDa): new nomenclature for the peripheral-type benzodiazepine receptor based on its structure and molecular function. *Trends Pharmacol Sci* **27**:402-409.

Paul SM and Purdy RH (1992) Neuroactive steroids. *FASEB J* **6**:2311-2322.

Peng Z, Hauer B, Mihalek RM, Homanics GE, Sieghart W, Olsen RW, and Houser CR (2002) GABA-A receptor changes in delta subunit-deficient mice: altered expression of alpha4 and gamma2 subunits in the forebrain. *J Comp Neurol* **446**:179-197.

Pieribone VA, Tsai J, Soufflet C, Rey E, Shaw K, Giller E, and Dulac O (2007) Clinical evaluation of ganaxolone in pediatric and adolescent patients with refractory epilepsy. *Epilepsia* **48**:1870-1874.

Pirker S, Schwarzer C, Wieselthaler A, Sieghart W, and Sperk G (2000) GABA-A receptors: immunocytochemical distribution of 13 subunits in the adult rat brain. *Neuroscience* **101**:815-850.

Pitkanen A, Roivainen R, and Lukasiuk K (2016) Development of epilepsy after ischaemic stroke. *The Lancet. Neurology* **15**:185-197.

Porcello DM, Huntsman MM, Mihalek RM, Homanics GE, and Huguenard JR (2003) Intact synaptic GABAergic inhibition and altered neurosteroid modulation of thalamic relay neurons in mice lacking delta subunit. *J Neurophysiol* **89**:1378-1386.

Porcu P, Barron AM, Frye CA, Walf AA, Yang SY, He XY, Morrow AL, Panzica GC, and Melcangi RC (2016) Neurosteroidogenesis today: Novel targets for neuroactive steroid synthesis and action and their relevance for translational research. *J Neuroendocrinol* **28**:12351-12371.

Prakash A, Bharti K, and Majeed AB (2015) Zinc: indications in brain disorders. Fundam. *Clin Pharmacol* **29**:131-149.

Puia G, Santi MR, Vicini S, Pritchett DB, Purdy RH, Paul SM, Seeburg PH, and Costa E (1990) Neurosteroids act on recombinant human GABA-A receptors. *Neuron* **4**:759-765.

Qian J, Xu K, Yoo J, Chen TT, Andrews G, and Noebels JL (2011) Knockout of Zn transporters Zip-1 and Zip-3 attenuates seizure-induced CA1 neurodegeneration. *J Neurosci* **31**:97-104.

Racine RJ (1972) Modification of seizure activity by electrical stimulation. II. Motor seizure. *Electroencephalogr Clin Neurophysiol* **32**:281-294.

Reddy DS (2003a) Is there a physiological role for the neurosteroid THDOC in stress-sensitive conditions? *Trends Pharmacol Sci* **24**:103-106.

Reddy DS (2003b) Pharmacology of endogenous neuroactive steroids. *Crit Rev Neurobiol* **15**:197-234.

Reddy DS (2006) Physiological role of adrenal deoxycorticosterone-derived neuroactive steroids in stress-sensitive conditions. *Neuroscience* **138**:911-920.

Reddy DS (2009a) The role of neurosteroids in the pathophysiology and treatment of catamenial epilepsy. *Epilepsy Res* **85**:1-30.

Reddy DS (2009b) Gender differences in antiseizure sensitivity of neurosteroids in the pilocarpine model of status epilepticus. *Epilepsia* **50**(Suppl 11):126.

Reddy DS (2011) Role of anticonvulsant and antiepileptogenic neurosteroids in the pathophysiology and treatment of epilepsy. *Front Endocrinol* **2**(38):1-11.

Reddy DS (2013a) Neuroendocrine aspects of catamenial epilepsy. *Hormones Behav* **63**:254-266.

Reddy DS (2013b) Role of hormones and neurosteroids in epileptogenesis. *Front Cell Neurosci* **7**(115):1-20.

Reddy DS (2014) Neurosteroids and their role in sex-specific epilepsies. *Neurobiol Dis* **72**(Pt B):198-209.

Reddy DS (2016a) Catamenial epilepsy: discovery of an extrasynaptic molecular mechanism for targeted therapy. *Front Cell Neurosci* **10**:1-14.

Reddy DS (2016b) The neuroendocrine basis of sex differences in epilepsy. *Pharmacol Biochem Behav* **152**:97-104.

Reddy DS (2016c) Neurosteroids for the potential protection of humans against organophosphate toxicity. *Ann N Y Acad Sci* **1378**:25-32.

Reddy DS (2017) The neuroendocrine basis of sex differences in epilepsy. *Pharmacol Biochem Behav* **152**:97-104.

Reddy DS (2018) GABA-A receptors mediate tonic inhibition and neurosteroid sensitivity in the brain. *Vitam Horm* **107**:177-191.

Reddy DS and Estes W (2016) Clinical potential of neurosteroids for CNS disorders. *Trends Pharmacol Sci* **37**:543-561.

Reddy DS and Jian K (2010) The testosterone-derived neurosteroid androstanediol is a positive allosteric modulator of GABA-A receptors. *J Pharmacol Exp Ther* **334**:1031-1041.

Reddy DS and Mohan A (2011) Development and persistence of limbic epileptogenesis are impaired in mice lacking progesterone receptors. *J Neurosci* **31**:650-658.

Reddy DS and Kulkarni SK (1998) Proconvulsant effects of neurosteroid pregnenolone sulfate and dehydroepiandrosterone sulfate in mice. *Eur J Pharmacol* **345**:55-59.

Reddy DS and Rogawski MA (2000a) Chronic treatment with the neuroactive steroid ganaxolone in the rat induces anticonvulsant tolerance to diazepam but not to itself. *J Pharmacol Exp Therap* **295**:1241-1248.

Reddy DS and Rogawski MA (2000b) Enhanced anticonvulsant activity of ganaxolone after neurosteroid withdrawal in a rat model of catamenial epilepsy. *J Pharmacol Exp Therap* **294**:909-915.

Reddy DS and Rogawski MA (2001) Enhanced anticonvulsant activity of neuroactive steroids in a rat model of catamenial epilepsy. *Epilepsia* **42**:337-344.

Reddy DS and Rogawski MA (2002) Stress-induced deoxycorticosterone-derived neurosteroids modulates GABA-A receptor function and seizure susceptibility. *J Neurosci* **22**:3795-3805.

Reddy DS and Rogawski MA (2009) Neurosteroid replacement therapy for catamenial epilepsy. *Neurotherapeutics* **6**:392-401.

Reddy DS and Rogawski MA (2010) Ganaxolone suppression of behavioral and electrographic seizures in the mouse amygdala kindling model. *Epilepsy Res* **89**:254-260.

Reddy DS and Rogawski MA (2012) Neurosteroids - Endogenous Regulators of Seizure Susceptibility and Role in the Treatment of Epilepsy In *Jasper's Basic Mechanisms of the Epilepsies*, ed. JL Noebels, M Avoli, MA Rogawski, RW Olsen, AV Delgado-Escueta. Bethesda (MD), pp-984-1002.

Reddy DS and Woodward R (2004) Ganaxolone: a prospective overview. *Drugs Future* **29**:227-242.

Reddy DS, Castaneda DC, O'Malley BW, and Rogawski MA (2014) Anticonvulsant activity of progesterone and neurosteroids in progesterone receptor knockout mice. *J Pharmacol Exp Ther* **310**:230-239.

Reddy DS, Gangisetty O, and Wu X (2017) PR-independent neurosteroid regulation of α2-GABA-A receptors in the hippocampus subfields. *Brain Res* **1659**:142-147.

Reddy DS, Gangisetty O, Briyal S (2010) Disease-modifying activity of progesterone in the hippocampus kindling model of epileptogenesis. *Neuropharmacology* **59**:573-581.

Reddy DS, Gould J, and Gangisetty O (2012) A mouse kindling model of perimenstrual catamenial epilepsy. *J Pharmacol Exp Ther* **341**:784-793.

Reddy DS, Kim HY, and Rogawski MA (2001) Neurosteroid withdrawal model of perimenstrual catamenial epilepsy. *Epilepsia* **42**:328-336.

Reddy DS, Yoshimura RF, Ramanathan G, Carver C, Johnstone TB, Hogenkamp DJ, and Gee KW (2018) Role of beta2/3-specific GABA-A receptor isoforms in the development of hippocampus kindling epileptogenesis. *Epilepsy Behav* **82**:57-63.

Reddy SD and Reddy DS (2015) Midazolam as an anticonvulsant antidote for organophosphate intoxication--A pharmacotherapeutic appraisal. *Epilepsia* **56**:813-821.

Reddy SD, Younus I, Clossen B, and Reddy DS (2015) Antiseizure activity of midazolam in mice lacking delta subunit extrasynaptic GABA-A receptors. *J Pharmacol Exp Therap* **353**:517-528.

Rogawski MA, Loya CM, Reddy K, Zolkowska D, and Lossin C (2013) Neuroactive steroids for the treatment of status epilepticus. *Epilepsia* **54**(Suppl 6):93-98.

Rosenthal ES, Claassen J, Wainwright MS, Husain AM, Vaitkevicius H, Raines S, Hoffmann E, Colquhoun H, Doherty JJ, and Kanes SJ (2017) Brexanolone as adjunctive therapy in super-refractory status epilepticus. *Ann Neurol* **82**:342-352.

Rudolph U, Crestani F, Benke D, Brunig I, Benson JA, Fritschy JM, Martin JR, Bluethmann H, and Mohler H (1999) Benzodiazepine actions mediated by specific GABA-A receptor subtypes. *Nature* **401**:796-800.

Ruiz A, Walker MC, Fabian-Fine R, and Kullmann DM (2004) Endogenous zinc inhibits GABA-A receptors in a hippocampal pathway. *J Neurophysiol* **91**:1091-1096.

Rupprecht R (2003) Neuroactive steroids: mechanisms of action and neuropsychopharmacological properties. *Psychoneuroendocrinology* **28**:139-168.

Rupprecht R, Reul JM, Trapp T, van Steensel B, Wetzel C, Damm K, Zieglgänsberger W, and Holsboer F (1993) Progesterone receptor-mediated effects of neuroactive steroids. *Neuron* **11**:523-530.

Russek SJ (1999) Evolution of GABA-A receptor diversity in the human genome. *Gene* **227**:213-222.

Saliba RS, Kretschmannova K, and Moss SJ (2012) Activity-dependent phosphorylation of GABA-A receptors regulates receptor insertion and tonic current. *EMBO J* **31**:2937-2951.

Scimemi A, Andersson A, Heeroma JH, Strandberg J, Rydenhag B, McEvoy AW, Thom M, Asztely F, and Walker MC (2006) Tonic GABA-A receptor-mediated currents in human brain. *Eur J Neurosci* **24**:1157-1160.

Shen H, Sabaliauskas N, Sherpa A, Fenton AA, Stelzer A, Aoki C, and Smith SS (2010) A critical role for alpha4betadelta GABA-A receptors in shaping learning deficits at puberty in mice. *Science* **327**:1515-1518.

Shin DJ, Germann AL, Steinbach JH, and Akk G (2017) The actions of drug combinations on the GABA-A receptor manifest as curvilinear isoboles of additivity. *Mol Pharmacol* **92**:556-563.

Shin DJ, Germann AL, Covey DF, Steinbach JH, and Akk G (2019) Analysis of GABA-A receptor activation by combinations of agonists acting at the same or distinct binding sites. *Mol Pharmacol* **95**:70-81.

Sieghart W (1995) Structure and pharmacology of gamma-aminobutyric acid A receptor subtypes. *Pharmacol Rev* **47**:181-234.

Sieghart W and Sperk G (2002) Subunit composition, distribution and function of GABA-A receptor subtypes. *Curr Top Med Chem* **2**:795-816.

Smart TG (1992) A novel modulatory binding site for zinc on the GABA-A receptor complex in cultured rat neurones. *J Physiol* **447**:587-625.

Smart TG, Moss SJ, Xie X, and Huganir RL (1991) GABA-A receptors are differentially sensitive to zinc: dependence on subunit composition. *Br J Pharmacol* **103**:1837-1839.

Smart TG, Xie X, Krishek BJ (1994) Modulation of inhibitory and excitatory amino acid receptor ion channels by zinc. *Prog Neurobiol* **42**:393-441.

Sperk G, Schwarzer C, Tsunashima K, Fuchs K, and Sieghart W (1997) GABA-A receptor subunits in the rat hippocampus I: immunocytochemical distribution of 13 subunits. *Neuroscience* **80**:987-1000.

Sperling MR, Klein P, and Tsai J (2017) Randomized, double-blind, placebo-controlled phase 2 study of ganaxolone as add-on therapy in adults with uncontrolled partial-onset seizures. *Epilepsia* **58**:558-564.

Spigelman I, Li Z, Banerjee PK, Mihalek RM, Homanics GE, and Olsen RW (2002) Behavior and physiology of mice lacking the GABA-A-receptor delta subunit. *Epilepsia* **43**(Suppl 5):3-8.

Spigelman I, Li Z, Liang J, Cagetti E, Samzadeh S, Mihalek RM, Homanics GE, and Olsen RW (2003) Reduced inhibition and sensitivity to neurosteroids in

hippocampus of mice lacking the GABA-A receptor delta subunit. *J neurophysiol* **90**:903-910.

Srivastava S, Cohen J, Pevsner J, Aradhya S, McKnight D, Butler E, Johnston M, and Fatemi A (2014) A novel variant in GABRB2 associated with intellectual disability and epilepsy. *Am J Med Genet A* **164A**:2914-2921.

Stell BM, Brickley SG, Tang CY, Farrant M, and Mody I (2003) Neuroactive steroids reduce neuronal excitability by selectively enhancing tonic inhibition mediated by delta subunit-containing GABA-A receptors. *Proc Natl Acad Sci USA* **100**:14439-14444.

Storustovu SI and Ebert B (2006) Pharmacological characterization of agonists at delta-containing GABA-A receptors: Functional selectivity for extrasynaptic receptors is dependent on the absence of gamma2. *J Pharmacol Exp Ther* **316**:1351-1359.

Sun C, Sieghart W, and Kapur J (2004) Distribution of alpha1, alpha4, gamma2, and delta subunits of GABA-A receptors in hippocampal granule cells. *Brain Res* **1029**:207-216.

Sun H, Zhang Y, Liang J, Liu X, Ma X, Wu H, Xu K, Qin J, Qi Y, and Wu X (2008) SCN1A, SCN1B, and GABRG2 gene mutation analysis in Chinese families with generalized epilepsy with febrile seizures plus. *J Hum Genet* **53**: 769-774.

Sun MY, Shu HJ, Benz A, Bracamontes J, Akk G, Zorumski CF, Steinbach JH, and Mennerick SJ (2018) Chemogenetic Isolation Reveals Synaptic Contribution of delta GABA-A Receptors in Mouse Dentate Granule Neurons. *J Neurosci* **38**:8128-8145.

Sutula TP (1990) Experimental models of temporal lobe epilepsy: new insights from the study of kindling and synaptic reorganization. *Epilepsia* **31**(Suppl 3): S45-54.

Szewczyk B (2013) Zinc homeostasis and neurodegenerative disorders. *Front Aging Neurosci* **5**:33.

Takeda A, Hanajima T, Ijiro H, Ishige A, Iizuka S, Okada S, and Oku N (1999) Release of zinc from the brain of El (epilepsy) mice during seizure induction. *Brain Res* **828**:174-178.

Tallarida RJ (2000). Drug synergism and dose-effect data analysis. Chapman & Hall/CRC, Boca Raton.

Tallarida RJ (2006) An overview of drug combination analysis with isobolograms. *J Pharmacol Exp Ther* **319**:1-7.

Tallarida RJ (2007) Interactions between drugs and occupied receptors. *Pharmacol Ther* **113**:197-209.

Tan HO, Reid CA, Single FN, Davies PJ, Chiu C, Murphy S, Clarke AL, Dibbens L, Krestel H, Mulley JC, Jones MV, Seeburg PH, Sakmann B, Berkovic SF,

Sprengel R, and Petrou S (2007) Reduced cortical inhibition in a mouse model of familial childhood absence epilepsy. *Proc Natl Acad Sci USA* **104**:17536-17541.

Tanaka M, Olsen RW, Medina MT, Schwartz E, Alonso ME, Duron RM, Castro-Ortega R, Martinez-Juarez IE, Pascual-Castroviejo I, Machado-Salas J, Silva R, Bailey JN, Bai D, Ochoa A, Jara-Prado A, Pineda G, Macdonald RL, and Delgado-Escueta AV (2008) Hyperglycosylation and reduced GABA currents of mutated GABRB3 polypeptide in remitting childhood absence epilepsy. *Am J Hum Genet* **82**:1249-1261.

Thurman DJ, Beghi E, Begley CE, Berg AT, Buchhalter JR, Ding D, Hesdorffer DC, Hauser WA, Kazis L, Kobau R, Kroner B, Labiner D, Liow K, Logroscino G, Medina MT, Newton CR, Parko K, Paschal A, Preux PM, Sander JW, Selassie A, Theodore W, Tomson T, Wiebe S; ILAE Commission on Epidemiology (2011) Standards for epidemiologic studies and surveillance of epilepsy. *Epilepsia* **52**(Suppl 7):2-26.

Tian M, Mei D, Freri E, Hernandez CC, Granata T, Shen W, Macdonald RL, and Guerrini R (2013) Impaired surface alphabetagamma GABA-A receptor expression in familial epilepsy due to a GABRG2 frameshift mutation. *Neurobiol Dis* **50**:135-141.

Tian Y, Yang Z, and Zhang T (2010) Zinc ion as modulator effects on excitability and synaptic transmission in hippocampal CA1 neurons in Wistar rats. *Neurosci Res* **68**:167-175.

Timofeeva O and Nadler JV (2006) Facilitation of granule cell epileptiform activity by mossy fiber-released zinc in the pilocarpine model of temporal lobe epilepsy. *Brain Res* **1078**:227-234.

Todd E, Gurba KN, Botzolakis EJ, Stanic AK, and Macdonald RL (2014) GABA-A receptor biogenesis is impaired by the gamma2 subunit febrile seizure-associated mutation, GABRG2(R177G). *Neurobiol Dis* **69**:215-224.

Tokuda K, O'Dell KA, Izumi Y, and Zorumski CF (2010) Midazolam inhibits hippocampal long-term potentiation and learning through dual central and peripheral benzodiazepine receptor activation and neurosteroidogenesis. *J Neurosci* **30**:16788-16795.

Turgeon SM and Albin RL (1992) Zinc modulates GABA-B binding in rat brain. *Brain Res* **596**:30-34.

Upasani RB, Yang KC, Acosta-Burruel M, Konkoy CS, McLellan JA, Woodward RM, Lan NC, Carter RB, and Hawkinson JE (1997) 3alpha-Hydroxy-3beta-(phenylethynyl)-5beta-pregnan-20-ones: synthesis and pharmacological activity of neuroactive steroids with high affinity for GABA-A receptors. *J Med Chem* **40**:73-84.

Urak L, Feucht M, Fathi N, Hornik K, and Fuchs K (2006) A GABRB3 promoter haplotype associated with childhood absence epilepsy impairs transcriptional activity. *Human Mol Genet* **15**:2533-2541.

Vaitkevicius H, Husain AM, Rosenthal ES, Rosand J, Bobb W, Reddy K, Rogawski MA, and Cole AJ (2017) First-in-man allopregnanolone use in super-refractory status epilepticus. *Ann Clin Transl Neurol* **4**:411-414.

Vezzani A, Fujinami RS, White HS, Preux PM, Blumcke I, Sander JW, Loscher W (2016) Infections, inflammation and epilepsy. *Acta neuropathol* **131**:211-234.

Vicini S, Losi G, and Homanics GE (2002) GABA-A receptor delta subunit deletion prevents neurosteroid modulation of inhibitory synaptic currents in cerebellar neurons. *Neuropharmacology* **43**:646-650.

Vogt K, Mellor J, Tong G, and Nicoll R (2000) The actions of synaptically released zinc at hippocampal mossy fiber synapses. *Neuron* **26**:187-196.

Wallace RH, Marini C, Petrou S, Harkin LA, Bowser DN, Panchal RG, Williams DA, Sutherland GR, Mulley JC, Scheffer IE, and Berkovic SF (2001) Mutant GABA-A receptor gamma2 subunit in childhood absence epilepsy and febrile seizures. *Nat Genet* **28**:49-52.

Wei W, Zhang N, Peng Z, Houser CR, and Mody I (2003) Perisynaptic localization of delta subunit-containing GABA-A receptors and their activation by GABA spillover in the mouse dentate gyrus. *J Neurosci* **23**:10650-10661.

Westbrook GL and Mayer ML (1987) Micromolar concentrations of Zn2+ antagonize NMDA and GABA responses of hippocampal neurons. *Nature* **328:**640-643.

Whissell PD, Lecker I, Wang DS, Yu J, and Orser BA (2015) Altered expression of δGABA-A receptors in health and disease. *Neuropharmacology* **88**:24-35.

Wiltgen BJ, Sanders MJ, Ferguson C, Homanics GE, and Fanselow MS (2005) Trace fear conditioning is enhanced in mice lacking the delta subunit of the GABA-A receptor. *Learn Mem* **12**:327-333.

Wisden W, Laurie DJ, Monyer H, and Seeburg PH (1992) The distribution of 13 GABA-A receptor subunit mRNAs in the rat brain. I. Telencephalon, diencephalon, mesencephalon. *J Neurosci* **12**:1040-1062.

Witsch J, Golkowski D, Hahn TT, Petrou S, and Spors H (2015) Cortical alterations in a model for absence epilepsy and febrile seizures: in vivo findings in mice carrying a human GABA-AR gamma2 subunit mutation. *Neurobiol Dis* **77**:62-70.

Wlodarczyk AI, Xu C, Song I, Doronin M, Wu YW, Walker MC, and Semyanov A (2013) Tonic GABA-A conductance decreases membrane time constant and increases EPSP-spike precision in hippocampal pyramidal neurons. *Front Neural Circuits* **7**:205.

Wohlfarth KM, Bianchi MT, and Macdonald RL (2002) Enhanced neurosteroid potentiation of ternary GABA-A receptors containing the delta subunit. *J Neurosci* **22**:1541-1549.

Wojda E, Wlaz A, Patsalos PN, and Luszczki JJ (2009) Isobolographic characterization of interactions of levetiracetam with the various antiepileptic drugs in the mouse 6 Hz psychomotor seizure model. *Epilepsy Res* **86**:163-174.

Wu X, Gangisetty O, Carver CM, and Reddy DS (2013) Estrous cycle regulation of extrasynaptic delta-containing GABA-A receptor-mediated tonic inhibition and limbic epileptogenesis. *J Pharmacol Exp Ther* **346**:146-160.

Xie XM and Smart TG (1991) A physiological role for endogenous zinc in rat hippocampal synaptic neurotransmission. *Nature* **349**:521-524.

Yorulmaz H, Seker FB, Demir G, Yalcin IE, and Oztas B (2013) The effects of zinc treatment on the blood-brain barrier permeability and brain element levels during convulsions. *Biol Trace Elem Res* **151**:256-262.

Younus I and Reddy DS (2017) A resurging boom in new drugs for epilepsy and brain disorders. *Expert Rev Clin Pharmacol* **23**:1-19.

Zheleznova NN, Sedelnikova A, and Weiss DS (2009) Function and modulation of delta-containing GABA-A receptors. *Psychoneuroendocrinology* **34**(Suppl 1):67-73.

Zhu J, Shao CY, Yang W, Zhang XM, Wu ZY, Zhou L, Wang XX, Li YH, Xia J, Luo JH, and Shen Y (2012) Chronic zinc exposure decreases the surface expression of NR2A-containing NMDA receptors in cultured hippocampal neurons. *PLoS One* **7**:e46012.